Investigations of Novel Reactions Inside the Resorcin[4]arene Hexamer and of HCl as Cocatalyst

Inauguraldissertation

zur

Erlangung der Würde eines Doktors der Philosophie

vorgelegt der

Philosophisch-Naturwissenschaftlichen Fakultät

der Universität Basel

von

Jesper Mathis Köster

2020

Genehmigt von der Philosophisch-Naturwissenschaftlichen Fakultät

auf Antrag von

Prof. Dr. Konrad Tiefenbacher, Prof. Dr. Marcel Mayor, Prof. Dr. Michal Juriček

---

Basel, den 15. Oktober 2019

Prof. Dr. Martin Spiess

Dekan

Die vorliegende Arbeit wurde von November 2015 bis August 2016 an der *Technischen Universität München* und von September 2016 bis November 2019 an der *Universität Basel* unter der Leitung von Prof. Dr. Konrad Tiefenbacher an der *Juniorprofessur für Organische Chemie* bzw. der *Assistenzprofessur für Organische Chemie* angefertigt.

Teile dieser Arbeit wurden veröffentlicht:

J.M. Köster, D. Häussinger, K. Tiefenbacher*, *Front. Chem.* **2019**, *6*, 639.

J.M. Köster, K. Tiefenbacher*, *ChemCatChem*, **2018**, *10*, 2941.

Acknowledgements

My deepest gratitude goes to Prof. Dr. Konrad Tiefenbacher, for accepting me in his group and offering the chance to pursue my PhD studies. His excellent and vast knowledge about chemistry and his experience have been of great help and a constant inspiration for my work. Although we did not always see eye to eye, I am deeply thankful for the invaluable advice he gave, and I will always look up to him as a remarkable supervisor. I wish you all the best for your future work and I am certain you will continue to inspire many more students in your group.

I gratefully acknowledge my colleagues from the Tiefenbacher group for making my time there the most enjoyable part of my studies. Special thanks go to Andreas Räder, who was an excellent supervisor during my Master's Thesis and to whom I owe a great deal of my theoretical and practical knowledge in the laboratory. I'd also like to commend his ability to keep daily life in the lab inspiring and entertaining. Additionally, I'd like to specially acknowledge Thomas Bräuer and Severin Merget for proofreading this manuscript and for being not only excellent colleagues but also very good friends.

During my PhD studies I had the chance to teach and supervise bright young students: Yu-Hsuan Lee and Michael Ehrenreich. I also thoroughly enjoyed my time supervising the OCA lab course in Munich as well as the Pharmapraktikum in Basel, teaching young students the basics of organic chemistry and watching them grow and develop their passion.

PD Dr. Daniel Häussinger is acknowledged for his immensely valuable help with conducting NMR kinetic experiments and NMR spectroscopy in general.

I would like to thank Ms Beatrice Erismann, Ms Esther Stalder, and Ms Isa Worni of the University of Basel for their great continuous help in handling all organizational questions.

My profound admiration goes to my girlfriend Jasmine Assefi for remaining calm in the face of late lab work, putting up with constant incoherent ramblings about chemistry, and for always supporting me. Thank you from the bottom of my heart for being a constant inspiration and helping me focus on the important things in life. You are truly special and keep inspiring me to do my absolute best.

Last but not least I want to thank my family for their unconditional love and support at all times.

Deutsches Abstrakt

Der auf der Selbstassemblierung von Resorcin[4]arene **60b** basierende supramolekulare Wirt **XII** zeigte katalytische Aktivität in mehreren Reaktionen. Die hexamere Struktur umschließt ein internes Volumen von 1400 Å³ und besitzt aufgrund ihres hoch dynamischen Charakters die Fähigkeit, Gäste reversibel aufzunehmen und wieder abzugeben. Die katalytische Aktivität rührt dabei von der Stabilisierung von Intermediaten und Übergangszuständen über Kation-π Wechselwirkungen mit den elektronenreichen Wänden der Kavität sowie der Ausbildung von H-Brücken her.

Während der Untersuchungen zur „tail-to-head“ Zyklisierung von Monoterpenen stellte sich heraus, dass HCl zwingend benötigt wird um katalytische Aktivität zu erhalten. Diese Erkenntnis zog eine genauere Betrachtung der bereits bekannten, von Wirt **XII** katalysierten Reaktionen nach sich, in deren Verlauf klar wurde, dass über kationische Intermediate verlaufende Reaktionen auf HCl als Kokatalysator angewiesen sind.

Die Aktivierung tertiärer Alkylfluoride sowie von primären und sekundären Benzylfluoriden in Gegenwart des molekularen Gefäßes **XII** wurde untersucht. Kinetische Messungen ergaben ein sigmoidales Reaktionsprofil, was auf ein enges katalytisches Zusammenspiel von Wirt und HF, das im Laufe der Reaktion freigesetzt wird, hindeutet.

Die von Hexamer **XII** katalysierte und bisher unbekannte Umsetzung von elektronenarmen Benzaldehyden mit Isocyaniden zu Iminen und Kohlenmonoxid wurde eingehend untersucht. Nach Betrachtung kinetischer Messungen und quantenmechanischer Berechnungen wurde ein Vorschlag zum Mechanismus der Reaktion formuliert, der einen schrittweisen Verlauf über Iminooxiran- und Aziridinon-Intermediate vorsieht.

English abstract

The readily accessible supramolecular host **XII,** based on the self-assembly of resorcin[4]arene **60b**, has been shown to facilitate a range of reactions. Its hexameric structure encloses an internal volume of 1400 Å³ and is capable of reversible guest encapsulation and release due to its highly dynamic nature. Its catalytic activity stems from the ability to stabilize intermediates and transition states *via* cation-π interactions with the electron-rich aromatic walls of the cavity and to form H-bonds.

Investigations into the tail-to-head cyclization of monoterpenes revealed a dependence on the presence of HCl for catalytic activity to arise. This sparked a closer scrutiny of reactions known to be catalyzed by host **XII**, which uncovered that the presence of HCl as cocatalyst is essential for reactions progressing through cationic intermediates.

The activation of tertiary alkyl fluorides and primary and secondary benzyl fluorides was investigated inside the supramolecular container **XII**. Kinetic measurements display a sigmoidal reaction progress, indicating synergistic catalysis by the host and HF released during the reaction.

An unprecedented transformation of electron-poor benzaldehydes and isocyanides to imines and carbon monoxide catalyzed by hexamer **XII** was investigated. A mechanistic proposal put forth after consulting kinetic measurements and quantum mechanical calculations, suggesting the reaction progresses *via* iminooxirane and aziridinone intermediates.

TABLE OF CONTENTS

1 Introduction

Supramolecular chemistry, often defined as chemistry beyond the molecule, is a relatively young research area that sits at the intersection of chemistry, biology and physics.[1] Its focus lies on the design of highly complex chemical systems arising from the assembly of simple building blocks *via* intermolecular, non-covalent interactions.[2] Essential for the spontaneous organization into higher-level structures is an individual subunit's ability of molecular recognition, encoded within its intrinsic conformational preferences and functional group decoration, which enables it to seek out other components and become part of a larger bonding network, *e.g.* through hydrogen bonding, metal-ligand coordination, or coulombic interactions. Self-assembly and guest uptake represent fundamental driving forces for the evolution of life as evidenced by the spontaneous formation of cell walls from lipids, thereby enabling the emergence of the first organisms.[3] Furthermore, the reversibility of self-assembly due to the weak nature of non-covalent interactions make these systems highly adaptive and therefore pliable for evolution.

Molecular recognition is also a key feature in enzymes, catalytically active proteins with well-defined three-dimensional structures arising from hydrogen bonds between residues specified by the individual amino acid sequence. The sheer number of essential processes catalyzed by enzymes is testament to their importance for biological life. The unmatched catalytic competence they display serves as eternal inspiration for supramolecular chemistry, their performance as constant benchmark and the pursuit of outclassing them remaining the ultimate goal.

1.1 Enzyme Catalysis

Imagining life on earth without the contribution from enzymes is impossible: All basic processes in life, such as the conversion of nutrients to energy and building blocks for proteins, lipids, and nucleic acids, rely on the catalytic prowess of enzymes to enable these transformations under mild, *in vivo* conditions. Over the course of hundreds of millions of years, evolution has shaped enzymes into versatile catalysts with high selectivities as well as excellent regio- and stereocontrol. Their exceptional catalytic power stems from active pockets, cavities in the tertiary structure of the

enzyme, which selectively bind substrates and reagents and transform them into products. Similar to a lock and key,[4] the three-dimensional structure of the catalytically active cavity accommodates exclusively substrates that match in size and shape through an interplay of non-covalent interactions with amino acid side chains (molecular recognition). Induced by the binding of a substrate the enzyme experiences subtle conformational changes to provide a better fit for the guest, forming an activated enzyme-substrate complex in the process.[5] Specifically, activation occurs by one or more of three basic modes: 1) stabilization of a transition state 2) lowering of the activation barrier by forming a higher-energy intermediate by temporarily reacting with the substrate 3) destabilizing the ground state by distorting the substrate's geometry.

Among natural products, terpenes occupy a special place with over 50,000 known individual representatives today,[6] with many possessing beneficial properties that have been exploited for use as anticancer drugs,[7] or antibiotic agents.[8] Based on the amount of carbon atoms of the underlying carbon skeleton (multiples of five, derived from isoprene) terpene natural products are classified as hemi- (C_5), mono- (C_{10}), sesqui- (C_{15}), di- (C_{20}), sester- (C_{25}), and triterpenes (C_{30}).[9] From only a handful of acyclic oligomers, such as geranyl phosphate (monoterpenes), farnesyl phosphate (sesquiterpenes), and geranylgeranyl phosphate (diterpenes) arise a multitude of cyclic structures.[6] The cyclization of these precursors by terpene cyclases to complex natural products is considered to be one of the most complex reactions encountered in nature. Two main biosynthetic pathways have been characterized, the "head-to-tail" branch (HT), which relies on electrophilic activation of a terminal prenyl unit (head), and the "tail-to-head" branch (TH), initiated by cleavage of an allylic pyrophosphate group (tail).[10] In addition to the activation mode, both branches differ in the direction of the propagation of the cationic charge along the substrate chain. In both case the generated cation undergoes cyclization by an intramolecular attack of a double bond. The newly formed cation propagates through additional cyclizations until the final product is released from the active pocket. This "non-stop" cyclization is a hallmark of terpene cyclases and is very hard to achieve with man-made catalysts.[11] Premature quenching of the cationic intermediates by recombination with lingering leaving groups or water is prevented by encapsulation of the intermediates in the active pockets of the cyclase enzyme, where they are stabilized via cation-dipole and cation-π interactions.

For a typical TH terpene cyclization, a cationic intermediate is generated by cleavage of the leaving group inside the active pocket of the cyclase enzyme, opening up several cyclization pathways (see figure 1).

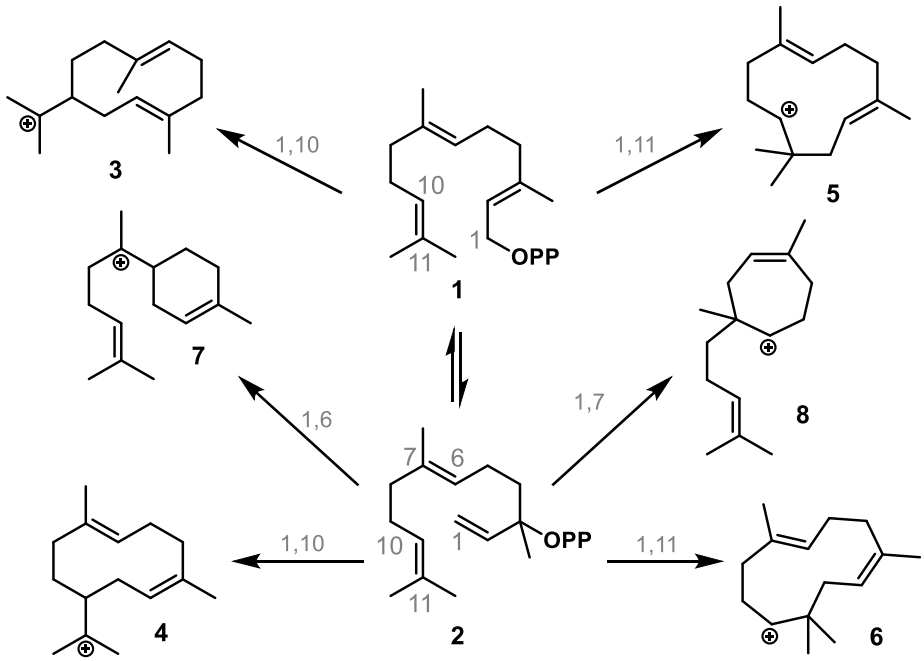

Figure 1. Possible enzyme-assisted cyclization pathways for farnesyl pyrophosphate (**1**) and nerolidyl pyrophosphate (**2**), giving rise to the formation of germacrenyl (**3**,**4**), humulyl (**5**,**6**), bisabolyl (**7**), and cycloheptenyl (**8**) carbon skeletons.[6]

In contrast to the multitude of possible pathways, the majority of terpene cyclases facilitates the formation of a single product in a highly enantioselective fashion. This is likely governed by the initial conformation of the acyclic precursor inside the catalytically active pocket.

With their unmatched stereoselectivity, terpene cyclases serve as ideal inspiration for the design of artificial enzyme mimics. Supramolecular systems display many characteristics of enzymes, such as molecular recognition of substrates, efficient uptake and selective transformations, that qualify them as suitable candidates for this objective. Within them also rests the potential to access new structures, that have been unavailable using the existing biomachinery and transfer the enzymes' impressive catalytic prowess to organic solvents.

1.2 Supramolecular Structures as Enzyme Mimetics

Supramolecular chemistry takes advantage of emergent properties when multiple subunits form larger, more complex structures through non-covalent interactions, such as hydrogen-bonding, metal coordination or π-interactions. The assembly process relies upon molecular recognition of individual subunits to spontaneously form well-defined supramolecular systems. The basic approach of designing a system to mimic enzymatic activity centers on recreating the active site of an enzyme, a well-defined cavity able to bind substrates, protect reactive intermediates from the bulk solution, and release the transformed products.

In 1987 PEDERSEN, CRAM, and LEHN were awarded the Nobel Prize in Chemistry for their respective contributions to supramolecular chemistry, a new field focusing on intermolecular interactions and host-guest complexation chemistry.[12] PEDERSEN synthesized so-called crown ethers, cyclic ethers with multiple oxygen donors, which were able to dissolve alkali metal salts in nonpolar solvents by forming strong coordination complexes.[13]

CRAM and LEHN built upon this discovery and disclosed their findings about three-dimensional analogues of crown ethers, namely cryptands and spherands, which displayed even higher affinities for alkali ions (see fig. 2).[14]

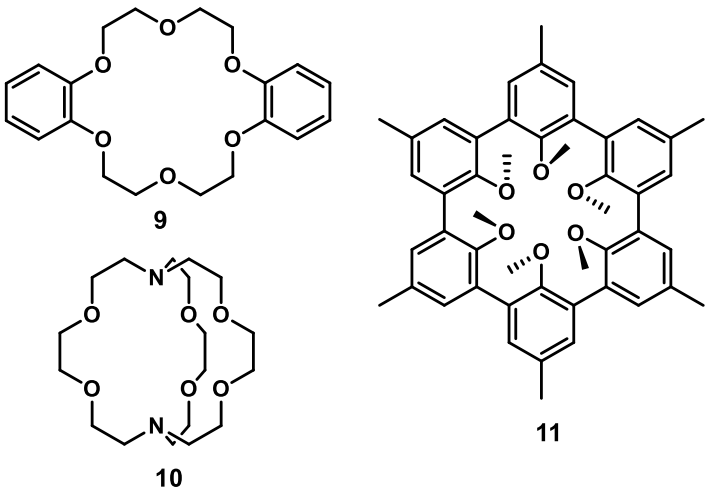

Figure 2. PEDERSEN's crown ether **9**, LEHN's cryptand **10,** and CRAM's spherand **11**.

The binding strength for alkali ions (*e.g.* K^+) increases with increasing rigidity of the backbone, in the order from **9** < **10** < **11**. Ensuing studies showed high affinities of crown ethers towards small protonated amine species, a finding that was then exploited to develop system **12**, which facilitates the cleavage of amino acid esters *via* thiolysis (see fig. 3).[14a]

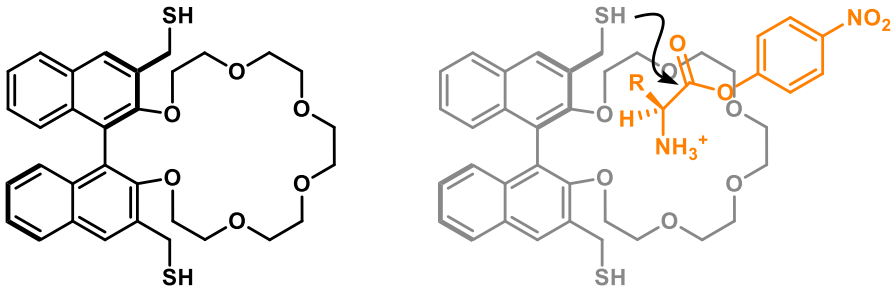

Figure 3. CRAM's transacetylation catalyst **12**; the crown ether moiety on the western part binds to the protonated amine moiety of the substrate, bringing the ester moiety in close proximity to the thiol group of **12**, facilitating cleavage of the ester.

This reaction highlights one of the possible ways supramolecular catalysts can accelerate reactions, by correctly orienting the substrate towards a reaction and its transition state. Other ways include raising the effective substrate concentration (*via* encapsulation) and stabilization of transition states of a reaction *via* positive interactions, such as hydrogen bonds or cation-π interactions.

Although other systems have been described making use of crown ether/cryptand binding sites,[15] none of these examples react in a truly catalytic fashion. Product inhibition along with severe constraints on substrate scope result in a strict limitation of the applicability of these systems. Tailored to binding specific substrates, changes in affinity often necessitate *de novo* synthesis of the supramolecular host to selectively bind different guests.

An alternative to, often painstakingly, building up supramolecular hosts in multistep syntheses *via* classical methods lies in taking advantage of self-assembling systems based on non-covalent interactions, such as metal-ligand interactions, hydrogen bonding, or coulombic interactions. So far, host structures based on metal-coordination,[16] hydrogen bonding,[17] the hydrophobic effect,[18] halogen bonding,[19] and ionic interactions have been reported.[20] Of these, metal-ligand assemblies form the largest sub-class of structures and have been studied the best.

1.2.1 Metal coordination-based assemblies

One approach to design a supramolecular container makes use of metal-ligand coordination, by employing multidentate ligands with rigid backbones and metal ions with fixed coordination geometries. The FUJITA group first published a Pd_6L_4 coordination capsule that formed *via* spontaneous self-assembly in aqueous solutions (see fig. 4).[21]

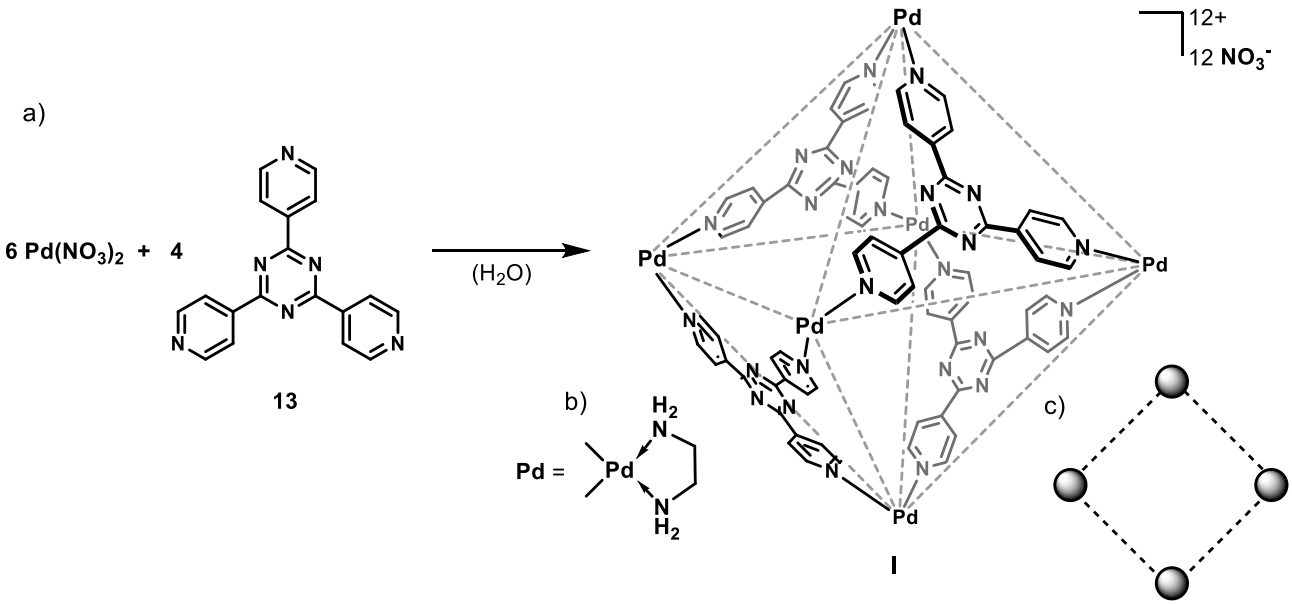

Figure 4. a) Self-assembly of the Pd_6L_4 capsule **I** by FUJITA from $Pd(NO_3)_2$ and tripyridyl ligand **13** b) coordination geometry of palladium ions c) schematic representation of capsule **I**.

The coordination cage **I** is made up of six palladium(II) ions with a square-planar coordination geometry at the vertices of an octahedron, connected by four tris(4-pyridyl)triazine (**13**) ligands in an alternating pattern. The inner compartment is comprised of a cavity with a volume of roughly 500 Å³ and has been shown to take up various organic compounds (*e.g. cis*-azobenzene and 1,3,5-tri-*tert*-butylbenzene) in aqueous solutions.[22] Cage **I** was used to catalyze the photodimerization of 1-methylacenaphthylene (**14**) with excellent regioselectivity, giving the head-to-tail *syn*-product **15** in >98% yield (see fig. 5).

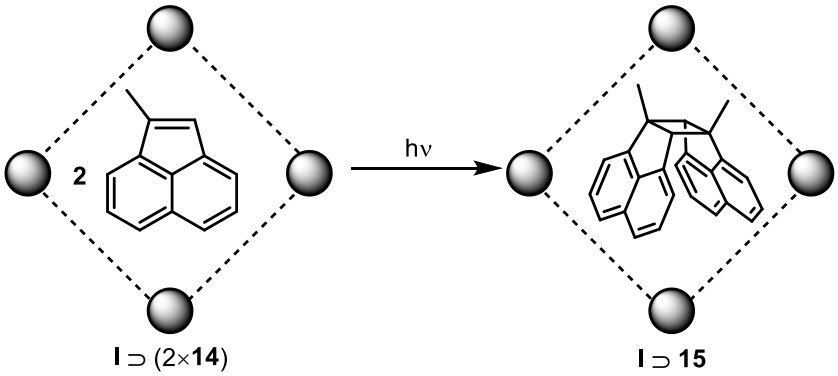

Figure 5. [2+2]-photodimerization inside coordination cage **I**.

In the absence of cage **I** no reaction could be observed. Furthermore, crossed photodimerizations of demethylated **14** with 1,4-naphthoquinones were catalyzed inside capsule **I**.[23] FUJITA *et al.* also found another interesting use for cage **I**, which is able to stabilize otherwise labile substrates and/or products in solution. This was showcased by the formation of cyclic siloxane trimers inside **I** in high yields from *m*-toluyltrimethoxysilane (**16,** see fig. 6).[24]

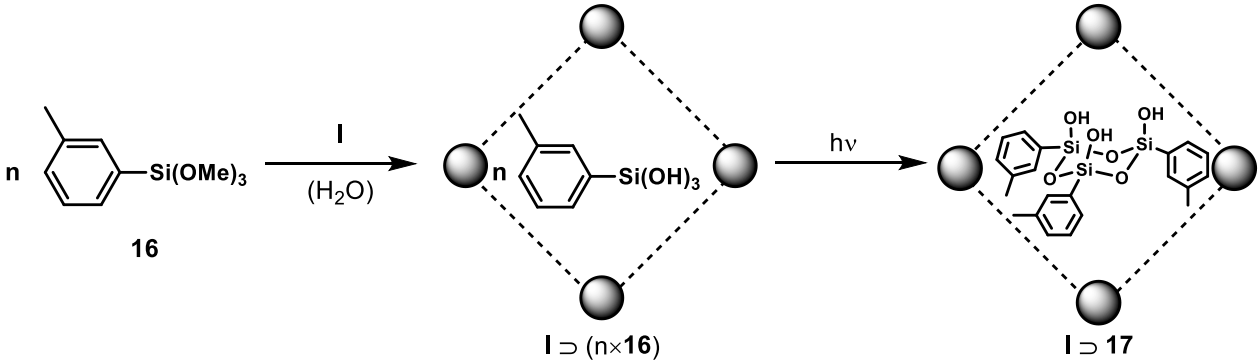

Figure 6. Hydrolysis of substrate **16** and encapsulation by coordination cage **I**, selective cyclization to trimer **17** within the cavity and protection from bulk solution conditions and further reactions.

Whereas in solution the cyclic trimer is rapidly converted, inside the cavity of cage **I** it proved to be stable for more than a month, displaying the ability of supramolecular catalysts to access different reactivities than traditional catalysts.

Another example of supramolecular catalysis was given by FUJITA *et al.* by showing that the KNOEVENAGEL reaction between aldehyde **18** and Meldrum's acid is accelerated by coordination cage **I** (see fig. 7).[25]

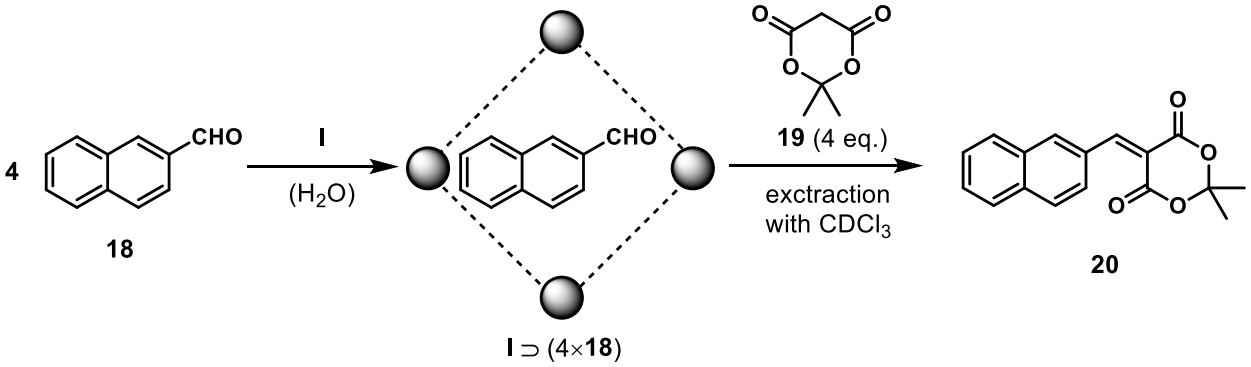

Figure 7. KNOEVENAGEL condensation of 2-naphthaldehyde (**18**) with Meldrum's acid (**19**) inside cage **I** at ambient temperature in aqueous solution. The condensation product **20** is too large to fit inside the interior cavity of **I** and is therefore expelled into solution.

This is a surprising result because of the dehydration step involved in the reaction mechanism and the reaction taking place under aqueous conditions, which would favor the formation of hydrated products. The mechanistic proposal is depicted in fig. 8.

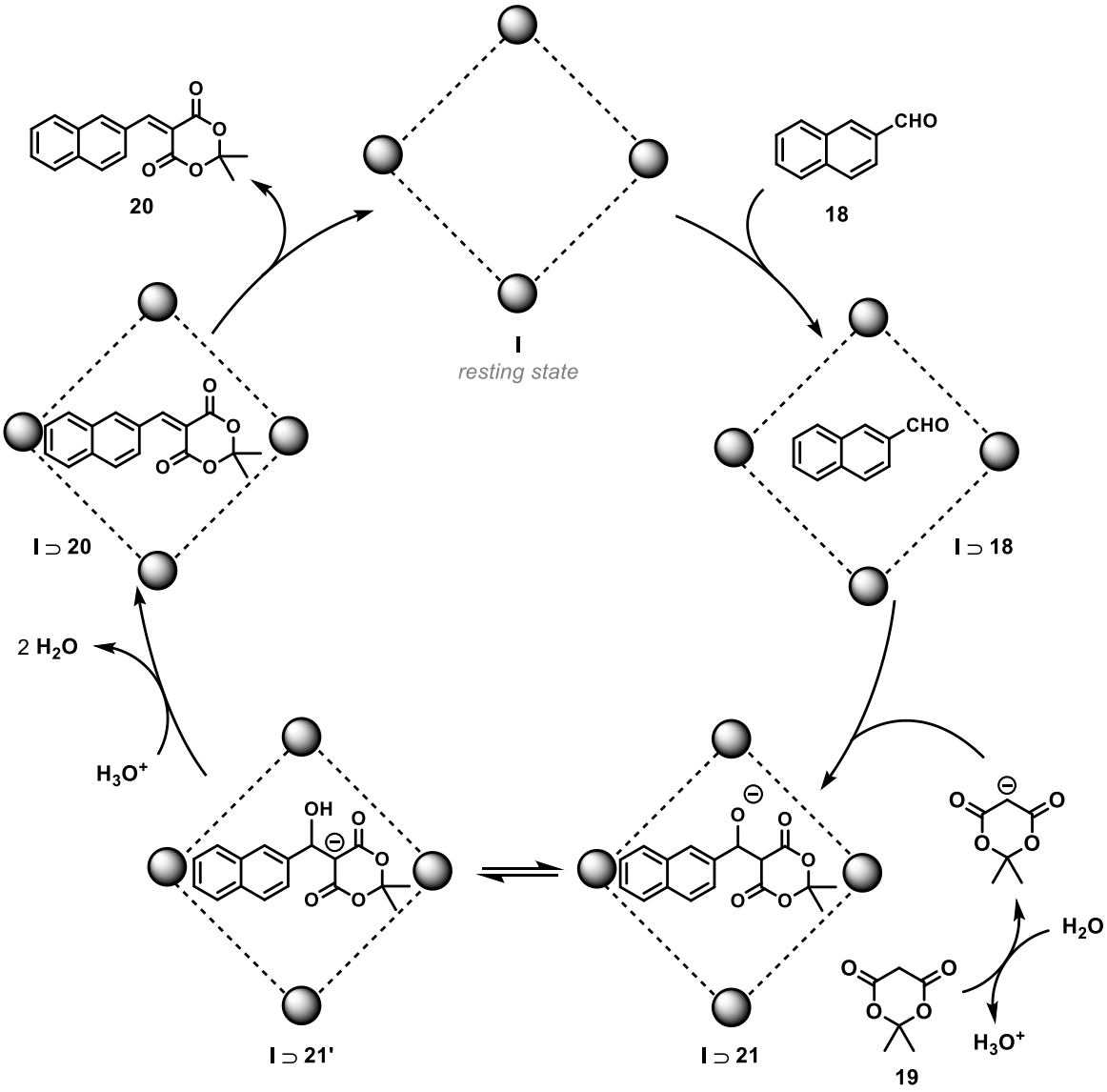

Figure 8. Mechanism of the KNOEVENAGEL reaction between aldehyde **18** and Meldrum's acid (**19**) inside coordination cage **I**.

Cage **I** is able to accommodate up to four molecules of aldehyde **18** in its inner cavity. Deprotonated **19**, present in the bulk solution, is able to enter the cavity and attack one molecule of **18**, leading to the formation of anionic intermediate **21**. Stabilized by the cationic charge of cage **I**, this intermediate isomerizes to the more stable **21'**, which is susceptible to protonation from the bulk solution. The hydrophobic interior of the supramolecular coordination cage facilitates the formation of the elimination product **20**, which is subsequently released from the cavity due to steric constraints.

Another mode of action was found for coordination cage **I** to act as a non-covalent protecting group for alkenes on diterpenes.[26] Diterpenes are too large to fit completely into the internal cavity of capsule **I**, instead adopting a coiled conformation, which leaves only the terminal alkenes open to electrophilic attacks from the bulk solution (see fig. 9).

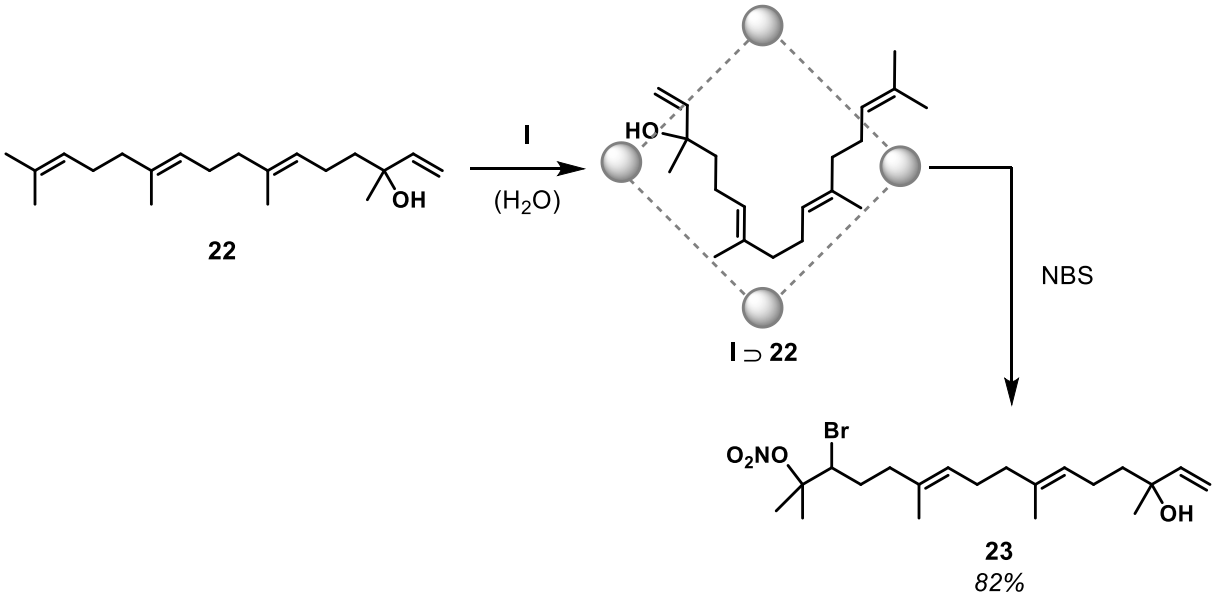

Figure 9. Nitroso-bromination of diterpene **22** inside coordination cage **I**, the coiled conformation **22** is forced to adopt in the internal cavity of **I** renders the internal tertiary alkenes inaccessible and therefore acts as a non-covalent protecting group.

The group of RAYMOND published a M_4L_6 coordination cage that self-assembles in aqueous solution from gallium(III) ions and catechol-based ligands **24** (see fig. 10).[27]

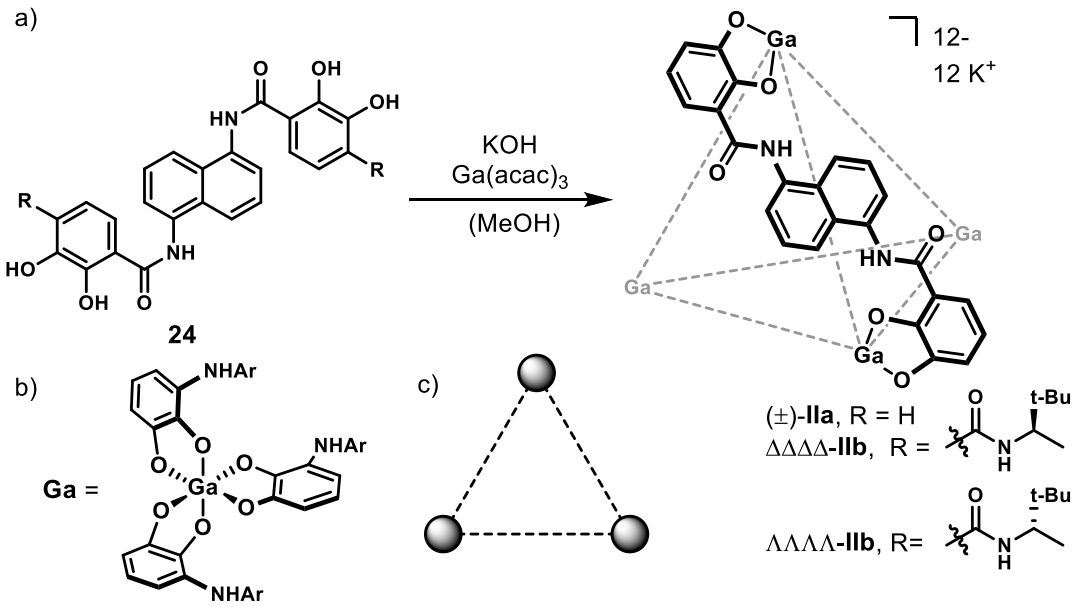

Figure 10. a) Self-assembly of coordination cages **IIa-b** by RAYMOND *et al.* in aqueous solution, remaining ligands omitted for clarity, b) coordination environment of Ga^{3+} ions, shown here in the Λ-configuration c) schematic representation of capsule **II**.

The capsule self-assembles under aqueous alkaline conditions, to facilitate deprotonation of the catechol units. The gallium ions at the vertices of the tetrahedral assembly are coordinated each by three catechol units, completing an octahedral coordination symmetry. The capsule's hydrophobic interior volume spans roughly 450 Å³. The gallium centers at the vertices exist in either the Δ or Λ configuration. Due to strong mechanical coupling of the ligands, the configuration of one gallium center is transferred to all remaining three gallium centers in the assembly, leading to the exclusive formation of either the ΔΔΔΔ- or the ΛΛΛΛ-capsule **IIa**. Further investigations showed that upon encapsulation of a chiral nicotinium cation template, the diastereomers formed of the ΔΔΔΔ- and ΛΛΛΛ-assemblies could be separated.[28] Employing enantiopure ligands with chiral amide residues lead to the exclusive formation of single diastereomers ΔΔΔΔ-**IIb** and ΛΛΛΛ-**IIb**, which also resulted in enhanced stability at elevated temperatures and against oxidation.[29]

Whereas capsule **I** from FUJITA is not fully closed, allowing guest exchange through large openings, capsule **II** presents a fully closed system. In spite of this, capsule **II** was shown to encapsulate small ammonium ions in solution and discriminate between different species (Me_4N^+, Pr_4N^+, Et_4N^+ in order of increasing affinity). The exchange occurs *via* reversible deformation of the host structure to create openings for guest molecules to enter and exit the interior cavity.[30]

Initial studies focused on encapsulating a cationic transition metal catalyst inside capsule **II** to render the supramolecular assembly catalytic. First examples include an iridium-based C-H-activation catalyst, which was shown to be taken up efficiently and catalyze the functionalization of aldehydes and ethers.[31]

Furthermore, a cationic rhodium catalyst was encapsulated and experiments for the isomerization of allylic alcohols were run. It was shown that the encapsulated catalysts impart high size and shape selectivity by adding an outer coordination layer.[32]

However, it was soon found that the M_4L_6 capsule **II** did not require an encapsulated guest/cocatalyst to be catalytically active: Upon addition of orthoformates, the anionic coordination cage was able to facilitate the hydrolysis of orthoformate ester in basic solutions, where one would not expect a reaction to occur (see scheme 1).[33]

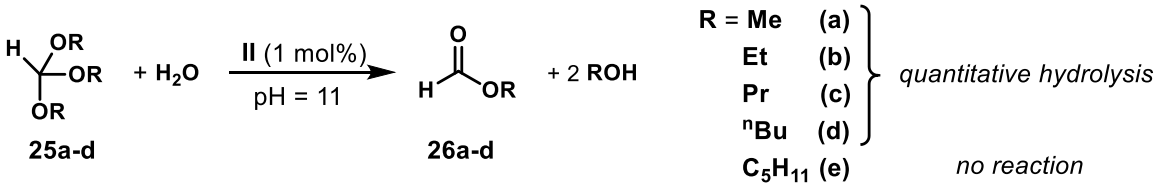

Scheme 1. Hydrolysis of trialkyl orthoformates **25a-d** catalyzed by capsule **II**; after expulsion from the interior cavity esters **26a-d** are hydrolyzed in the bulk solution.

The capsule shows a clear substrate size selectivity, effecting quantitative hydrolysis for smaller alkyl residues up to *n*-butyl chains, but showing no reaction at all for *n*-pentyl substituted orthoformates. A mechanistic proposal for this puzzling transformation is shown in fig. 11.

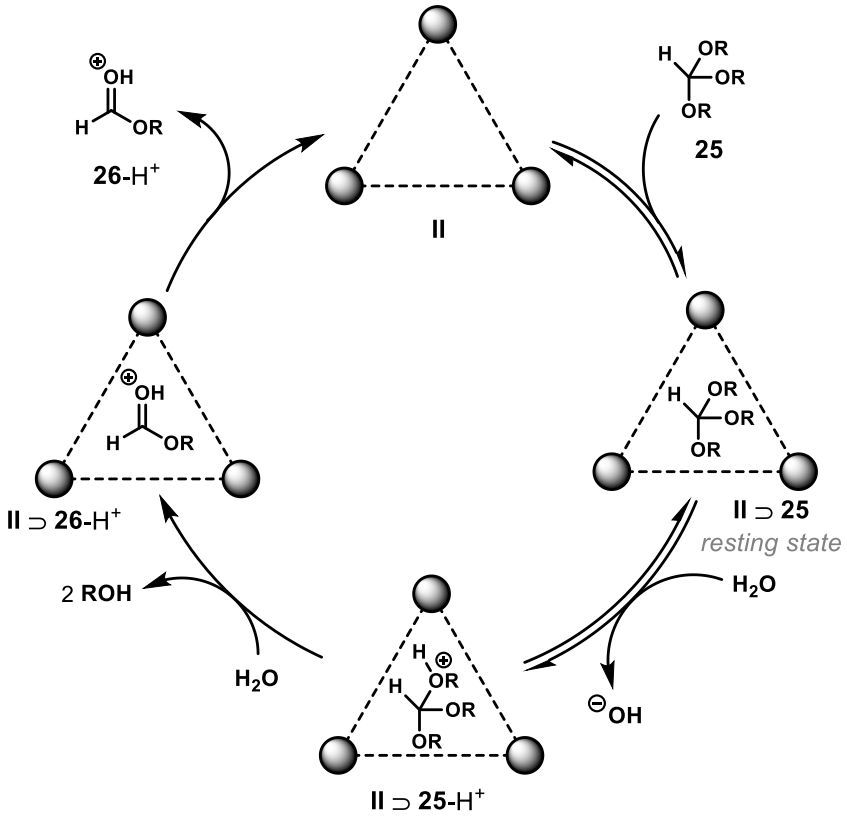

Figure 11. Mechanism of the orthoformate hydrolysis mediated by capsule **II** in basic aqueous solutions.

Orthoformate **25** is encapsulated within the hydrophobic cavity of **II** to form host-guest complex **II** ⊃ **25**, which represents the resting state of the catalyst. Water from the bulk solution enters the interior and transfers a proton to the orthoformate. The protonated host-guest complex **II** ⊃ **25-H**$^+$ is stabilized by electrostatic interactions between the anionic cage and the cationic intermediate. After elimination of one alcohol molecule, the resulting carbenium ion is stabilized inside the cavity and subsequently attacked by a water molecule from the bulk solution. Another molecule of alcohol is eliminated, giving the protonated ester species **II** ⊃ **26-H**$^+$, which then leaves the cavity and is deprotonated in the bulk solution where it is further hydrolyzed to give the carboxylate anion. The reaction follows MICHAELIS-MENTEN kinetics, showing a fast pre-equilibrium step of encapsulation and first-order kinetics for the hydrolysis reaction (first order in substrate, capsule **II**, and proton concentration). In the case of tripropyl orthoformate **25c**, the rate was found to be accelerated by a factor of 890 inside cage **II**. Addition of a high-affinity guest (NEt_4^+) led to a complete halt of turnover, further confirming the need for encapsulation for catalysis to occur.

Studies with a lower affinity guest (NPr_4^+) led to the conclusion of competitive inhibition for the hydrolysis reaction.

Exploiting the high affinity of **II** towards cationic ammonium species, the [3.3]-sigmatropic Aza-COPE rearrangement of allyl enammonium cations was found to be catalyzed as well by the anionic cage (see scheme 2).[34]

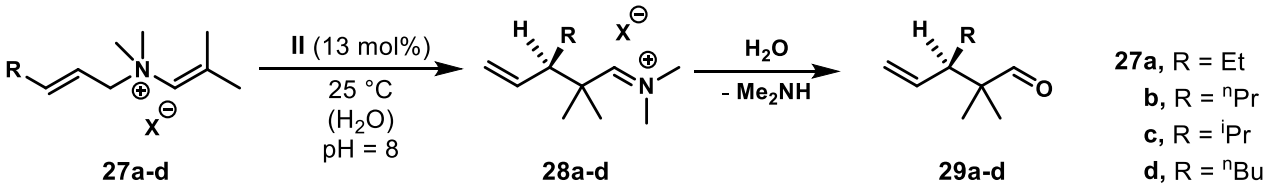

Scheme 2. Aza-COPE rearrangement of allyl enammonium cations **27a-d** inside cage **II** and subsequent hydrolysis to aldehydes **29a-d** in bulk solution.

A range of allyl enammonium ions were tested under catalytic conditions. In the case of **27c** the rate compared to the uncatalyzed reaction in bulk solution was found to be accelerated by a factor of 854. For **27a** and **27b**, the rates were accelerated by a factor of 141 and 150 respectively. The mechanism for this reaction is shown in fig. 12.

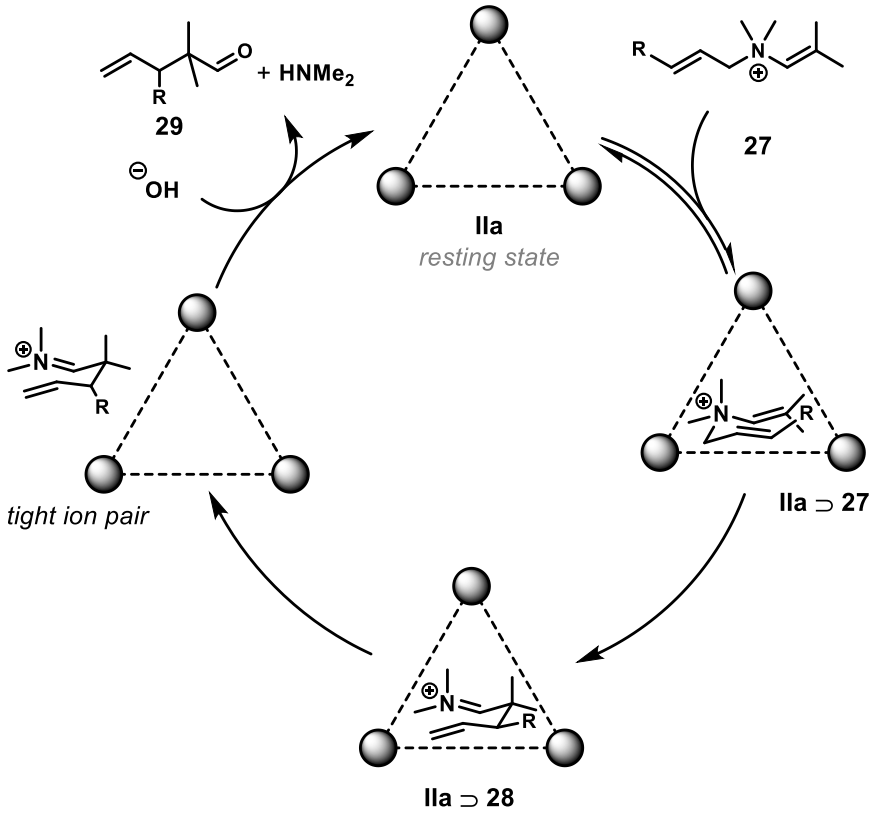

Figure 12. Proposed catalytic cycle for the Aza-COPE rearrangement of allyl enammonium cation **27** inside the cavity of anionic cage **IIa**.

Due to its cationic charge substrate **27** is easily taken up by cage **IIa**. Once encapsulated it is forced to adopt a reactive conformation due to steric restraints, which facilitates the rearrangement to occur. The resulting iminium ion **28** then leaves the interior of **IIa** but remains tightly bound to the outside of the assembly. After release from the exterior of the highly charged cage, hydroxide ions from the bulk solution are able to attack iminium ion **28** and release the product aldehyde **29**.

Conducting the Aza-COPE rearrangement with optically pure ΔΔΔΔ-**IIa** (20 mol% loading) in D_2O at 50 °C for 2 hours led to a remarkable increase in enantioselectivity of up to 78% *ee*.[35]

Exploring the goal of developing enzyme-like catalysts, the groups of RAYMOND and BERGMAN turned their attention towards the PRINS cyclization of aldehydes.[36] Investigating the reaction of (±)-Citronellal (**30**) in presence of capsule **IIa** in aqueous solutions, they found that the formation of isopulegols **31a-d** was favored over the formation of diol **32**, as was observed before in this reaction in bulk solution with acid catalysts (see scheme 3).

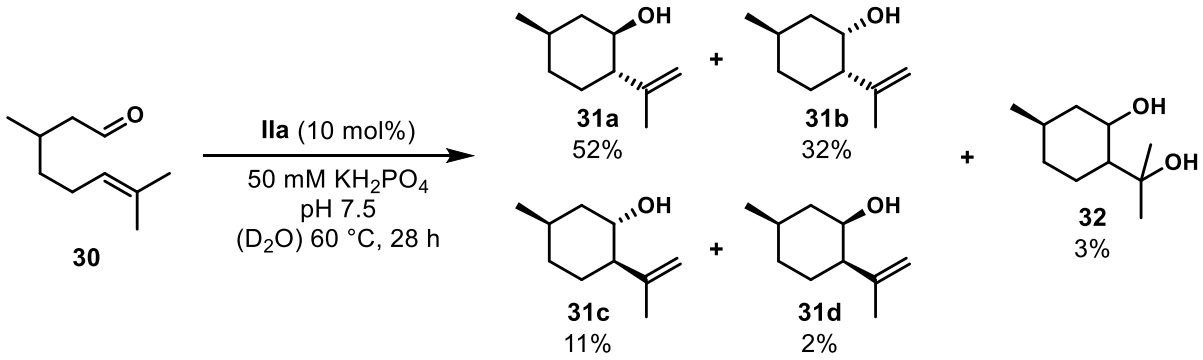

Scheme 3. PRINS cyclization of **30** in presence of capsule **IIa**.

The change in selectivity was attributed to the hydrophobic interior of capsule **IIa**, which prevents water from entering and trapping the transient cation, leading instead to the elimination products **31a-d**.

The reaction scope was further extended to include the Aza-PRINS cyclization as well, building upon the group's earlier work with the Aza-COPE rearrangement (see scheme 4).[37]

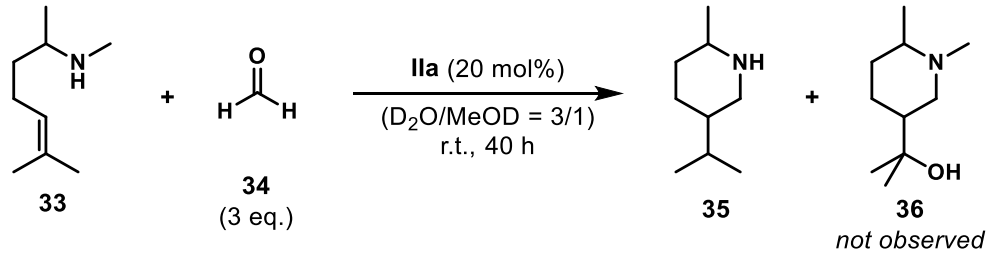

Scheme 4. Aza-PRINS cyclization of amine **33** in presence of capsule **IIa**.

As was the case in the PRINS cyclization mentioned above, a change in selectivity from the reaction run in bulk solution was observed. Employment of coordination cage **IIa** led to the exclusive formation of piperidine **35** instead of product **36**. This was rationalized by the encapsulation of the substrate, which energetically favors the adoption of a more spherical transition state (see fig. 13).

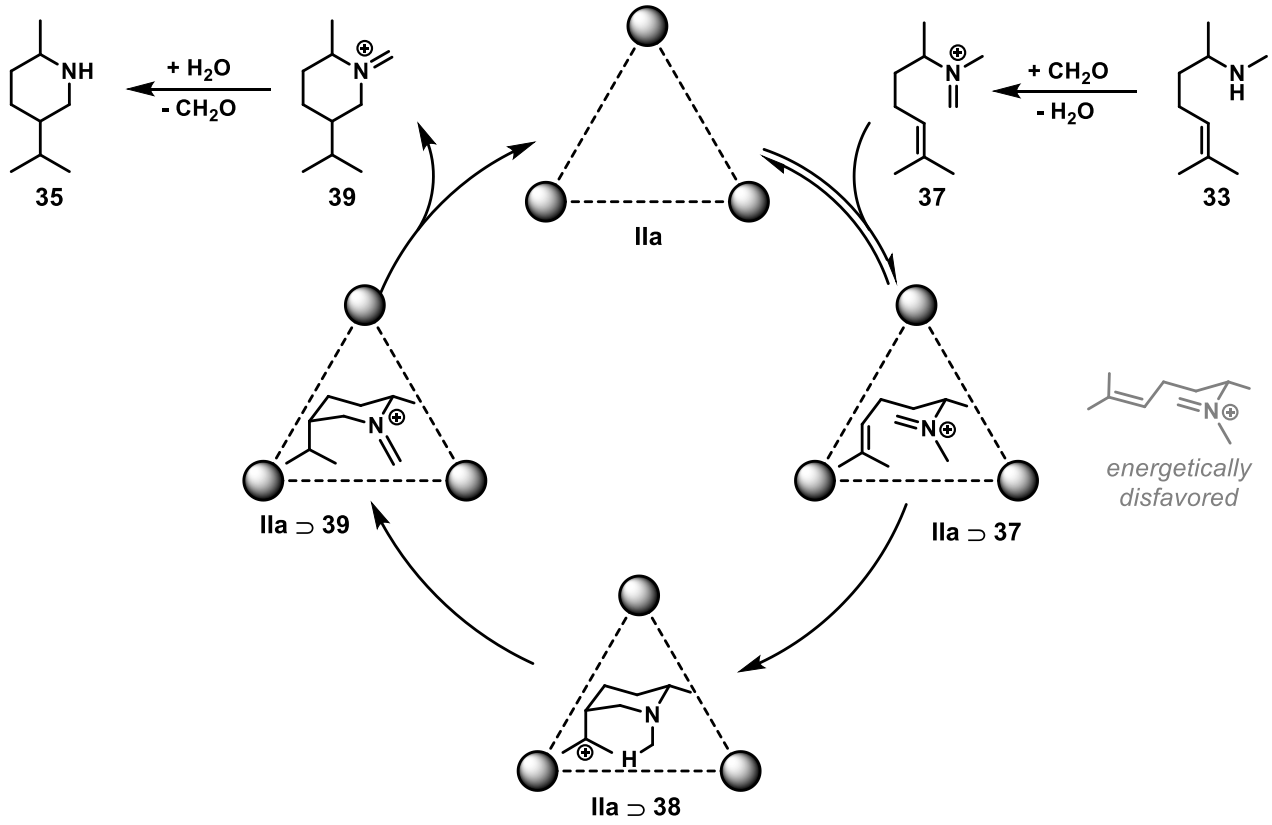

Figure 13. Mechanistic proposal for the Aza-PRINS cyclization of amine **33** and formaldehyde catalyzed by the coordination cage **IIa**; the change in selectivity presumably arises from the adoption of a more spherical transition state inside the cavity of **IIa**.

The group of NITSCHKE has published work on similar supramolecular capsules based on metal-ligand coordination cages, in their case focusing on Fe^{2+} centers and iminopyridine bidentate ligands (see fig. 14).[38]

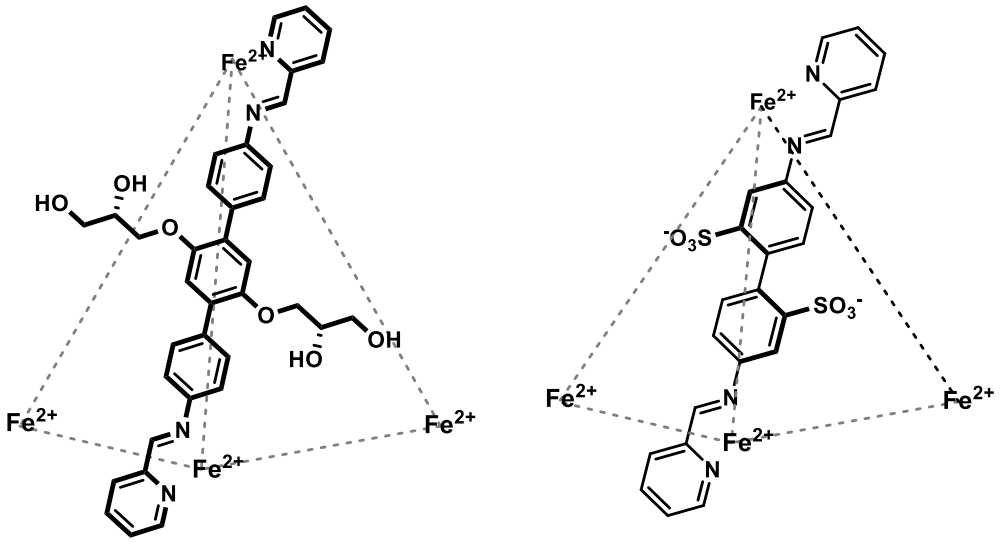

Figure 14. Schematic representation of two exemplary water-soluble capsules **III** and **IV** by NITSCHKE *et al.*, remaining ligands have been omitted for clarity.

The tetrahedral capsules **III** and **IV** self-assemble in aqueous solutions, enclosing a hydrophobic cavity in the process. A remarkable property of both capsules is the transfer of remote stereochemical information to the metal centers, as both capsules could be obtained in an enantiopure fashion by employing optically pure ligands. Capsule **III** has been shown to encapsulate a wide array of molecules and catalyze the hydrolysis of organophosphates.[38] Capsule **IV** was used as catalyst in the cascade reaction of furan (**40**, see fig. 15) with singlet oxygen and further reacted with nitromethane.[39]

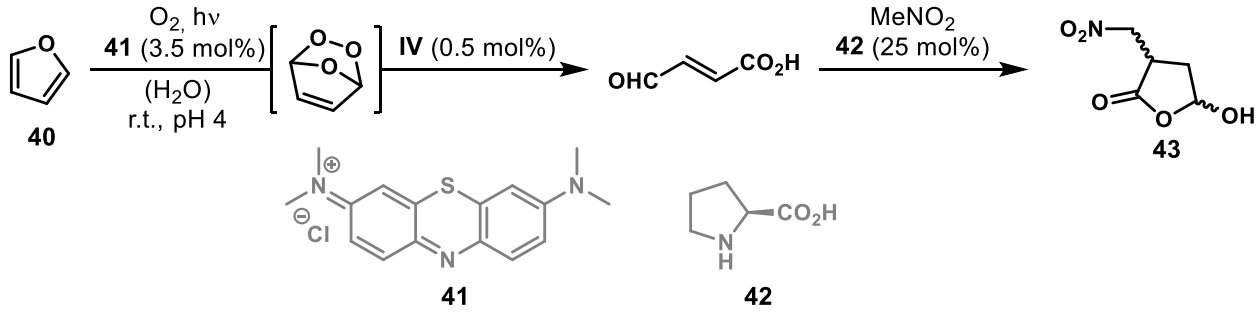

Figure 15. Catalytic relay consisting of methylene blue (**41**), cage **IV**, and *L*-proline (**42**) in one pot transforming furan (**40**) to butanolide **43**.

In this multicatalytic cascade furan is first reacted with singlet oxygen, generated by irradiation of methylene blue (**41**), to form the respective endoperoxide, which is then opened inside the cavity of cage **IV**. A final 1,4-addition of nitromethane catalyzed by *L*-proline leads to the formation of butanolide **43** in 30% overall yield. Remarkably, all three catalytic systems operate in tandem without any interference, showcasing the great potential of coordination cage **IV** and similar structures for more complex transformations.

The group of REEK made use of both metal-ligand coordination and cation-dipole interactions to design a new supramolecular host. By using a ligand with multiple additional binding sites for metal complexes, *e.g.* porphyrins, they were able to encapsulate the active transition metal catalyst by creating a second coordination sphere.[40] The first synthetic application of the ligand-template strategy lead to host **V**, based on the selective binding of Zn-porphyrins **44** to the tri-pyridyl phosphine ligand **45** (see fig. 16).[41]

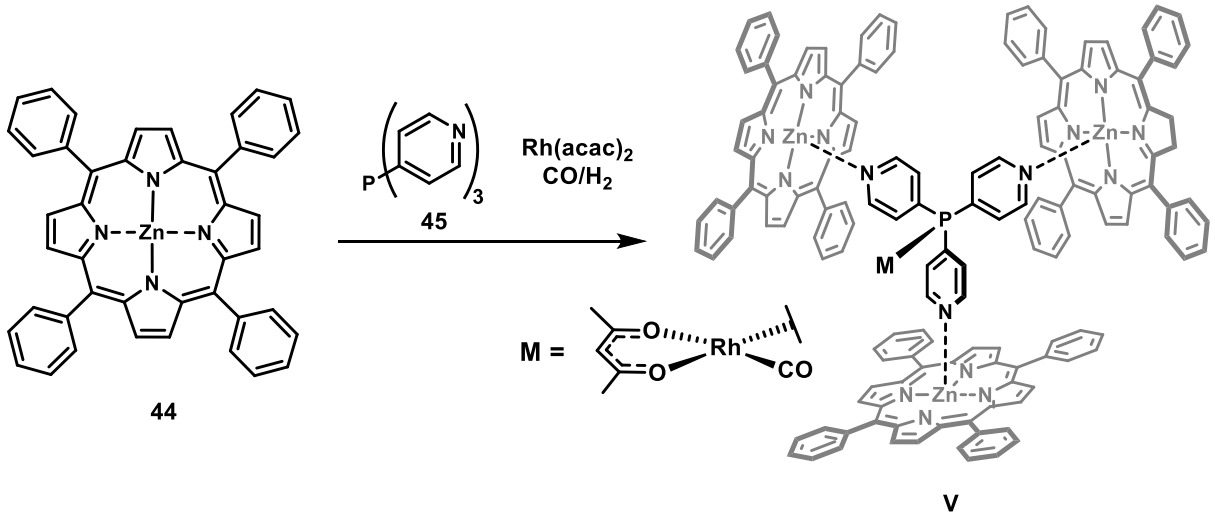

Figure 16. Synthesis of supramolecular hydroformylation catalyst **V** from Zn-porphyrin **44**, phosphine **45**, $Rh(acac)_2$ and synthesis gas (CO/H_2).

Addition of a Rh^{II} salt and synthesis gas (CO/H_2) to the supramolecular assembly of ligand **45** with Zn-porphyrin **44** resulted in the formation of the active hydroformylation catalyst **V**. Steric constraints prevent the formation of a bis-phosphine complex. The approach is highly modular, enabling the facile synthesis of multiple hosts by variation of either ligand or porphyrin components.[42]

The supramolecular catalyst **V** was then employed in the hydroformylation of linear alkenes (see scheme 5).[40-41, 43]

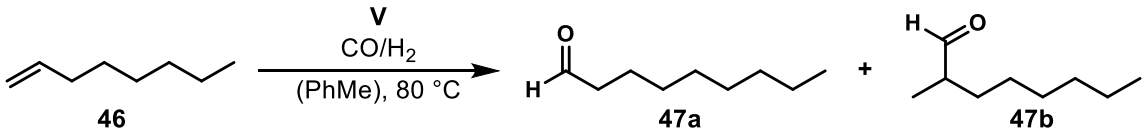

Scheme 5. Hydroformylation of 1-octene (**46**) catalyzed by supramolecular Rh-complex **V** and linear aldehyde product **47a** and branched product **47b**.

Well-defined transition metal catalysts such as the Rh-complex with ligand **45** are known to catalyze the hydroformylation and lead predominantly to the formation of the linear aldehyde product **47a**. When the supramolecular catalyst **V** was used in the reaction the activity was increased by nearly 100% and the selectivity had changed towards the branched product **47b**. This was rationalized by the complete encapsulation of the active rhodium metal center by the coordinating porphyrin units, which provide a sterically constrictive cavity, in which the formation of the more spherical branched product **47b** is favored. This selectivity is not achievable with traditional homogeneous transition metal catalysts.

The selectivity only applies to terminal alkenes. The synthetically more appealing chiral aldehydes derived from hydroformylation of internal alkenes are not accessible using this catalyst. To achieve this, the group developed a second-generation catalyst based on bis-(Zn-salphen) and phosphoramidite ligand **48** (see fig. 17).[44]

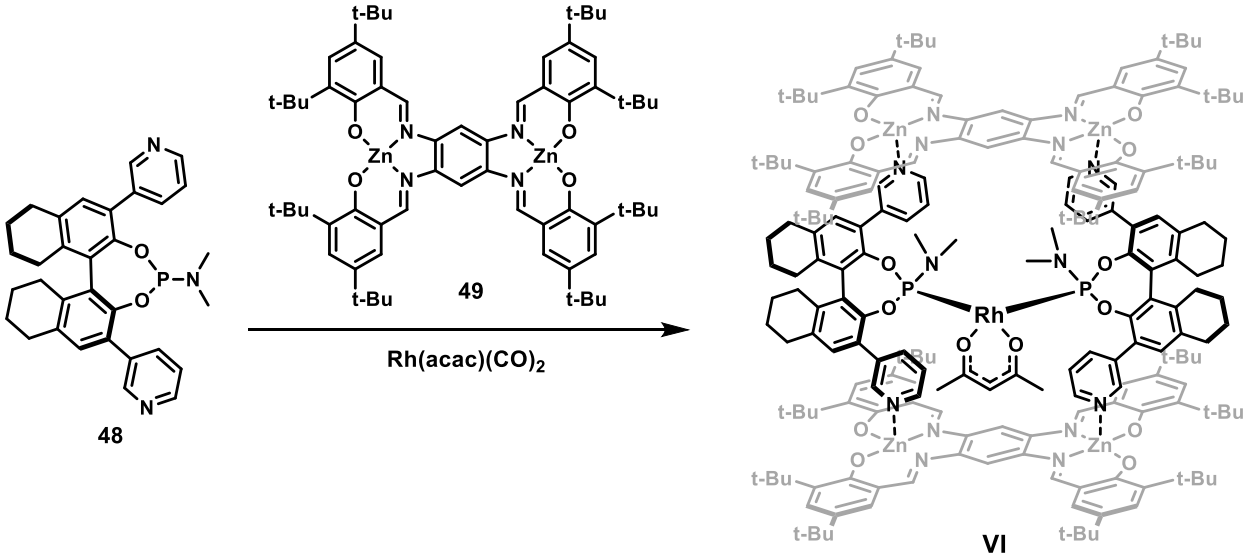

Figure 17. Synthesis of the bidentate supramolecular "box" complex **VI** from phosphoramidite **48** and bis-(Zn^{II}-salphen) **49**.

The phosphoramidite **48** and bis-(Zn-salphen) **49** self-assemble in solution to form a supramolecular box, in which the two phosphorus atoms are oriented in a suitable distance to act as a bidentate ligand for Rh^{I}, confining the active site in a chiral supramolecular environment. The catalyst **VI** was able to successfully hydroformylate internal alkenes with a high degree of stereochemical control (65% overall yield of *R*-**52**, see scheme 6).

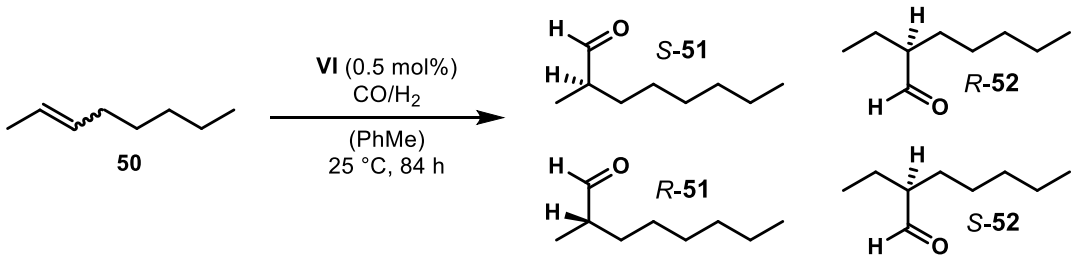

Scheme 6. Hydroformylation of internal alkene **50** catalyzed by supramolecular Rh-complex **VI** leading predominantly to the formation of the *R*-enantiomer of the innermost aldehyde **52**.

Although the overall conversion reached only 20%, very high selectivities for the innermost aldehyde product **52** were obtained (**51/52** = 30/70, 86% *ee* for *R*-**52**) when using *cis*-**50** as starting material. For the *trans*-alkene an overall conversion of 10% was achieved with a regioselectivity of **51/52** = 40/60 and 72% *ee* for *R*-**52**, showcasing the system's impressive ability to confer enantioselectivity on achiral substrates.

1.2.2 Hydrogen-bond based assemblies

Another approach to designing supramolecular structures is based on the self-assembly of subunits *via* non-covalent interactions, such as hydrogen bonds, halogen bonds, hydrophobic effect, and electrostatic interactions. Although assemblies based on halogen bonds have been disclosed by DIEDERICH and RISSANEN,[20] the majority of catalytically active systems reported so far rely on hydrogen bonds. Their highly directional nature and lower binding energy compared with metal-ligand coordination means that assemblies based on H-bonds are highly dynamic in nature. In contrast to metal-ligand hosts, guest exchange requires partial or full breakdown of the hydrogen bond network of the assemblies.[45] Furthermore, suitable building blocks are required to display some degree of curvature to make up for the lack of metal centers, which impart a geometric preference on the supramolecular structure through well-defined coordination modes.

The group of REBEK pioneered research in this specific area of supramolecular chemistry, focusing initially on glycoluril-derived structures, *e.g.* the "tennis ball", which forms dimeric structures in chloroform and benzene (see fig. 18).[46]

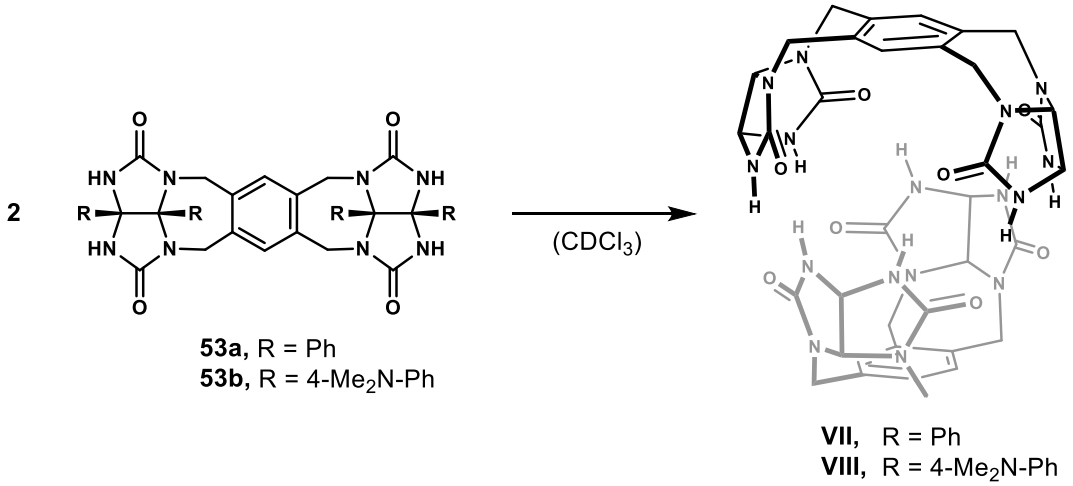

Figure 18. Formation of the dimeric "tennis ball" structure from glycolurils **53a-b** in water-saturated chloroform and structural representation of the dimer; residues on the glycolurils have been omitted for clarity.

The curved geometry of **53**, enforced by the *cis*-configuration of the phenyl substituents on the glycoluril units and the conformation of the seven-membered rings connecting the central benzene moiety with the outer glycolurils, facilitates the formation of the pseudo-spherical dimeric structure **VII**, which is held together by eight hydrogen bonds between complementary urea units.

Molecular modeling indicated an interior volume of 50 – 55 Å³, which would suffice to accommodate small molecules.[47] Indeed, ^{1}H NMR experiments showed that the assembly in $CDCl_3$ is present as two distinct species, as an empty "shell" and filled with one molecule of $CDCl_3$. Further experiments confirmed the ability of structure **VII** to encapsulate small molecules such as dichloromethane, ethylene, and methane. The largest binding constant was measured for CH_4, owing to its size which ideally fills the interior of dimer **VII**. The encapsulation is an energetically disfavored process, restricting the translational freedom of guests. This entropic decrease is countered by stabilization of the guest *via* VAN-DER-WAALS interactions with the host structure. The encapsulation of larger species was rationalized by the lengthening of the hydrogen bonds between the individual subunits.[47]

Switching substituents on the glycolurils (**53b**, **VIII**) enables template-assisted dimerization even in polar, aprotic solvents, *e.g.* DMF-d_7, that compete for hydrogen bonds. Upon addition of suitable guests (CH_4, xenon) the dimeric structure could be detected *via* ^{1}H-NMR. This process could be reversed by addition of acid to the solution, leading to the breakdown of the assembly.[48] Larger assemblies, accessible by changing the spacer between the glycoluril units from benzene to naphthalene and ethenoanthracene, were able to encapsulate larger guests. When comparing the binding properties of guests, it became apparent that guest size and shape govern the encapsulation.[49] Further studies concluded that in absence of specific interactions between host and guest, the highest binding rates are achieved when 55% of the internal cavity are occupied by the guest.[50]

One of the larger structures derived from extending the spacers between the glycoluril units is shown in fig. 20.[51] To retain the curved geometry necessary for dimer formation, monomers **54a** and **54b** were outfitted with an ethylene bridge on the central ring. The increased internal volume permits the uptake of multiple solvent molecules, that in turn can be displaced by suitable guests, such as derivatives of adamantane or ferrocene.

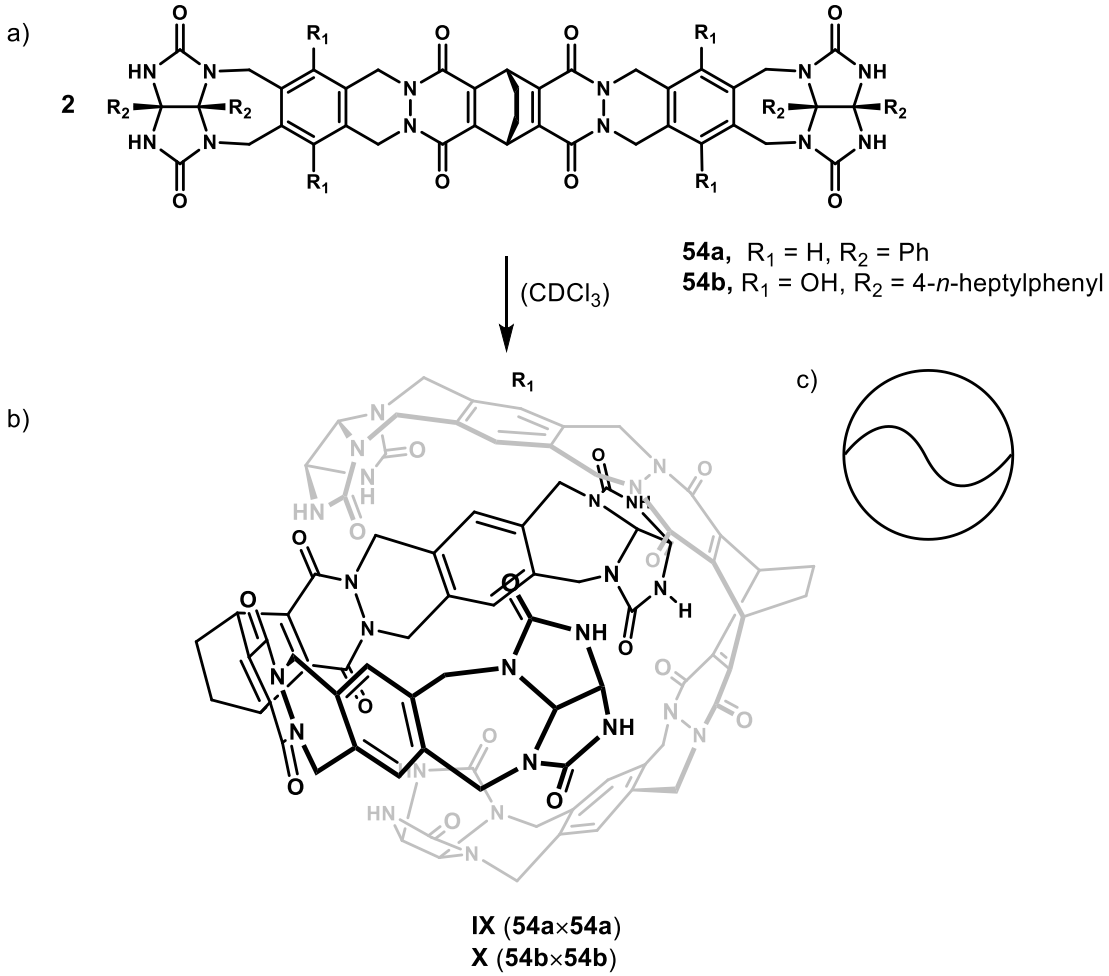

Figure 19. (a) Assembly of extended glycoluril building blocks **54a-b** to (b) "softball" structure I**X** in apolar solvents, phenyl substituents omitted for clarity; schematic representation of dimers I**X** and **X**.

The encapsulation is, contrary to observations from the smaller dimer **VII**, driven by entropy (release of multiple solvent molecules *vs.* a single guest) and not by enthalpic gains. Furthermore, the encapsulation is a slow exchange process, *i.e.* the signals of both the empty and occupied host are easily distinguished. Since "softballs" **IX** and **X** were able to take up multiple molecules of larger solvents, *e.g.* *p*-xylene-d_{10}, the assemblies' potential for catalysis of bimolecular reactions was investigated. As a model reaction the DIELS-ALDER cycloaddition of *p*-benzoquinone (**55**) and cyclohexadiene (**56**) was performed in presence of dimer **X** in *p*-xylene-d_{10} (see scheme 7).[52]

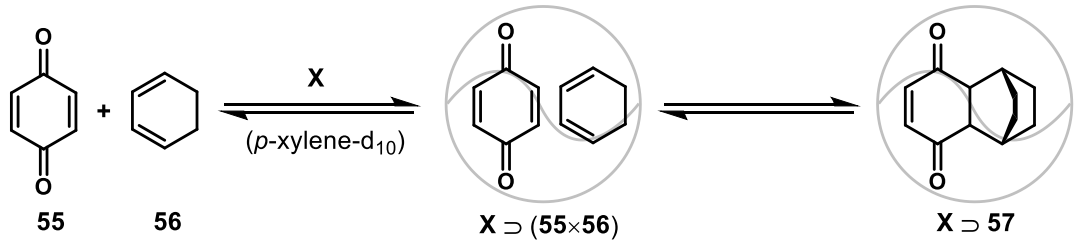

Scheme 7. DIELS-ALDER cycloaddition between *p*-benzoquinone (**55**) and cyclohexadiene (**56**) accelerated by dimer **X** to adduct **X** ⊃ **57** .

The reaction proceeds *via* pairwise encapsulation of **55** and **56**, displacing two molecules of deuterated *p*-xylene in the process. Owing to the greatly increased local concentration of both components inside the "softball", the reaction rate is accelerated by a factor of over 200. However, because of the perfect fit of product **57** within the interior of **X** ($K_a > 10^5$ M^{-1}) the catalytic cycle stops short due to product inhibition.

This problem was overcome by using 2,5-dimethyl thiophene dioxide (**58**, see fig. 20) as the diene component, since the resulting cycloaddition adduct **59** shows a much lower affinity to the softball than the starting material **55** and is consequently displaced from the interior by two molecules of starting material **55** ($K_a = 1.9 \cdot 10^5$ M^{-2}).[53]

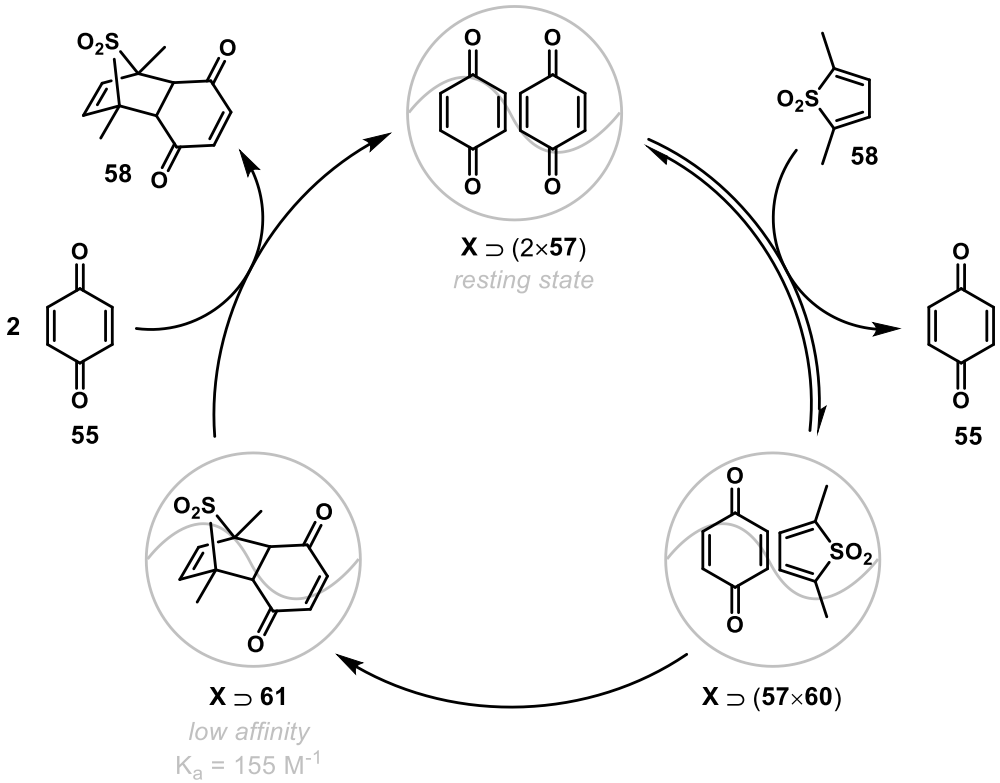

Figure 20. Catalytic cycle of the encapsulation driven DIELS-ALDER cycloaddition of *p*-benzoquinone (**55**) and 2,5-dimethyl thiophene dioxide (**58**) by REBEK *et al.*

Venturing onto even larger capsules, REBEK *et al.* investigated the hexameric capsule arising from self-assembly of resorcin[4]arenes in apolar solvents (see fig. 21). The hexameric structure **XI** was first reported in the solid state by ATWOOD *et al.*[54] and soon after confirmed to be present in solution by COHEN *et al.*[55]

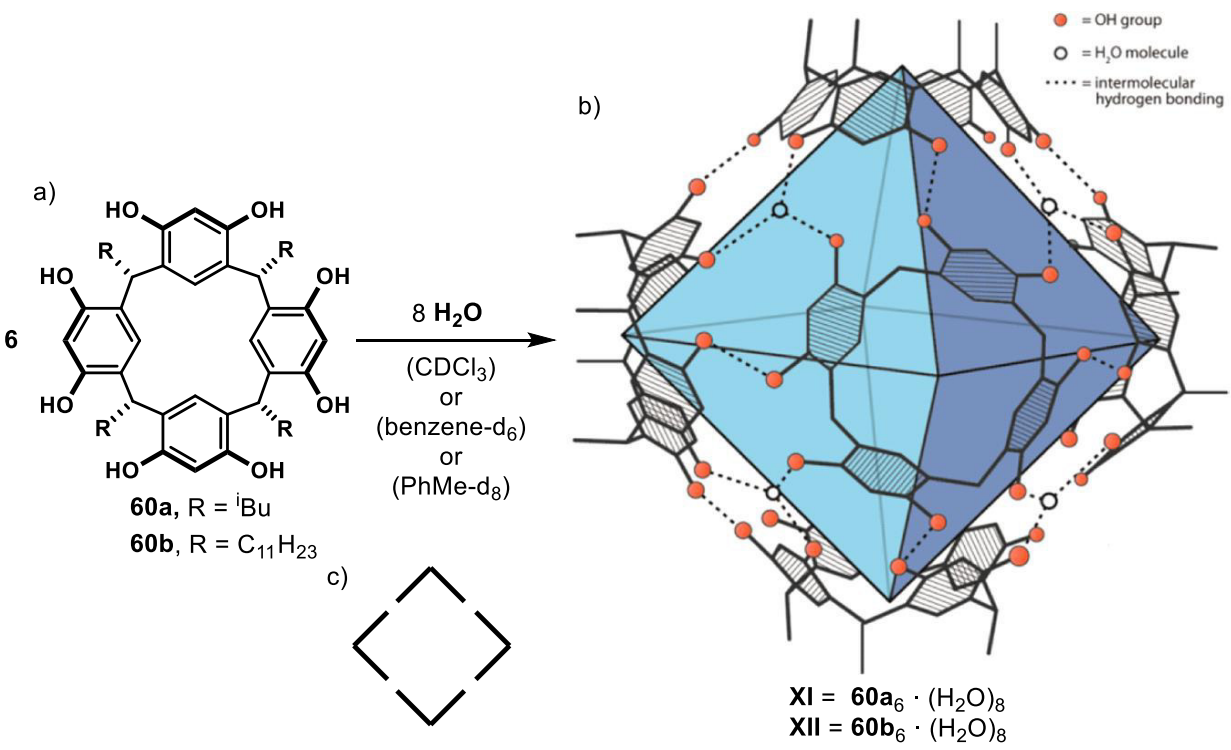

Figure 21. Self-assembly of resorcin[4]arene subunits (a) to the hexameric capsules **XI**, **XII** (b, R feet omitted for clarity) in apolar solvents under incorporation of eight water molecules; schematic representation of the hexameric assembly (c); figure adapted from ref. 56.

The hexamer possesses a roughly octahedral shape, with each monomer taking up position at one of the vertices. At each face of the octahedral assembly a "portal" is located, made up of a water molecule bound to surrounding monomer units *via* hydrogen bonds to the resorcinol hydroxy groups. In total, the assembly is held together by 60 hydrogen bonds, comprising an interior volume of roughly 1400 Å³.[54] Owing to the relatively weak hydrogen bonds, the structure is highly dynamic in solution, with individual subunits diffusing away from the assembly and being replaced from the bulk solution. This dynamic process is also thought to apply for the uptake and release of guest molecules.[45]

The molecular recognition properties of resorcin[4]arenes were well known for monomeric and dimeric structures,[56] but the disclosure of the hexameric capsule with its large interior volume stimulated more detailed investigations. Initial studies showed high affinities of the system towards tetraalkylammonium and phosphonium cations,[57] as well as a great sensitivity towards the addition of polar solvents, *e.g.* methanol, that disrupt the hydrogen bond network and force the

capsule to disassemble.[58] The affinity towards small positively charged guests was rationalized by cation-π interactions between guests and the interior cavity walls of the host hexamer.[57]

Capsule **XII** has been used as a supramolecular container for catalytically active gold and photoredox catalysts by the groups of REEK and SCARSO.[59] It was also found that the assembly catalyzes reactions on its own, for example, the hydration of isonitriles to formamides (see scheme 8).[60]

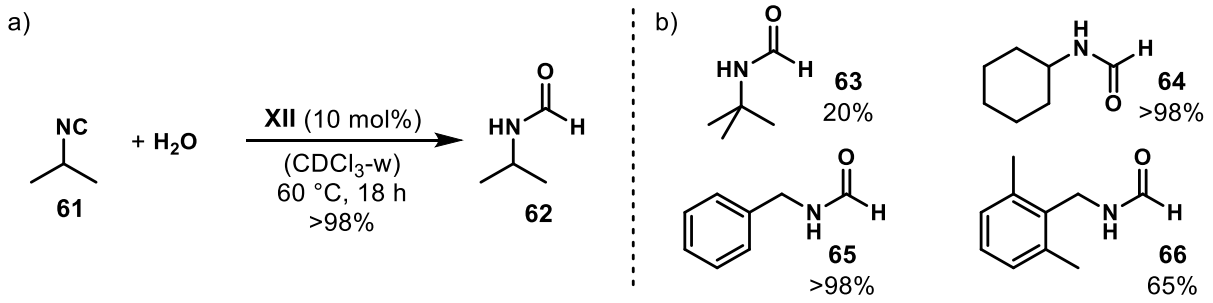

Scheme 8. a) Hydration of isocyanide **61** to formamide **62** inside capsule **XII** and b) scope of the reaction.

The reaction was found to be highly sensitive towards substrate size, the slightly larger *tert*-butyl substituted **63** was formed in only 20% yield whereas the isopropyl-substituted **62** was obtained in 98% yield. The agreed upon mechanism sees the protonation of the terminal carbon atom as the first step, after which the positively charged intermediate would be stabilized inside capsule **XII** *via* cation-π interactions.[60] Another example for catalysis was disclosed with the cycloaddition of diazoacetates and electron-poor alkenes, *e.g.* acrolein, by SCARSO *et al.* (see fig. 22).[61]

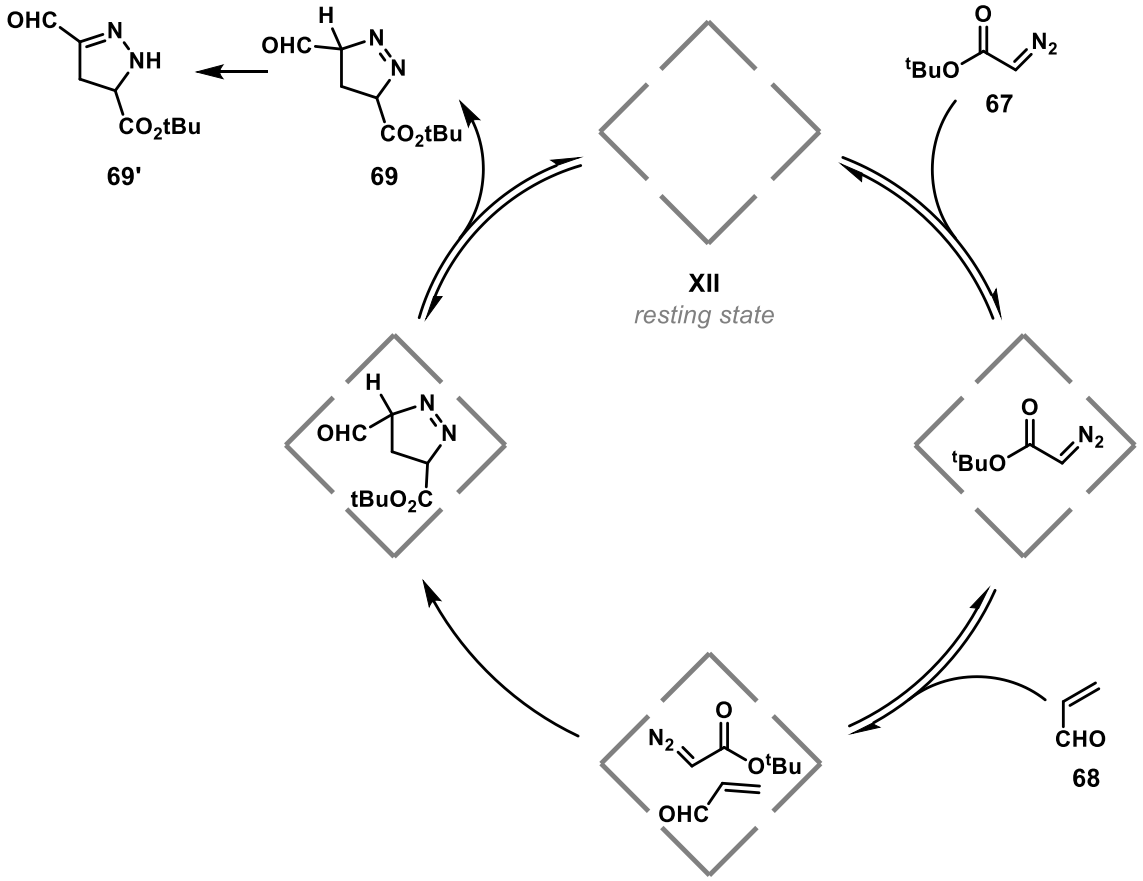

Figure 22. Catalytic cycle for the cycloaddition reaction between *tert*-butyl diazoacetate (**67**) and acrolein (**68**) inside capsule **XII**, published by SCARSO *et al.*

Capsule **XII** is able to accommodate up to six molecules of solvent in its resting state, which are then partially replaced by both starting materials. The greatly increased local concentration inside the cavity leads to an acceleration of the cycloaddition reaction; in absence of **XII** no reaction could be observed under identical conditions (water-saturated $CDCl_3$, r.t., 20 h reaction time). The cycloaddition adduct **69** is then released from the cavity and tautomerizes to the more stable **69'**, while the interior of the capsule takes up either solvent molecules from the bulk solution or new starting material to begin a new catalytic cycle.

Further examples of catalysis by SCARSO *et al.* include cycloadditions of isocyanides and azides,[62] size-selective amide couplings,[63] the oxidation of sulfides with hydrogen peroxide,[64] the hydration of alkenes to ketones,[65] and the MEINWALD rearrangement of epoxides.[66]

TIEFENBACHER *et al.* found that the hexameric assembly acts as a BRØNSTED acid (pK_a = 5.5 - 6) and used this finding to influence a size-selective WITTIG reaction as well as catalyze a highly

selective acetal hydrolysis.[67] They were further able to show that capsule **XII** is able to catalyze the cyclization of monoterpenes in a tail-to-head fashion in tandem with HCl as cocatalyst, which until then had been difficult to achieve in solution (see fig. 23).[68]

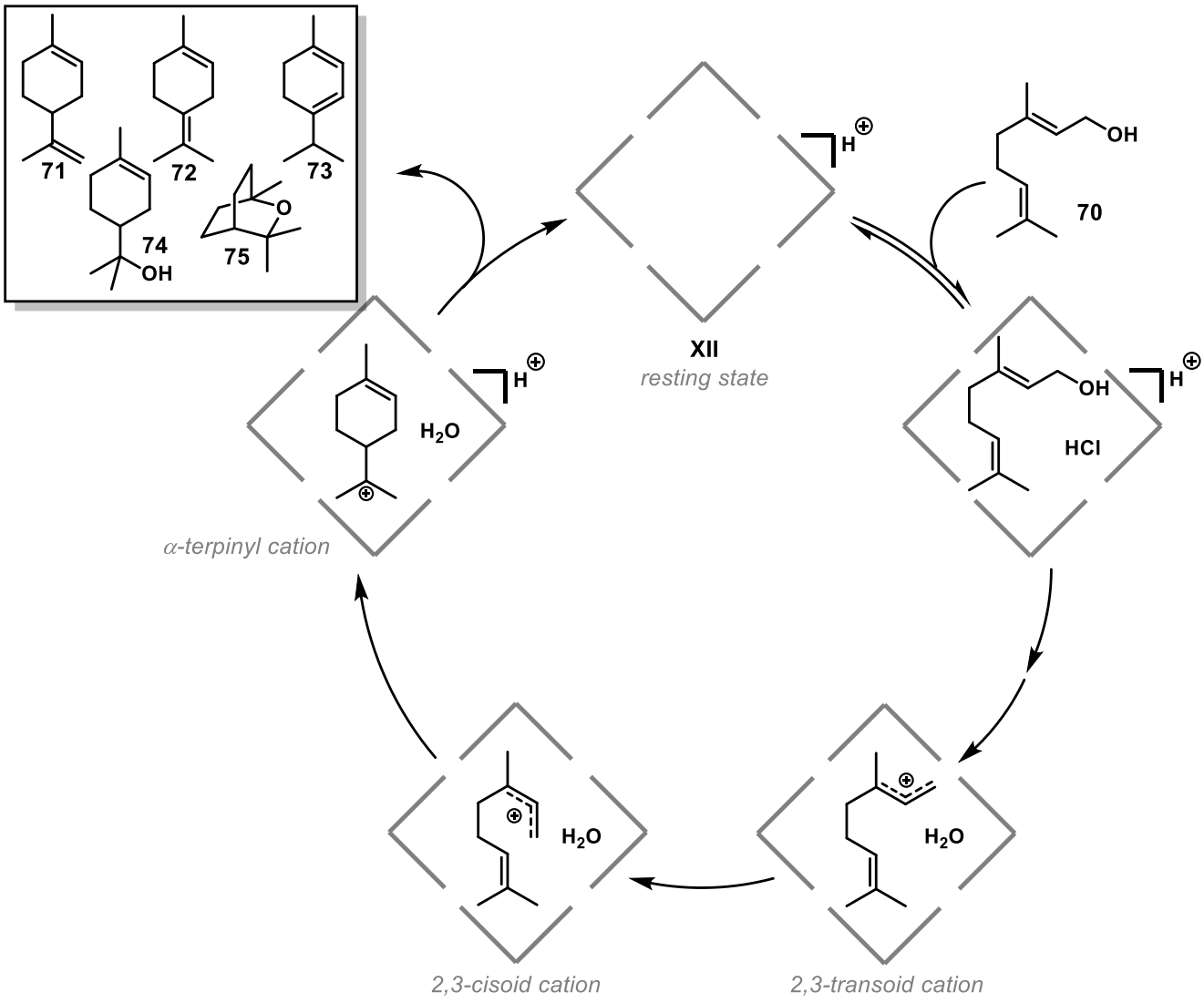

Figure 23. Catalytic cycle for the tail-to-head terpene cyclization of geraniol (**70**) inside capsule **XII** to multiple products **71**-**75**.

The reaction proceeds *via* encapsulation of the substrate geraniol (**70**) by the protonated capsule **XII** (from the cocatalyst HCl). After transfer of a proton to the hydroxy group of **70**, water is released to form the 2,3-transoid allyl cation. Stabilized by cation-π interactions inside the cavity of **XII**, the cation isomerizes to the 2,3-cisoid form, which can cyclize to the α-terpinyl cation.

Starting from this intermediate, a plethora of subsequent reactions is facilitated, mirrored by the variety of product structures obtained from this reaction. Limonene (**71**) and terpinolene (**72**) are formed by elimination of a proton; α-terpinene (**73**) by 1,2-*H*-shift and subsequent elimination of a proton; α-terpineol (**74**) is formed by nucleophilic interception of the α-terpinyl cation by water, subsequent acid-catalyzed cyclization leads to the formation of eucalyptol (**75**). The main product obtained from geraniol is α-terpinene (**73**). Different selectivities can be obtained by using different leaving groups (see scheme 9).

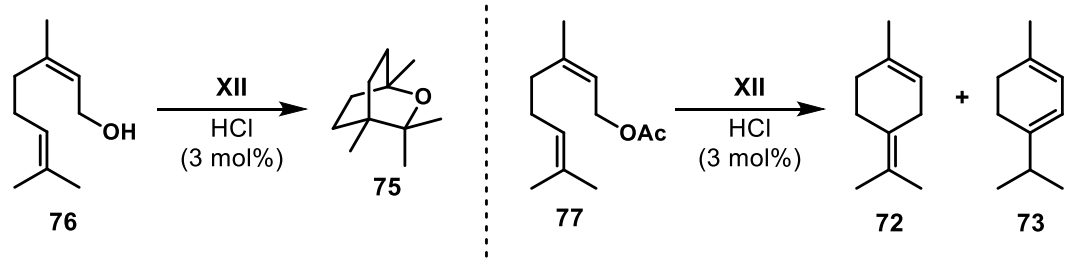

Scheme 9. Difference in reactivity between nerol (**78**) and neryl acetate (**79**), only most abundant products listed.

The cyclization of nerol (**76**) leads predominantly to the formation of eucalyptol *via* α-terpineol, whereas mostly terpinolene and α-terpinene are obtained from neryl acetate (**77**). The cleaved leaving group, *e.g.* water in the case of nerol, remains encapsulated and in close proximity to the generated cation, and is therefore able to intercept the α-terpinyl cation intermediate, leading to the formation of α-terpineol and subsequently eucalyptol. Exchanging the leaving group for a less nucleophilic one suppresses this pathway, steering the product distribution more towards the elimination products **71**, **72**, and **73**.[68b] The most selective reaction was found to be the cyclization of geranyl acetate to α-terpinene **73** in 35% yield.

Facilitating this pathway, that had been difficult to achieve with man-made catalysts, signifies a breakthrough for supramolecular catalysis and promises great potential for vastly improved total syntheses of terpene natural products.

Utilizing acyclic sesquiterpene substrates, TIEFENBACHER *et al.* were able to significantly shorten the total step count for the total synthesis of longifolene (eleven steps) and isolongifolene (10 steps) to four steps in total.[69] In further studies, the selective cyclization of (2*E*,6*Z*)-farnesyl acetate (**78**)

could be harnessed to complete the first total synthesis of δ-selinene (**79**, see scheme 10).[69-70] This also marks the first total synthesis of a natural product that utilizes the cyclization of an acyclic precursor inside a supramolecular catalyst.

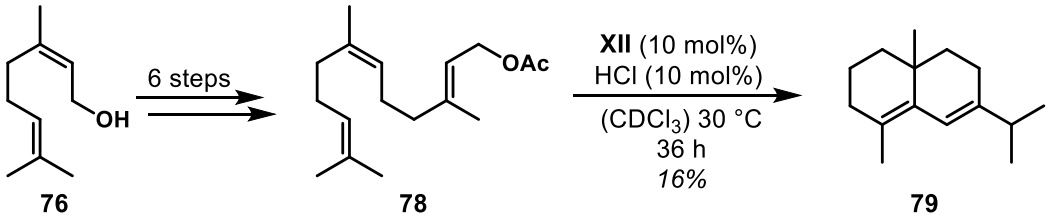

Scheme 10. Total synthesis of δ-selinene from **76**, accessible from commercially available nerol in 6 steps.

The catalytic olefin-metathesis between two unsaturated substrates is one of the most powerful synthetic methods for the formation of new C-C bonds, its importance underlined by the awarding of the Nobel prize in chemistry in 2005 to CHAUVIN, GRUBBS, and SCHROCK.[71] While closely related, and equally useful synthetically, the carbonyl-olefin metathesis has received far less attention due to the requirement for either harsh conditions or stoichiometric use of metal reagents. The laboratory of SCHINDLER achieved a breakthrough using catalytic amounts of LEWIS acids, *e.g.* $FeCl_3$, $GaCl_3$, under mild conditions.[72] TIEFENBACHER *et al.* found this reaction to also be catalyzed by host **XII** and HCl as cocatalyst (see scheme 11).[73]

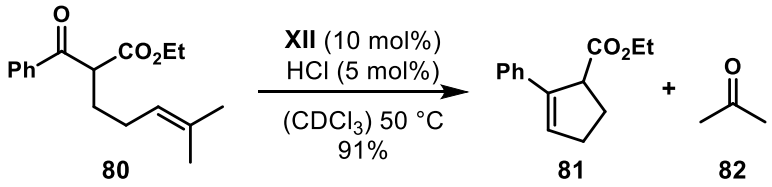

Scheme 11. Carbonyl-Olefin metathesis (COM) reaction of benzoyl acetate **80** catalyzed by capsule **XII**.

The reaction proceeds cleanly over the course of four days to give cyclopentene **81** and acetone (**82**) as products. The proposed mechanism is shown in fig. 24.

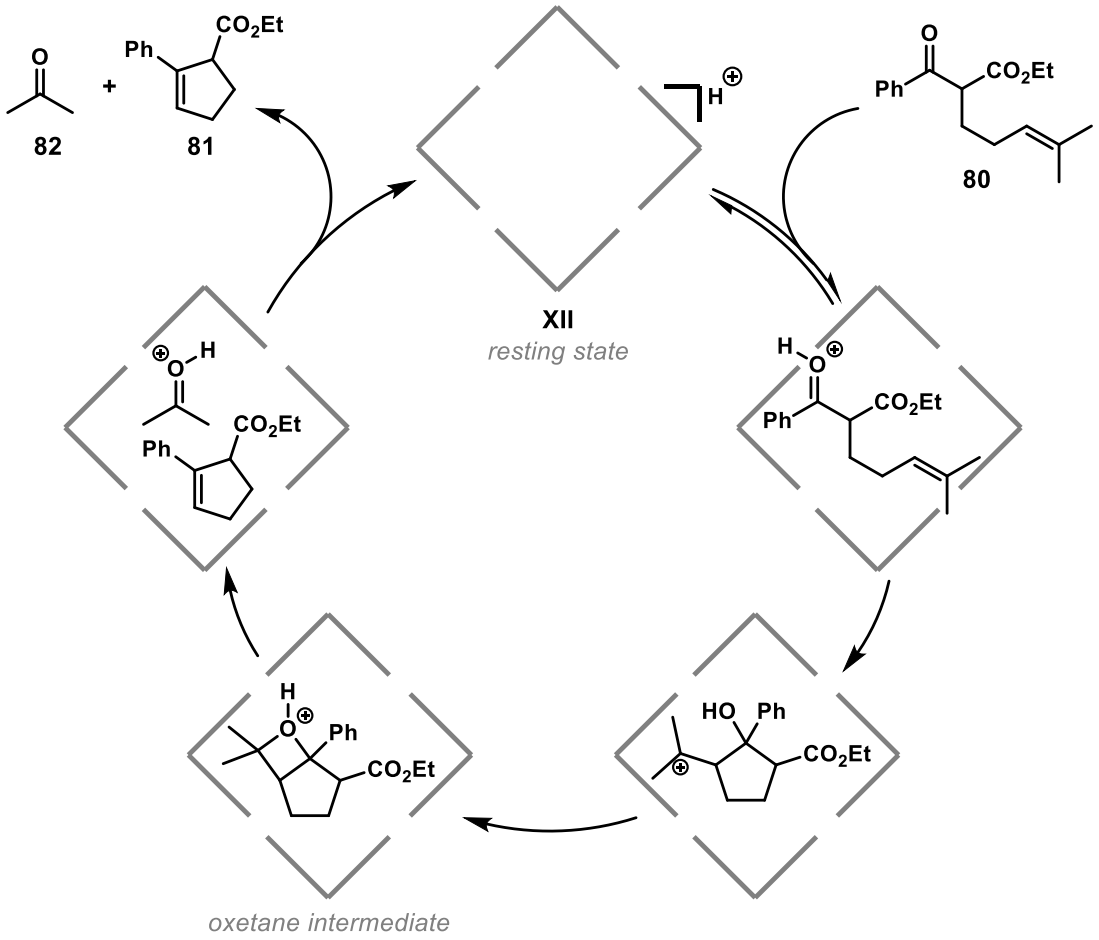

Figure 24. Catalytic cycle for the carbonyl-olefin metathesis of substrate **80** in presence of capsule **XII**.

After encapsulation of substrate **80** the aryl ketone is activated for a nucleophilic attack *via* protonation by host **XII** (protonated by the cocatalyst HCl). The alkene moiety then attacks the carbonyl carbon atom intramolecularly, leading to the formation of a cyclopentane core. The residual cation, situated at the isopropyl substituent, is intercepted by the alcohol newly formed from the former carbonyl group, forming a bicyclic oxetane intermediate. Cycloreversion of the oxetane formation releases the cyclopentene product **81** and protonated acetone (**82**).

The reaction has been shown to give increased yields compared with SCHINDLER's method, highlighting the potential of supramolecular chemistry for challenging transformations.

Other examples of catalytic processes facilitated by capsule **XII** investigated by TIEFENBACHER *et al.* include the intramolecular hydroalkoxylation of alkenes,[74] a cyclodehydration-rearrangement cascade,[75] and the cavity-assisted reversal/amplification of enantioselective iminium catalysis.[76]

Recently, the laboratory of NERI published further reactions catalyzed by hexameric host **XII**: a [2+3]-dipolar cycloaddition between nitrones and unsaturated aldehydes,[77] and the conjugate addition of pyrroles to nitroalkenes.[78] Additionally, a mild procedure for the activation of benzyl chlorides for Friedel-Crafts alkylations was disclosed,[79] and further expanded for the use of water as solvent.[80] Quantum chemical investigations hinted at the formation of a hydrogen bond from a water molecule of the hydrogen bond network of assembly **XII** to the chlorine atom of the substrate as the likely source of activation in this reaction, paving the way for further reactions exploiting this pathway.

Pursuing the exceptional activities and selectivities displayed by enzymes, supramolecular catalysts aim to mimic their catalytically active pockets, showing great promise in catalytic applications and leading to novel products previously inaccessible to classical synthetic methods. The "non-stop" cyclization of acyclic monoterpenes catalyzed by the hexameric capsule **XII** serves as an impressive first step towards the ultimate goal of outperforming enzymes, however, many constrictions have yet to be overcome. Catalytic efficiency in biologically relevant reactions, expressed in the ratio of k_{cat}/k_{uncat}, is up to ten orders of magnitude higher for enzymes.[81] Furthermore, most reactions published so far are intramolecular conversions and of limited synthetic relevance. In order to compete with enzymatic systems on equal terms, the prerequisites for catalytic activity need to be fully understood, to then harness that knowledge for the design of more selective supramolecular hosts.[82] Finally, to become more relevant to the synthetic community, efforts are under way to develop optically active assemblies for enantioselective catalysis.

2 Objective of this Thesis

The hexameric assembly **XII** has been shown to catalyze a wide variety of reactions so far, ranging from [2+3]-cycloadditions to complex terpene cyclizations. However, its role in the respective catalytic processes, has not been fully characterized yet.

During detailed studies on the terpene cyclization, we discovered that residual traces of hydrochloric acid in solution, generated by photolysis of the solvent chloroform, were essential for catalytic activity.[68b] This thesis sets out to investigate whether the presence of HCl is essential for other reactions catalyzed by capsule **XII** as well.

Additionally, this thesis aims to elucidate the reaction mechanism and scope of the defluorination of benzyl and tertiary alkyl fluorides observed in presence of capsule **XII**. This reaction is known to be catalyzed by strong BRØNSTED and LEWIS acids, however, the mild conditions inside the cavity may offer new synthetic possibilities.

Furthermore, the formal carbonyl-isocyanide metathesis reaction, in which electron-deficient benzaldehydes react with isocyanides to form imines under release of carbon monoxide shall be investigated in detail.

3 Results and Discussion

3.1 Publication summaries

The following pages of this chapter function as a short summary of the publications that were prepared during the course of this dissertation.

3.1.1 Elucidating the Importance of Hydrochloric Acid as a Cocatalyst for Resorcinarene-Capsule-catalyzed reactions[83]

A detailed study of the terpene cyclization reaction revealed the presence of traces of hydrochloric acid (generated by photolysis of the solvent chloroform) was essential for catalytic turnover with capsule **XII**. Since this factor had not been considered in earlier examples of catalysis, we set out to test which reactions required the presence of this cocatalyst to facilitate the published transformations.

To this end, we reviewed all examples of catalysis by capsule **XII** and selected nine reactions to investigate in greater detail. These include the [2+3]-cycloaddition reactions, the hydration of isocyanides and of alkynes respectively, and the oxidation of sulfides, published by the group of SCARSO. From the group of TIEFENBACHER we selected the hydrolysis of acetals, the hydroalkoxylation, the cyclodehydration-rearrangement cascade, and the terpene cyclization as examples for further investigation (see table 1).

The hydrolysis of acetals, the terpene cyclization, and the intramolecular hydroalkoxylation were found to be highly dependent upon the presence of HCl as cocatalyst. The hydrolysis of acetaldehyde diethyl acetal (**83**) only required the addition of 0.1 mol% HCl to reproduce the published results, underlining the interplay of capsule **XII** and the cocatalyst at minuscule amounts. In presence of only one of either components the published reactivity could not be reproduced. The cyclodehydration-rearrangement cascade was found to be catalyzed solely by **XII**, however, the addition of HCl accelerated the reaction noticeably, doubling the yield.

Table 1. Overview of reactions investigated including yields obtained. Reactions were performed in triplicate and standard deviations were determined; all reactions were performed in $CDCl_3$ filtered through basic Al_2O_3 to remove acid traces and with 10 mol% of capsule **XII**; Additives: A – no additives; B – 3 mol% HCl added; C – literature inhibition conditions (TBAB or $TEABF_4$); D – literature inhibition conditions (TBAB or $TEABF_4$) and 3 mol% HCl added.

#	reaction	A	B	C	D
1	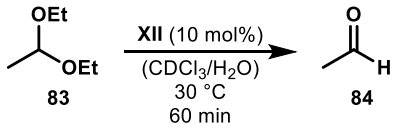	0 ± 1	**86 ± 5**[a]	0[b]	0[a,b]
2	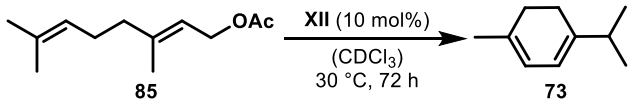	0	**27 ± 3**	0[b]	0[b]
3	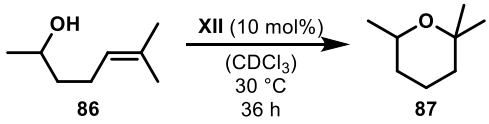	0	**95 ± 2**	0[b]	7 ± 2[b]
4	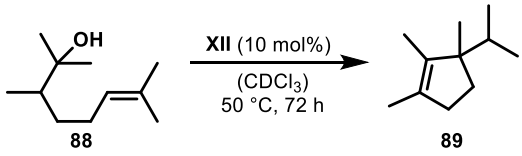	32 ± 1	**65 ± 1**	0[b]	3 ± 2[b]
5	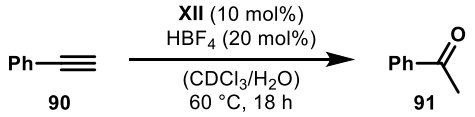	81 ± 3	79 ± 3 acid HBF_4 is present in all cases	2 ± 0[c]	12 ± 5[c]
6	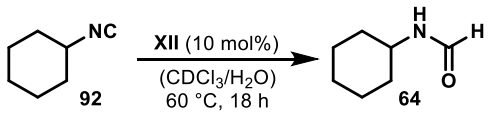	95 ± 4	95 ± 1	13 ± 0[c]	14 ± 1[c]
7	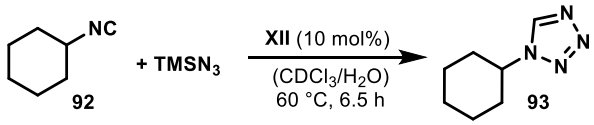	90 ± 4	92 ± 5	43 ±1[c]	41 ± 1[c]
8	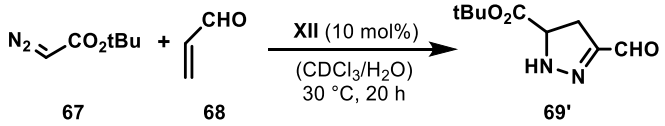	93 ± 2	90 ± 1	0[c]	0[c]
9	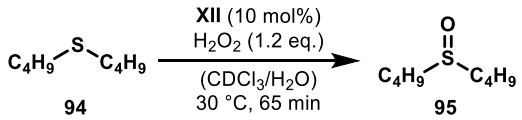	92 ± 1	94 ± 1	70 ±1[c]	70 ± 0[c]

[a]0.1 mol% HCl added [b]1.5 eq.TBAB added [c]10 eq. $TEABF_4$ added

The reactions published by SCARSO *et al.* were shown to not rely on the presence of the cocatalyst HCl except for the hydration of alkynes and isocyanides. The alkyne hydration was shown beforehand to depend on the presence of a strong BRØNSTED acid cocatalyst, HBF_4, which was added in 20 mol%. The hydration of isocyanides was presumed to proceed *via* initial protonation of the terminal carbon atom and subsequent nucleophilic attack of water to form the respective *N*-formamide. However, the findings from this work suggest a different mechanism may be at work.

3.1.2 Activation of primary and secondary benzylic and tertiary alkyl (sp^3)C-F bonds inside a self-assembled molecular container[84]

Alkyl fluorides, long believed to be inert due to the high energy of the C-F bond (105.4 kcal/mol, for comparison C-H 98.8 kcal/mol), were shown to be activated by strong BRØNSTED or LEWIS acids under harsh conditions. We set out to investigate whether the hexameric capsule **XII** could serve as a mild alternative. Initial studies suggested that tertiary alkyl fluorides were activated in presence of the hexamer at 40 °C in otherwise acid-free conditions. We then set out to determine the scope and limitation of this process, learning that primary and secondary alkyl fluorides remain inert but that primary and secondary alkyl fluorides were prone to activation under reaction conditions.

Table 2. Substrate overview with yields; product denominations: a – alcohol, e – cyclic ether, i – internal alkene, t - terminal alkene; all reactions run in filtered $CDCl_3$ at 40 °C in presence of 10 mol% of capsule **XII**.

entry	substrate	products	background
1	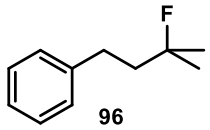 **96**	**96i** 69%[a] (16 h) **96t** 13%[a]	0[b] 0[c]
2	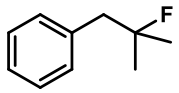 **97**	**97i** 45%[a] (16 h) **97a** 16%[a] **97t** 35%[a]	0[b] 0[c]
3	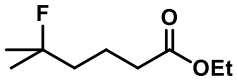 **98**	**98l** 60%[a] (20 h) 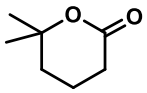 **98l** **98i** 29%[a] **98t** 3%[a]	0[b] 0[c]
4	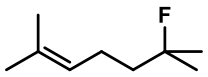 **99**	**99e** 81%[a] (21 h) 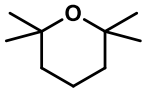 **99e** **99i** 11%[a]	0[b] 0[c]
5	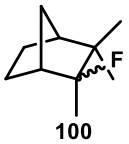 **100**	**100t** 98%[a] (2 h)	**100t** 98%[b] (20 h) 0[c]
6	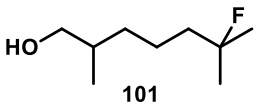 **101**	**101e** 72%[a] (4 h) 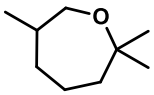 **101e**	**101e** 71%[b] (7d) 0[c]
7	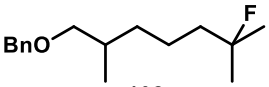 **102**	**102i** 65%[a] (4 h) **102t** 6%[a]	**102i** 5%[b] (7d) 0[c]
8	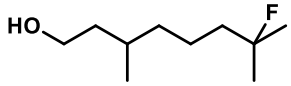 **103**	**103i** 60%[a] (4 h) **103t** 6%[a] **103a** 16%[a]	**103i** 52%[b] (7d) **103t** 6%[b] **103a** 13%[a] 0[c]

all reactions run in $CDCl_3$ (filtered over basic Al_2O_3 prior to use) at 40 °C; [a] determined *via* ^1H NMR [b]addition of TBAB (1.5 eq. relative to capsule **XII**), reaction run for 7 d at 40 °C [c] addition of HOAc (10 mol%), no hexamer present, 7 d, 40 °C

In the absence of nucleophiles the main pathway observed was elimination, with the formation of higher substituted alkene products favored (see table 2). In presence of intramolecular nucleophiles (**98**, **101-103**) the formation of lactones and ethers could be observed. The activation of fluoroalkene **99** yielded cyclic ether **99e**, resulting from interception of the cation by water from either the interior of capsule **XII** or from the hydrogen bond network of the supramolecular assembly itself. Kinetic studies revealed a sigmoidal reaction progress, indicative of an

autocatalytic process. Control reactions with HF, however, showed only sluggish conversion of alkyl fluorides, which points to HF assuming the role of cocatalyst for hexamer **XII** (see fig. 25).

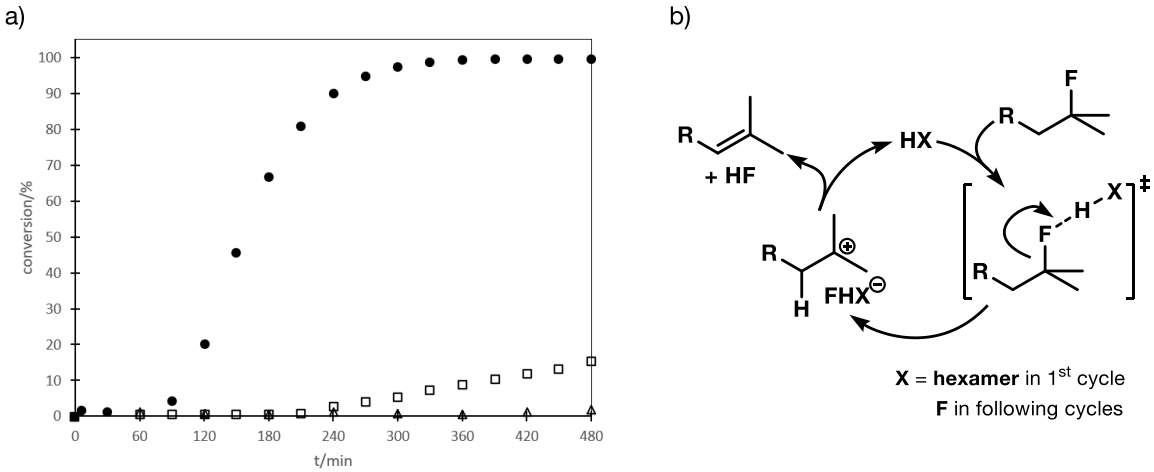

Figure 25. a) Reaction profile of the consumption of fluoride **96** in presence of capsule **XII** at 30 °C (□), 40 °C (●), 10 mol% HF in absence of **XII** (Δ), b) mechanistic proposal for the activation of alkyl fluorides catalyzed by capsule **XII**.

Furthermore, these findings indicate that the main mode of activation of C-F bonds by **XII** is by hydrogen bonding from the supramolecular hydrogen bond network, thereby establishing that the resorcin[4]arene-based assembly is able to catalyze reactions either *via* its inherent BRØNSTED acidity or by hydrogen bonding. Kinetic studies with deuterated **96** pointed towards the abstraction of the fluoride as rate-determining.

Additionally, experiments with primary and secondary benzyl fluorides in presence of host **XII** and suitable arene nucleophiles showed the formation of FRIEDEL-CRAFTS benzylation products (see scheme 12).

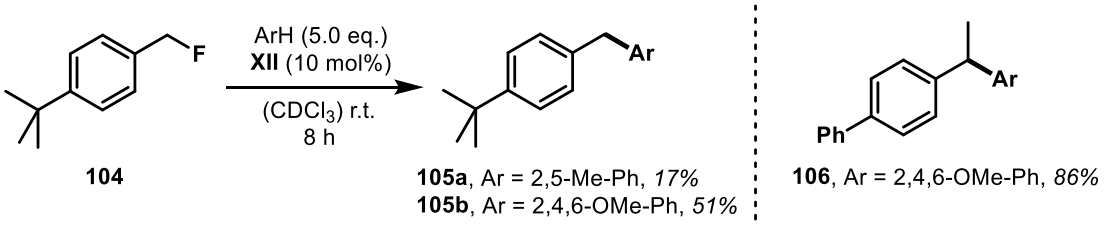

Scheme 12. FRIEDEL-CRAFTS benzylation of arene nucleophiles with primary benzyl fluoride **104** and formation of product **106** from a secondary benzylic fluoride.

3.2 Unusual Reactivity of Isocyanides with Aromatic Aldehydes within a Self-Assembled Capsule

3.2.1 Results and Discussion

This work was performed in collaboration with the SCARSO group and is currently being prepared for publication.

Supramolecular catalysis has received increasing attention in the last decades not only for the impressive substrate and product selectivities these systems achieve, but also for opening up new modes of catalysis.[16, 85],[26, 42e, 73, 79, 84, 86] Resorcin[4]arene (**60b**, Fig. 26a), which self-assembles in apolar solvents (chloroform, benzene) to form hexameric capsule **XII** (fig. 27b),[55, 87] is a highly versatile system and has been used as a nanometer-sized reaction chamber as well as a catalyst itself.[59, 64, 67-68, 75-76, 88] It incorporates eight molecules of water, which serve to connect the subunits in a network of 60 hydrogen bonds.[54, 89]

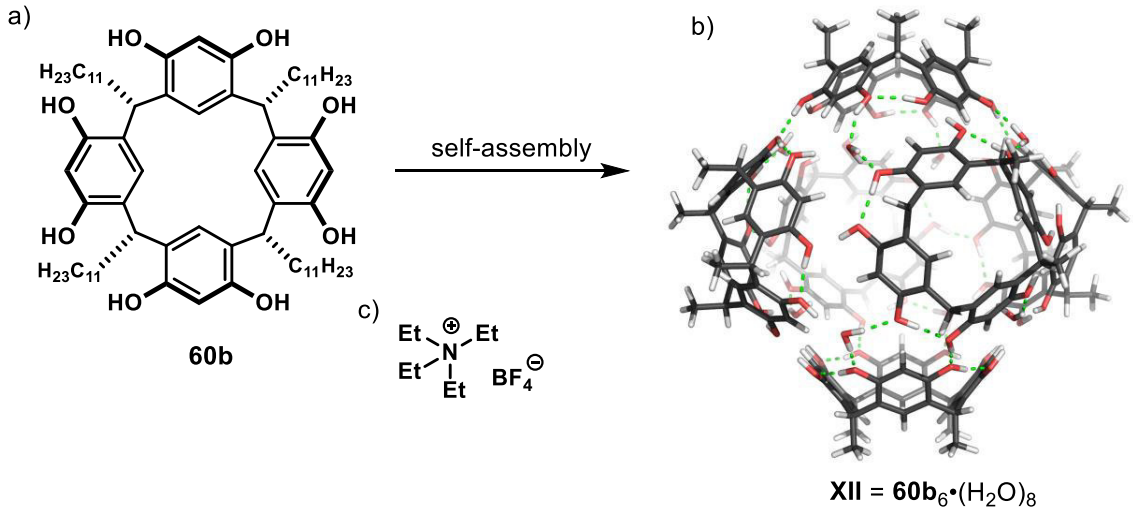

Figure 26. Resorcin[4]arene **62b** (a) self-assembles in apolar solvents to form hexamer **XII** (b), high affinity guest tetraethylammonium tetrafluoroborate ($TEABF_4$, c).

Its interior cavity comprises a volume of roughly 1400 Å³ and readily encapsulates small tetraalkylammonium cations thanks to its electron rich internal surfaces.[57] Encapsulation occurs *via* a portal mechanism, during which one of the subunits diffuses away from the dynamic assembly to expose the interior cavity to the bulk solution. After entry of a guest molecule a subunit

approaches from the solution and closes the assembly again.[45] Guest release and exchange proceed in likewise fashion.

Isocyanides have been shown to be suitable guests for capsule **XII**, which are also being activated for attack by nucleophiles such as water,[60] and azides, [62] inside the supramolecular assembly. They are of enormous synthetic interest due to the unique properties of the carbon atom in the isocyanide moiety which can behave as either an electrophile or a nucleophile.[90] The most well-known reactions involving isocyanides are the PASSERINI and UGI multicomponent reactions,[91] in which these versatile molecules react with carbonyl compounds and carboxylic acids (and amines) to give α-acyloxy amides, or bis-amides respectively. These reactions incorporate the full isocyanide moiety into the product structure.

Herein we present the reaction of isocyanides with electron-poor benzaldehydes promoted by capsule **XII**, leading to the formation of imines (see scheme 13). To the best of our knowledge, this reaction is without precedent in the literature.

Scheme 13. Reaction between isocyanide **107** and benzaldehyde **108**, catalyzed by capsule **XII**, leading to the formation of imine **109**.

Based on earlier findings,[60, 62] the reaction of isocyanide **107** with aldehydes was investigated in presence of capsule **XII**. The reaction with electron-poor benzaldehyde **108** yielded an unexpected product, an imine containing one carbon less than the expected structure. This immediately sparked enormous interest to gain further insight into this novel reaction and efforts to optimize reaction conditions were made. It was found that running the reaction at 50 °C in acid-free chloroform (filtered through basic Al_2O_3) with 10 mol% of capsule **XII** (13.3 M) at an isocyanide/aldehyde ratio of 2/1 gave a total yield of 46% of imine **109**. The formation of imine **109** was confirmed by ^{1}H-NMR as well as GC-MS. Control reactions were performed to identify the role of capsule **XII** in this reaction (see table 3).

Table 3. Control experiments for the reaction between 4-Nitrobenzaldehyde (**108**) and isocyanide **107**.

#	I	Additive	Yield [%][a]
1	-	-	-
2	+	-	46
3	-	HOAc (10 mol%)	-
4	-	*n*-Hex-resorcinol (24 eq.)	-
5	+	$TEABF_4$ (10 eq.)	7

[**107**]= 266 mM, [**XII**]= 13.3 mM, [**108**]= 133 mM, 0.5 mL $CDCl_3$-w, 50 °C, 24 h,
+: presence; -: absence; [a]determined by ^{1}H-NMR spectroscopy.

In the absence of **XII** no reaction was observed (see table 3, entry 1). Adding 10 mol% of acetic acid (comparable pK_a of 4.7, pK_a(**XII**) ~ 5.5)[67] failed to facilitate the formation of imines, indicating that the reaction is not catalyzed by the inherent BRØNSTED acidity of **XII** (entry 3). Running the reaction with 24 eq. of *n*-hexyl-resorcinol (comparable subunits of **XII**, which mimic its hydrogen bonding ability) also failed to produce the imine product (entry 4), pointing towards encapsulation and stabilization of intermediates as the possible mode of catalysis for capsule **XII**. This hypothesis was confirmed by the addition of 10 eq. of high-affinity guest $TEABF_4$ to the reaction (entry 5), which blocks the uptake of new guests and severely decreased the yield from 46 to 7%, highlighting the necessity for the interior of **XII** to be accessible in order for catalysis to occur.

The general applicability of the reaction was investigated with isocyanide **107** and a series of electron-poor benzaldehydes **110**-**120** (see fig. 27). Benzaldehydes containing electron-donating groups as well as aliphatic aldehydes containing protons in α-position did not show the desired reactivity (**117**-**120**). Furthermore, we explored the reaction of isocyanides **107, 121**-**126** with aldehyde **115** (see fig. 27). Sterically more demanding isocyanides did not lead to any reaction. Yields for all reactions ranged from 40-90%, with no reaction observed in the absence of

capsule **XII** and significantly lower yields after addition of high-affinity guest TBAB, confirming the necessity for an accessible interior cavity for catalysis.

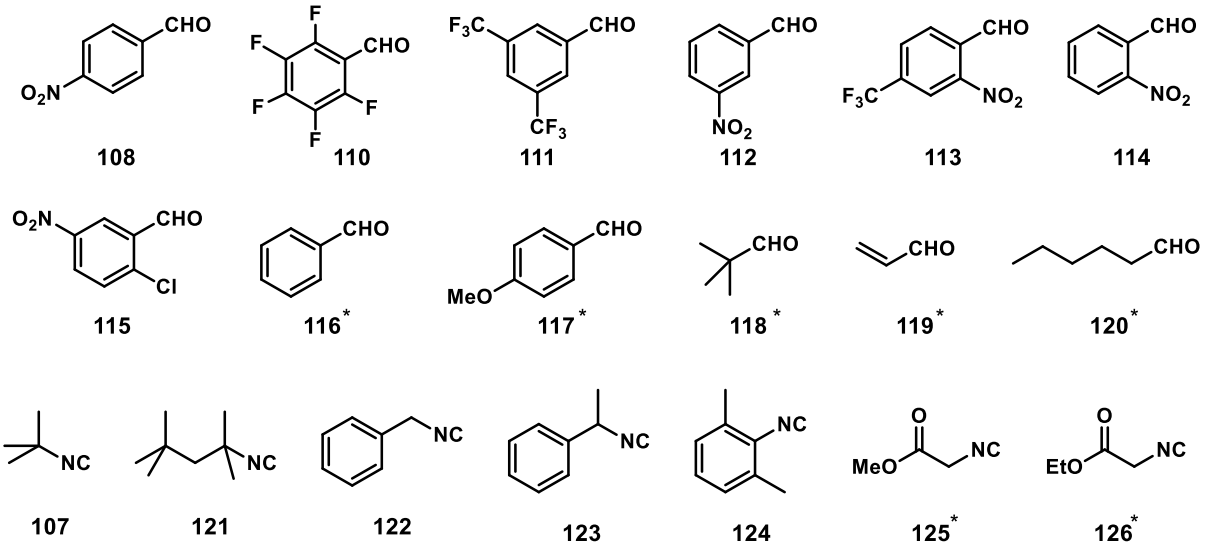

Figure 27. Scope and limitations of the observed reaction between isocyanides and electron-poor benzaldehydes, *no reaction observed

In order to investigate the mechanism of this reaction we prepared ^{13}C-labelled 1-adamantyl isocyanide (**127**, scheme 14) after a recent procedure and reacted it with aldehyde **115**.[92] The imine product resulting from this reaction was found to be unlabelled, indicating that the N-C bond of the isocyanide is cleaved in the process and carbon presumably released as carbon monoxide. This hypothesis was confirmed in a different setup by the detection of carbon monoxide.

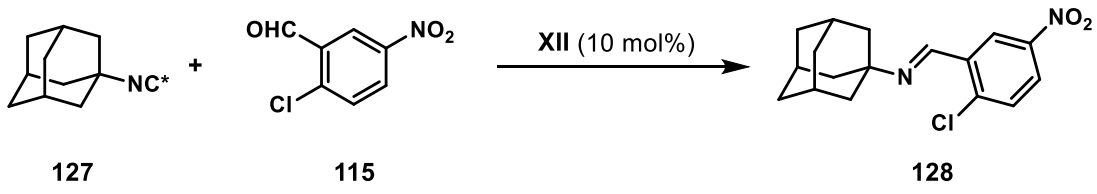

Scheme 14. Reaction of ^{13}C-labelled isocyanide **127** with aldehyde **115** leading to the formation of unlabelled imine **128** and carbon monoxide (not monitored in this reaction).

There is very little precedent in the literature covering the cleavage of the N-C bond of isocyanides,[93] so we set out to determine the kinetics of the reaction between isocyanide **107** and aldehyde **108** to gain more insight, which proved to be challenging due to the ready hydrolysis of the imine products by capsule **XII**. The results indicate first order kinetics for isocyanide, aldehyde, and capsule, respectively. Calculations based on these results pointed towards two possible mechanistic pathways (see fig. 28):

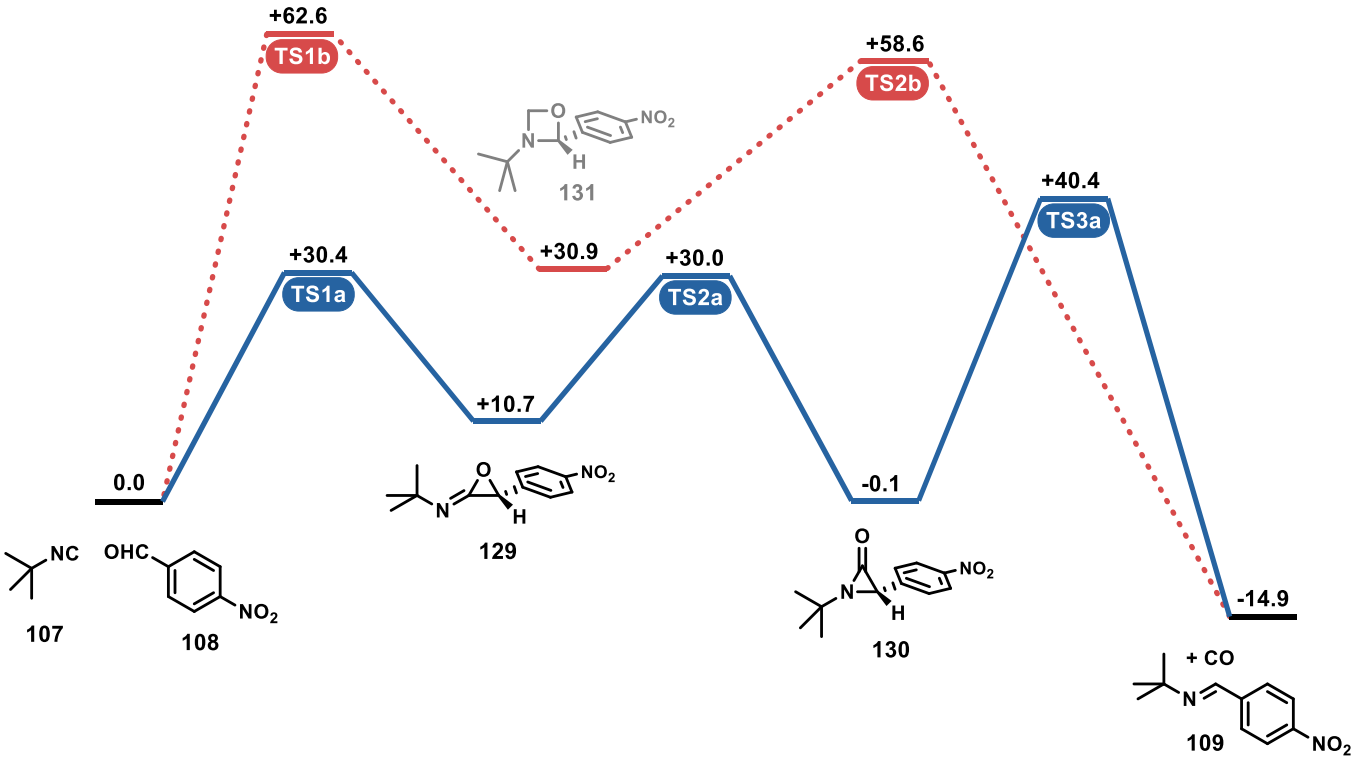

Figure 28. Energy profiles for the proposed mechanisms *via* formation of iminooxirane **129** (pathway **a**, blue) or oxazetidine **131** (pathway **b**, red), relative energies given in kcal/mol.

Pathway **a** (blue) proceeds *via* formation of iminooxirane **129**, which rapidly isomerizes to aziridinone **130**.[94] The α-lactam **130** then decomposes to imine **109** and carbon monoxide with a relatively high activation barrier of 40.5 kcal/mol, identifying this step as likely rate-determining. In pathway **b** (red) oxazetidine **131** is formed in a concerted fashion with a very high activation barrier of 62.6 kcal/mol. The four-membered intermediate **131** then undergoes a metathesis-like decomposition to imine **109** and carbon monoxide with a much lower activation barrier of 27.7 kcal/mol, indicating that the formation of **131** would be rate-determining in this pathway.

The thermal decomposition of aziridinones to either carbonyl compounds and isocyanides (major pathway) or imines and carbon monoxide (minor pathway) was published by SHEEHAN *et al.* in 1968.[95] The iminooxirane intermediate, suspected to be the missing link in this process, was detected spectroscopically in a later study, lending further credibility to this pathway for the reaction.[94] For pathway **b** no precedent in the literature could be found. The lower activation barriers for pathway **a** (30.4 *vs.* 62.6 kcal/mol for the initial step) and the literature precedence for the rearrangement of the iminooxirane to the aziridinone indicate that the reaction is more likely to proceed through this mechanism. We therefore propose the following catalytic cycle for the reaction (see fig. 29):

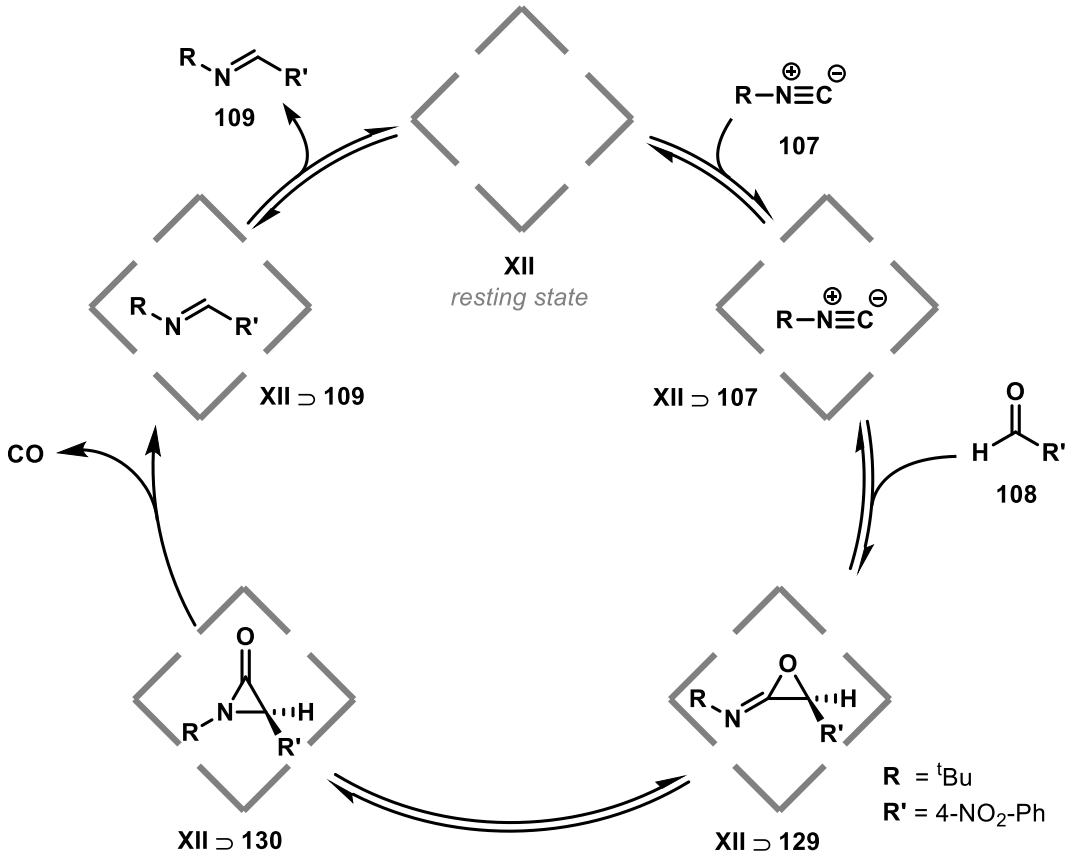

Figure 29. Proposed catalytic cycle for the formation of imine **109** from isocyanide **107** and electron-poor benzaldehyde **108**, catalyzed by capsule **XII**.

The "empty" capsule **XII** takes up one equivalent of isocyanide **107**, leading to the formation of host-guest complex **XII** ⊃ **107**. Upon encapsulation of aldehyde **108** (of much lower affinity to **XII** than isocyanide **107**) both components reversibly react to form iminooxirane **129**, either in a

concerted or a step-wise manner. Rapid isomerization leads to aziridinone **130**, which then decomposes to imine **109** and carbon monoxide.

In conclusion, we described an unprecedented reaction between isocyanides and electron-poor benzaldehydes catalyzed by the hexameric capsule **XII**. The reaction is likely catalyzed by encapsulation of the isocyanide and stabilization of the intermediate structures. Molecular dynamics simulations of the reaction led to a proposed a mechanism *via* formation of an iminooxirane, isomerization to an aziridinone, and collapse to an imine and carbon monoxide. Inhibition experiments with high-affinity ammonium guests confirm the reaction is catalyzed by the interior of the capsule.

3.2.2 Experimental details

3.2.2.1 General Information

Reactions were carried out under an atmosphere of argon unless otherwise indicated. Analytical thin-layer chromatography (TLC) was performed on *Merck* silica gel *60 F_{254}* glass-baked plates, which were analyzed under UV light (λ = 254 nm) or after exposure to standard staining reagents (basic $KMnO_4$ or CAM: cerium ammonium molybdate). All NMR experiments were performed on a *Bruker Avance Neo* spectrometer operating at 500 MHz. The instrument was equipped with a direct observe 5-mm *BBFO FB* probe with a self-shielded z-gradient. The experiments were performed at 323 K and the temperature was calibrated using a water standard showing accuracy within ± 0.2 K. Chemical shifts of ^{1}H NMR and ^{13}C NMR are given in ppm. The proton signal of the deuterated solvent was used as reference: $CDCl_3$ $\delta(^1H)$ = 7.26 ppm, $\delta(^{13}C)$ = 77.16 ppm; acetone $\delta(^1H)$ = 2.05 ppm. Coupling constants (*J*) are reported in Hertz (Hz). Standard abbreviations indicating multiplicity were used as follows: s (singlet), d (doublet), dd (doublet of doublets), m (multiplet). GC analyses were conducted on a *Shimadzu GC-2010 Plus* instrument equipped with a FID and a *Rtx-5* capillary column (length = 30.0 m). Hydrogen was used as carrier gas and constant-pressure mode (pressure = 106.9 kPa) with a split ratio of 1:20 was employed. The following temperature-program was used: 60 °C for 1 min, 15 °Cmin^{-1} to 250 °C, and 250 °C for 5 min. GC-MS analyses were performed on a *GC Trace* GC 2000 equipped with a HP5-MS column (30 m, I.D. 0.25 mm, film 0.25 μm) using He gas carrier and coupled with a quadrupole *MS Thermo Finnigan* Trace MS with *Full Scan* method.

Sources of chemicals: All solvents used for synthesis were purchased from *Sigma-Aldrich* and *Acros Organics* with the highest commercially available purity and employed without further treatment. All isocyanides and aldehydes were purchased from *Sigma-Aldrich* and *Alfa Aesar*. $CDCl_3$ (99.8%, stabilized with silver foil) and acetone-d_6 were purchased from *Cambridge Isotope Laboratories*. All imine products were identified by ^{1}H-NMR spectroscopy and GC-MS chromatography.

General: Transfer of liquids with a volume ranging from 1 to 10 µL or from 10 to 100 µL was performed with a *Microman M1* pipette (*Gilson*, systematic error: 1.40 – 1.60%) equipped with 10 or 100 µL pipette tips respectively. The weighing of substrates, catalyst, internal standard, and products was performed using a *AB135-S/Fact Mettler Toledo Classic Plus* balance.

3.2.2.2 Synthesis of *C*-Undecylcalix[4]resorcinarene (60b)

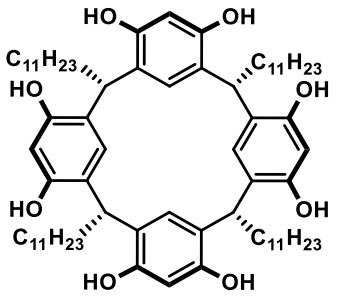

$C_{72}H_{112}O_8$
1105.68 g/mol

Resorcin[4]arene **60b** was synthesized according to a modified literature procedure.[96] To a stirred solution of 99.9% ethanol (270 mL) and 37% aqueous HCl (90 mL), resorcinol (70.9 g, 644 mmol, 1.0 eq.) was added. After complete dissolution and cooling to 0 °C, a solution of dodecanal (143 mL, 119 g, 644 mmol, 1.0 eq.) in 99.9% ethanol (180 mL) was added dropwise into the reaction mixture over the course of 40 min. The resulting solution was allowed to warm to r.t. and subsequently refluxed at 100 °C for 18 h. Upon cooling to r.t. a yellow precipitate formed from the dark red solution. The precipitate was dispersed in cold methanol, filtered, and subsequently washed with cold methanol until the washings were light yellow. The solid was recrystallized from methanol (150 mL). To remove remaining yellow impurities the solid was washed extensively with a mixture of methanol/water (50/50, 8 × 100 mL). The crystalline material was dried under reduced pressure (15 mbar) at 55 °C using a rotary evaporator. The drying process was continued until the residual methanol was completely removed. In order to obtain a satisfying water content the material was moistened with cold methanol, washed with water (8 × 100 mL), and dried under reduced pressure at 55 °C. Compound **60b** (109 g, 98.5 mmol, 61%) was obtained as a white to slightly yellowish powder. After dissolving **60b** (11.0 mg) in $CDCl_3$ (0.5 mL), a water content of 13.5 eq. H_2O/hexamer was determined *via* integration of the ^1H NMR spectrum. The spectroscopic data matched those reported in the literature.

3.2.2.3 Synthesis of products

Imine products were synthesized to fully identify products of the catalytic reactions from the respective aldehydes and amines according to a procedure by STAHL *et al.*[97]

N-tert-butyl-1-(4-nitrophenyl)methanimine (109)

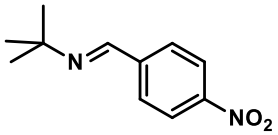

106

$C_{11}H_{14}N_2O_2$
206.1055 g/mol

^{1}H NMR (500 MHz, $CDCl_3$): δ[ppm] = 8.33 (s, 1H), 8.26 (d, ^3J = 8.8 Hz, 2H), 7.92 (d, ^3J = 8.7 Hz, 2H), 1.32 (s, 9H).

^{13}C NMR (151 MHz, $CDCl_3$): δ[ppm]: 153.1, 148.9, 142.8, 128.7, 123.9, 58.4, 29.6.

N-tert-butyl-1-(perfluorophenyl)methanimine (132)

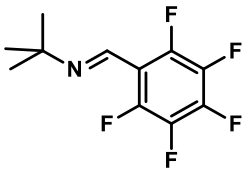

129

$C_{11}H_{10}F_5N$
251.0733 g/mol

^{1}H NMR (300 MHz, $CDCl_3$): δ[ppm] = 8.32 (s, 1H), 1.30 (s, 9H).

1-(3,5-bis(trifluoromethyl)phenyl)-*N*-(*tert*-butyl)methanimine (133)

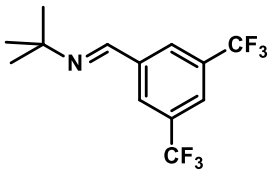

130

$C_{13}H_{13}F_6N$
297.0952 g/mol

^{1}H NMR (300 MHz, $CDCl_3$): δ[ppm] = 8.35 (s, 1H), 8.24 (s, 2H), 8.05 (s, 1H), 1.28 (s, 9H).

***N-tert*-butyl-1-(3-nitrophenyl)methanimine (134)**

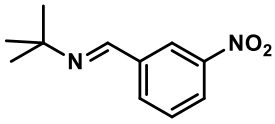

$C_{11}H_{14}N_2O_2$
206.1055 g/mol

131

^{1}H NMR (300 MHz, $CDCl_3$): δ[ppm] = 8.60 (s, 1H), 8.34 (s, 1H), 8.10 (d, ^3J =7.6 Hz ,1H), 7.80 (d, ^3J = 7.9 Hz, 1H), 7.58 (m, 1H), 1.25 (s, 9H).

***N-tert*-butyl-1-(2-nitro-4-(trifluoromethyl)phenyl)methanimine (135)**

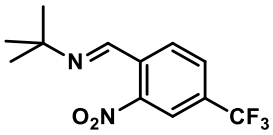

$C_{12}H_{13}F_3N_2O_2$
274.0929 g/mol

132

^{1}H NMR (300 MHz, $CDCl_3$): δ[ppm] = 8.70 (s, 1H), 8.31 (s, 1H), 8.22 (d, ^3J = 8.0 Hz ,1H), 7.91 (d, ^3J = 8.1 Hz, 1H), 1.33 (s, 9H).

***N-tert*-butyl-1-(2-nitrophenyl)methanimine (136)**

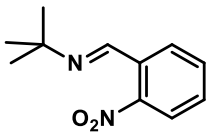

$C_{11}H_{14}N_2O_2$
206.1055 g/mol

133

^{1}H NMR (300 MHz, $CDCl_3$): δ[ppm] = 8.68 (s, 1H), 8.28 (d, ^3J = 12.5 Hz, 1H), 7.97 (d, ^3J = 8.3 Hz, 1H), 7.78 (m, 2H), 1.27 (s, 9H).

***N-tert*-butyl-1-(2-chloro-5-nitrophenyl)methanimine (137)**

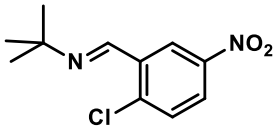

$C_{11}H_{13}ClN_2O_2$
240.0666 g/mol

134

^{1}H NMR (300 MHz, $CDCl_3$): δ[ppm] = 8.78 (d, ^3J = 2.8 Hz, 1H), 8.67 (s, 1H), 8.19 (d, ^3J = 2.8 Hz, 1H), 8.16 (d, ^3J = 2.8 Hz, 1H), 1.31 (s, 9H).

1-(2-chloro-5-nitrophenyl)-*N*-(2,4,4-trimethylpentan-2-yl)methanimine (138)

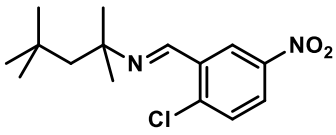

$C_{15}H_{21}ClN_2O_2$
296.1292 g/mol

135

^{1}H NMR (400 MHz, $CDCl_3$): δ[ppm] = 8.82 (d, ^3J = 2.8 Hz, 1H), 8.56 (s, 1H), 8.08 (dd, ^3J = 8.8, 2.8 Hz, 1H), 7.54 (d, ^3J = 8.8 Hz, 1H), 1.67 (s, 2H), 1.29 (s, 6H), 0.89 (s, 9H).

^{13}C NMR (100 MHz, $CDCl_3$) δ[ppm] = 149.61, 130.89, 125,62, 123.52, 62.60, 56.56, 31.91, 29.72.

***N*-benzyl-1-(2-chloro-5-nitrophenyl)methanimine (139)**

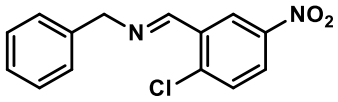

$C_{14}H_{11}ClN_2O_2$
274.0509 g/mol

136

^{1}H NMR (300 MHz, $CDCl_3$): δ[ppm] = 9.29 (s, 1H), 8.97 (d, ^3J = 2.8 Hz, 1H), 8.51 (d, ^3J = 2.7 Hz, 1H), 8.20 (dd, ^3J = 8.8, 2.8 Hz, 1H), 7.38 (m, 5H), 4.90 (m, 2H).

1-(2-chloro-5-nitrophenyl)-*N*-(1-phenylethyl)methanimine (140)

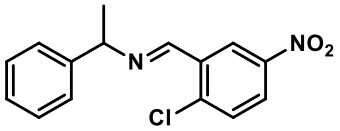

$C_{15}H_{13}ClN_2O_2$
288.0666 g/mol

137

^{1}H NMR (300 MHz, $CDCl_3$): δ[ppm] = 9.00 (d, ^3J = 2.6 Hz, 1H), 8.82 (s, 1H), 8.61 (d, ^3J = 2.6 Hz, 1H), 8.48 (d, ^3J = 2.4 Hz, 1H), 7.48 (m, 5H), 4.70 (dd, ^3J = 13.1 Hz, ^4J = 6.5 Hz, 1H), 1.65 (s, 3H).

1-(2-chloro-5-nitrophenyl)-*N*-(2,6-dimethylphenyl)methanimine (141)

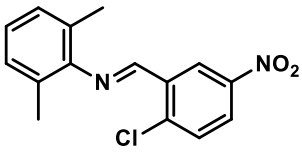

$C_{15}H_{13}ClN_2O_2$
288.0666 g/mol

138

^{1}H NMR (300 MHz, $CDCl_3$): δ[ppm] = 9.17 (d, ^3J = 2.8 Hz, 1H), 8.73 (s, 1H), 8.31 (d, ^{3}J = 2.9 Hz, 1H), 8.28 (d, ^3J = 2.8 Hz, 1H), 7.10 (m, 3H), 2.20 (s, 6H).

3.2.2.4 Determination of yields

General procedure (NMR analysis): Reactions in presence of capsule **XII** were conducted using stock solutions of *C*-Undecylcalix[4]resorcinarene in $CDCl_3$. Prior to usage, $CDCl_3$ was filtered through a basic Al_2O_3 plug (5-6 mL through 2-3 g Al_2O_3) to remove trace amounts of HCl/DCl, potentially generated by photodegradation of $CDCl_3$. The stock solution for *C*-Undecylcalix[4]resorcinarene was prepared by weighing in monomer (440 mg, 0.40 mmol) in a 1 mL volumetric flask, which was then filled to less than full capacity with filtered $CDCl_3$ and homogenized in an ultrasonic water bath. In case of incomplete dissolution, the flask was heated to approx. 40 °C with a heat gun under agitation. After complete dissolution, the flask was then filled to the calibration mark with filtered $CDCl_3$ and again agitated to give a clear yellow solution.

The stock solutions for isocyanides and aldehydes were prepared by weighing the respective starting materials into a GC vial and filling up with calculated amounts of filtered $CDCl_3$ to reach a final concentration of 1.33 M (isocyanide) and 0.67 M (aldehyde). The small contribution of the starting materials to the total volume of the stock solution was neglected. Isocyanides (100 µL, 1.33 mol/L, 133 µmol) and aldehydes (100 µL, 0.67 mol/L, 66.7 µmol) were added as stock solutions in filtered $CDCl_3$. In all cases the amount of added $CDCl_3$ was adjusted to maintain an overall volume of 500 µL.

Stock solutions of isocyanide (100 µL, 133 µmol, 20 eq.), aldehyde (100 µL, 66.7 µmol, 10 eq.), *C*-Undecylcalix[4]resorcinarene stock solution (100 µL, 40 µmol, 6.0 eq), and 200 µL of filtered $CDCl_3$ were added to a GC vial (1 mL size). Immediately upon mixing a small aliquot (20 µL) was taken from the reaction mixture and diluted with 0.5 mL of acetone-d_6 and subjected to ^{1}H-NMR spectroscopy. The GC vial was then kept at 50 °C (±1 °C) using a thermostated aluminum heating block. The progress of the reaction was monitored *via* ^{1}H NMR. For this purpose, the GC vials containing the reaction mixture were removed from the heating block and upon cooling to r.t. a small aliquot (20 µL) was taken, diluted with 0.5 mL of acetone-d_6 and subjected to NMR spectroscopy. The influence of the temperature drop during removal of aliquots was neglected. Further measurements were taken in the same fashion.

The yields were calculated by employing the following equations (3.1 – 3.3)

$$n(sm)_0 = \frac{(I_{sm})_0}{(I_{sm})_{0,exp}} = x \tag{3.1}$$

$$n(p)_n = \frac{(I_p)_n}{(I_p)_{n,exp}} = z \tag{3.2}$$

$$yield(p) = \frac{x}{z} * 100\% \tag{3.3}$$

$n(sm)_0$ = amount of starting material in the initial measurement; $(I_{sm})_0$ = integral of a suitable starting material signal in the initial measurement after normalizing an integral value of a hexamer **I** resonance (methine group = 24H); $(I_{sm})_{0,exp}$ = expected integral of the corresponding resonance assuming 10.0 eq. of starting material; $n(p)_n$ = amount of product in the n-th measurement (full conversion/equilibrium reached); $(I_p)_n$ = integral of a characteristic product resonance in the n-th measurement, after normalizing an integral value of a hexamer **I** resonance; $(I_p)_{n,exp}$ = expected integral of the corresponding resonance assuming complete and selective conversion of 10.0 eq. of substrate.

General procedure (GC analysis): After addition of all reactants as described above, a small aliquot (10 – 15 µL) was taken from the reaction mixture, diluted with heptane (900 µL, contains 0.08% vol. DMSO) and cooled to –20 °C for 20 minutes. Upon cooling and centrifugation, the catalyst precipitated and was removed. The samples were then subjected to GC analysis. This process was repeated for further measuring points. In order to precisely calculate the conversion and yield, response factors to *n*-decane as internal standard (IS) were determined for the investigated substrates and their corresponding products. Stock solutions of *n*-decane, substrates and products were prepared as described in table 4, utilizing filtered $CDCl_3$ as solvent. 40 µL aliquots of *n*-decane stock solution (242 mmol/L) were added to 25 µL, 50 µL or 100 µL aliquots of analyte (302 mmol/L) for 4-Nitrobenzaldehyde (**108**). For imine **109** 40 µL aliquots of *n*-decane stock solution were added to 13 µL, 25 µL, and 50 µL aliquots of analyte. After dilution with $CDCl_3$ to a total volume of 500 µL, analyte to *n*-decane ratios of 0.25, 0.5, 1, or 2 were obtained.

Table 4. Preparation of stock solutions.

compound	molar mass [g/mol]	pure compound	$CDCl_3$ [µL]
n-decane	142.29	5.68 mg	165
108	151.12	19.7 mg	430
109	206.11	8.81 mg	142

Approximately 10 µL of each sample was diluted with 0.1 mL heptane (contains 0.08% vol. DMSO) and subjected to GC analysis. The response factors were calculated according to equation 3.4 and are listed in table 5.

$$RF = \frac{(A_X \cdot C_{IS})}{(A_{IS} \cdot C_X)} \tag{3.4}$$

RF = response factor; A_X = GC area of analyte; A_{IS} = GC area of internal standard; C_X = concentration of analyte; C_{IS} = concentration of internal standard.

For GC analysis, conversions and yields were calculated by employing the following equations (3.5 - 3.8).

$$n(sm)_0 = \frac{(A_{sm})_0}{RF_{sm} \cdot (A_{IS})_n} = x \tag{3.5}$$

$$n(sm)_n = \frac{(A_{sm})_n}{RF_{sm} \cdot (A_{IS})_n} = y \tag{3.6}$$

$$conversion(sm) = \left(\frac{x - y}{x}\right) \cdot 100\% \tag{3.7}$$

$$n(p)_n = \frac{\left(A_p\right)_n}{RF_p \cdot (A_{IS})_n} = z \tag{3.8}$$

$n(sm)_n$ = amount of starting material in the n-th measurement; $(A_{sm})_0$ = area of starting material in the initial measurement; $(A_{IS})_0$ = area of internal standard in the initial measurement; $(A_{sm})_n$ = area of starting material in the n-th measurement; $(A_{IS})_n$ = area of internal standard in the n-th measurement; $(A_p)_n$ = area of product in the n-th measurement; RF_{sm} = response factor of starting material; RF_p = response factor of product;

Table 5. GC Response factors.

compound	C_X/C_{IS}	A_X/A_{IS}	RF	Ø
	0.5	0.31	0.63	
108	1	0.64	0.64	0.65
	2	1.37	0.68	
	0.25	0.32	1.30	
109	0.5	0.66	1.31	1.29
	1	1.27	1.27	

3.2.2.5 Unreactive Aldehydes

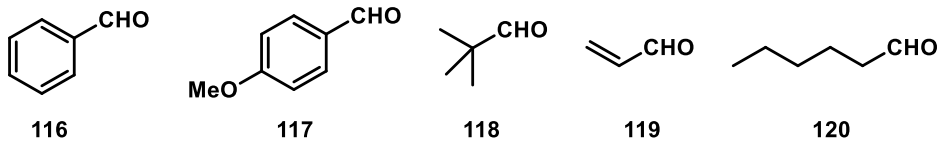

Figure 30. Aldehydes that did not show formation of imines with *tert*-butyl isocyanide (**107**).

Employing benzaldehydes with electron-donating groups (**117**) as well as the parent benzaldehyde (**116**) in the reaction with *tert*-butyl isocyanide (**107**) did not give any imine product under standard reaction conditions. The same holds true for aliphatic aldehydes with (**120**) and without protons in α-position (**118**) and with conjugated double bonds (**119**). This illustrates the necessity for benzaldehydes with electron-withdrawing substituents for the reaction to proceed.

3.2.2.6 Elucidation of reaction mechanism

Uptake studies

The uptake of isocyanide **107** and benzaldehyde **108** was investigated in ^{1}H-NMR studies (see fig. 31).

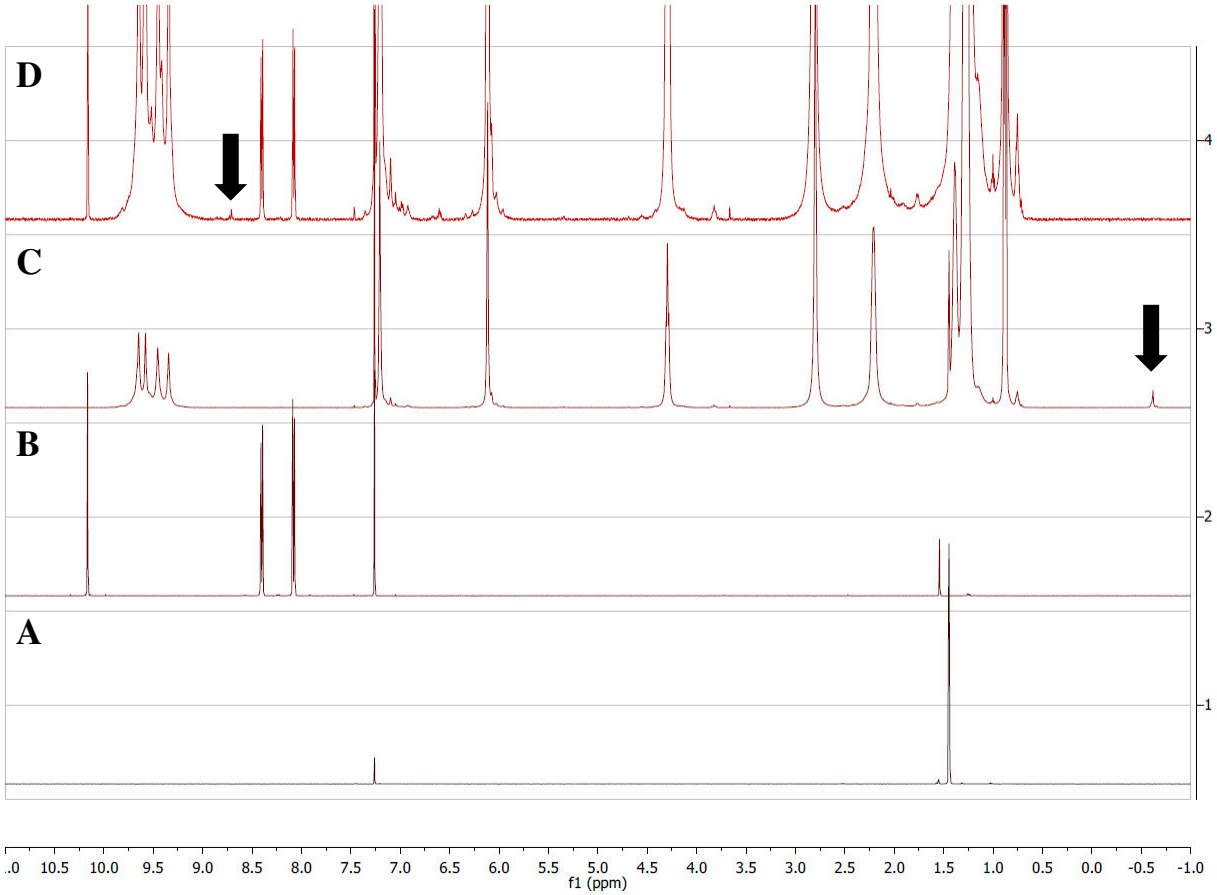

Figure 31. ^{1}H NMR spectra in $CDCl_3$: A) isocyanide **107** B) aldehyde **108** C) isocyanide **107** (1.0 eq.) and capsule **XII** D) aldehyde **108** (1 eq.) and capsule **XII**, ↓ - encapsulated substrate.

As seen in fig. 31, the isocyanide is readily taken up by the supramolecular host while the aldehyde shows negligible encapsulation. This points to the encapsulation of the isocyanide as a first step in a proposed mechanism.

3.2.2.7 ^{13}C-labelled substrates

The isotopically labelled substrate **127** was synthesized from 1-adamantanol and ^{13}C-labelled trimethylsilyl cyanide according to a procedure from KITANO *et al.*[92] It was then reacted with 2-Chloro-5-Nitrobenzaldehyde (**115**) in presence of 10 mol% of capsule **XII** at 60 °C (see scheme 15).

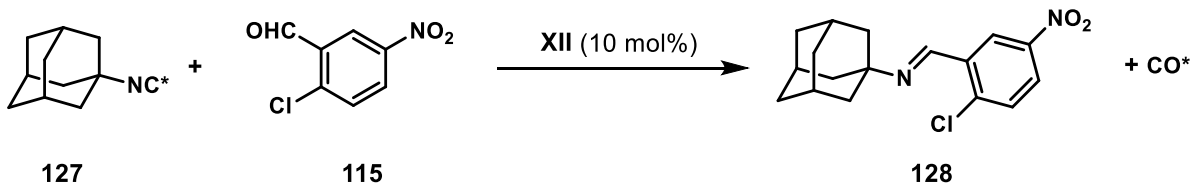

Scheme 15. Reaction of isotopically labelled isocyanide **127** and benzaldehyde **115** in presence of capsule **XII**.

After 24 h the formation of the corresponding imine product was confirmed *via* ^{1}H-NMR and GC-MS, giving the expected mass of 318 u for the imine, indicating that the ^{13}C-label was cleaved from the isocyanide during the reaction (see fig. 32).

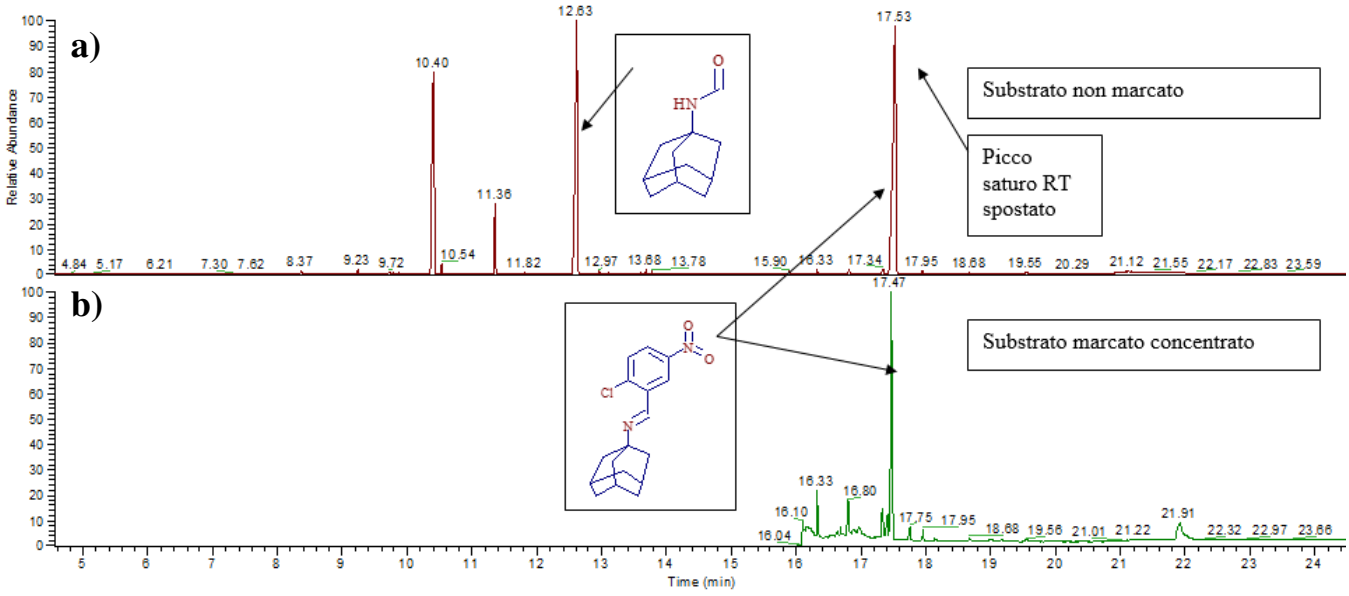

Figure 32. GC-MS trace of the reaction of a) unlabeled **127** with aldehyde **115** and b) of isotopically labeled **127** with **115**, confirming the formation of the unlabeled imine product **128**.

As is clearly visible from the GC-MS trace both cases show the formation of unlabeled imine product, along with non-negligible amounts of the *N*-Formyl amide, resulting from hydration of

the isocyanide substrate. To corroborate this finding the reaction was repeated with aldehyde **113**, leading to the formation of the unmarked imine product as well (see figure 33).

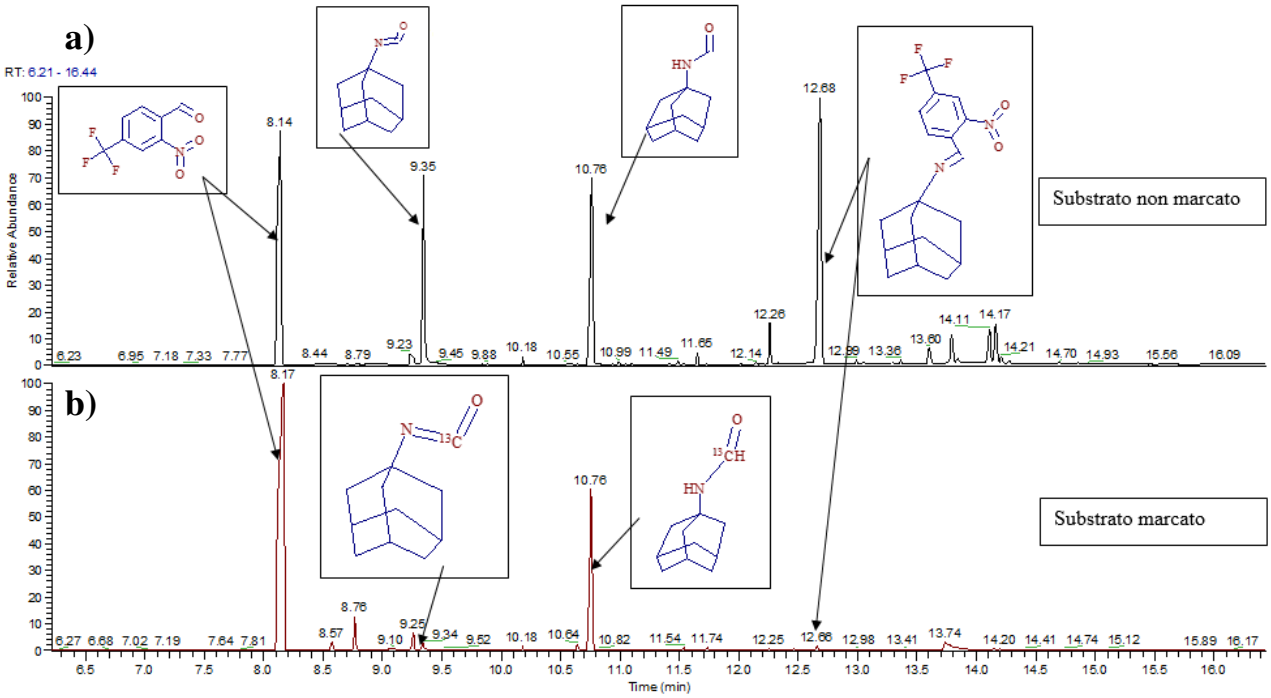

Figure 33. GC-MS trace of the reaction of a) unlabeled isocyanide **127** with benzaldehyde **113** and b) of labeled **127** with **113** each in presence of 10 mol% of capsule **XII**.

As observed before, in both reactions (with unlabeled and labeled isocyanide **127**) the formation of the unlabeled imine product was observed. This is a strong indication that the N-C bond of the isocyanide is cleaved during the reaction, presumably to form carbon monoxide.

3.2.2.8 Detection of carbon monoxide

The reaction between 4-Nitrobenzaldehyde (**108**) and *tert*-butyl isocyanide (**107**) in presence of catalytic amounts of C-Undecylcalixresorcin[4]arene (**60b**) was carried out on larger scale (1.3 mmol of isocyanide) overnight at 50 °C in a Schlenk flask (see figure 34). After 16 h reaction time the stopcock of the flask was opened and the overhead volume in the flask was blown towards an *Industrial Scientific MX4 iQuad* gas detector with the help of an argon balloon attached to the flask. Readings of the gas detector confirmed the formation of carbon monoxide from the reaction mixture. Multiple control experiments were conducted successfully to exclude the possibility of the detector being triggered by *tert*-butyl isocyanide, a problem encountered in detection attempts using a different method.[98] The formation of carbon monoxide during the course of this reaction could be confirmed with a high degree of certainty.

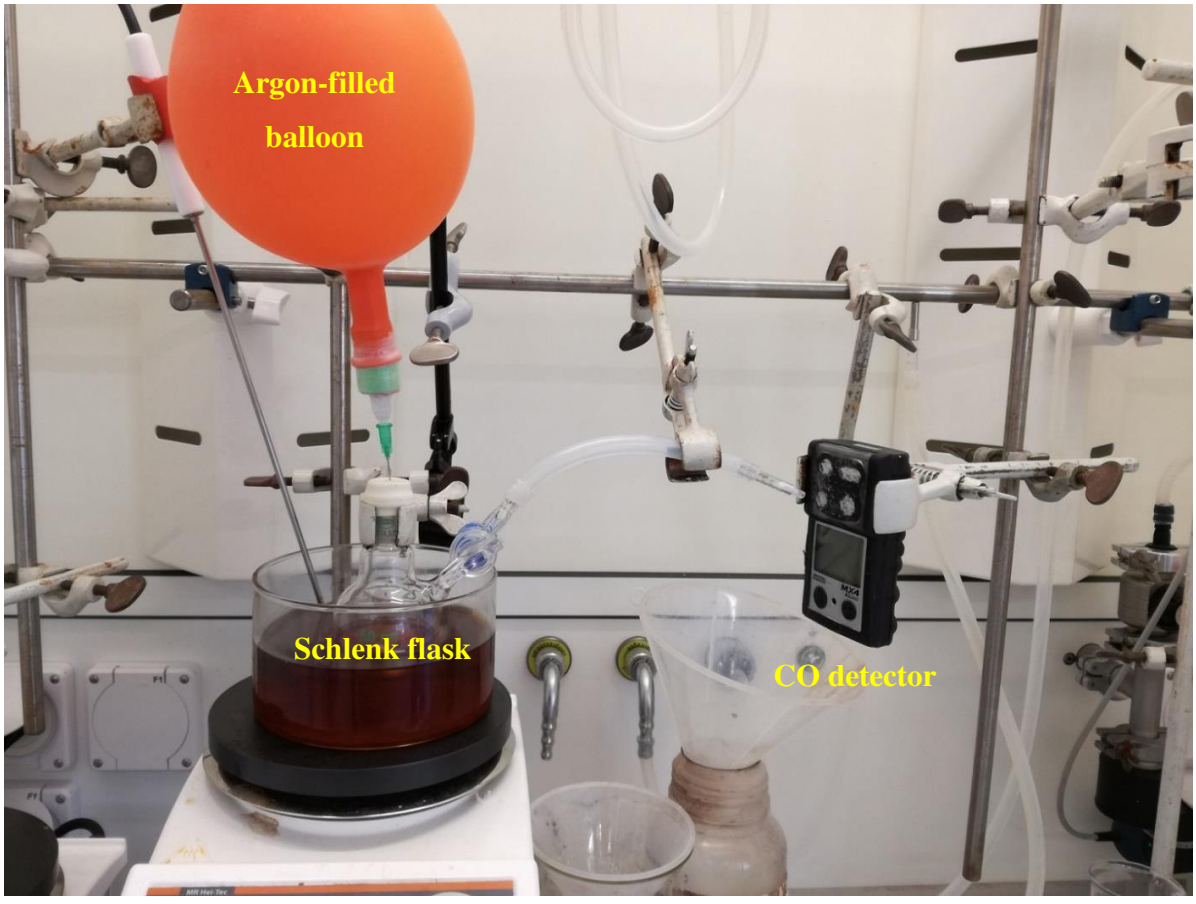

Figure 34. Reaction setup for the detection of carbon monoxide using an electronic gas detector.

3.2.2.9 Kinetic measurements

Hydrolysis of imine products

Low yields observed after prolonged reaction times coupled with a known lability of imines towards acidic reaction conditions led to the hypothesis that most of the imine product was rapidly hydrolyzed upon formation inside capsule **XII**. To test this hypothesis, imine **109** was synthesized and added to capsule **XII** under standard reaction conditions (10 mol% **XII**, 50 °C, filtered $CDCl_3$). The concentration was monitored *via* GC (see fig. 35). The graph shows rapid hydrolysis regardless of the starting concentration and reaches a plateau afterwards. Starting from 1 eq. of imine **109**, after 1 h approximately 10% of the initial concentration remained, at 10 eq. approx. 55% remained.

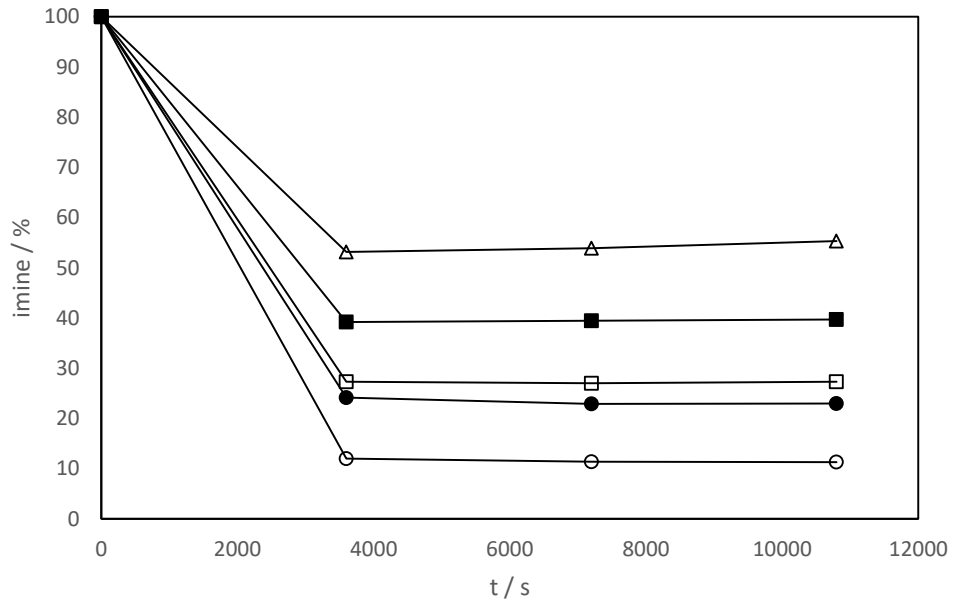

Figure 35. Hydrolysis of imine **109** under reaction conditions (10 mol% capsule **XII**, 50 °C, filtered $CDCl_3$) at different starting concentrations of **109** (○- 1 eq, ● - 2 eq., □ - 3 eq., ■ - 5 eq., Δ - 10 eq.).

Another control experiment was conducted to mimic the steady formation of imine **109** under reaction conditions. One equivalent of **109** was added to the reaction mixture, which was then left to equilibrate for 15 min at 50 °C. Samples were taken immediately after addition of **109** and after 15 min (see fig. 36).

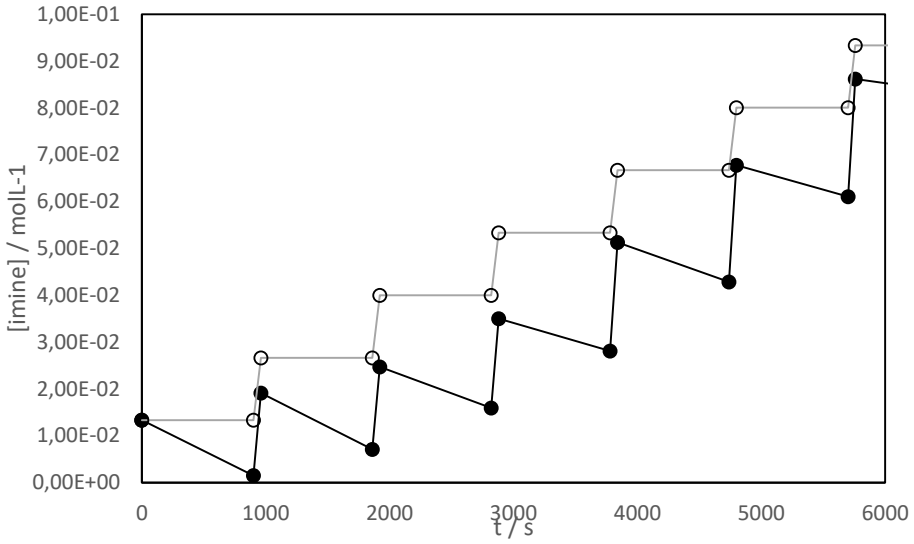

Figure 36. Hydrolysis of imine **109** under standard reaction conditions (10 mol% **XII**, 50 °C, filtered $CDCl_3$); steps mark addition of 1 eq. of **109** to the reaction mixture (● – measured concentration, ○ – theoretical concentration).

As observed before, rapid hydrolysis of the imine occurs within 15 min after addition. This holds true for the addition of up to 7 eq. of **109**, after which the gap between measured and theoretical concentration closes. This indicates a saturation of capsule **XII** with hydrolysis products, namely *tert*-butyl amine, which is likely protonated (earlier findings showed the protonation and subsequent encapsulation of amine bases, *e.g.* NEt_3).[67]

Control reactions with the additive *tert*-butyl amine showed a considerably slower formation of the imine product under standard conditions after 24 h (yield reduced by 43%).

Determination of reaction order

Kinetic measurements were conducted to determine the reaction order of all components to gain insight into the reaction mechanism.

$$rate = -\frac{d[sm]}{dt} = \frac{d[P]}{dt} \tag{3.9}$$

$$rate = k \cdot [aldehyde]^m \cdot [isocyanide]^n \cdot [capsule]^o \tag{3.10}$$

$$\ln(rate) = m \cdot \ln[aldehyde] + n \cdot \ln[isocyanide] + o \cdot \ln[capsule] + \ln k \tag{3.11}$$

sm = starting material; P = product

In accordance with eq. 3.9 – 3.11, the reaction order (m, n, and o respectively) can be obtained by plotting the rates of the reaction against the initial concentration of the respective components on a logarithmic scale. To determine the reaction order, for example, of the aldehyde, both the concentrations of isocyanide and capsule need to remain constant. This is achieved by employing a large excess of isocyanide (10 eq. relative to aldehyde). Capsule **XII** acts as a catalyst, its concentration therefore remains constant over the course of the reaction.

Analyzing the reaction is challenging, not the least because the isocyanide cannot not be reliably monitored *via* ^{1}H NMR nor GC. The monitoring of the imine product was found to give the most reliable data, since the consumption of the aldehyde starting material suffers from side reactions.

Table 6. Initial rates for the reaction of aldehyde **108** and isocyanide **107** under standard reaction conditions (10 mol% capsule **XII**, 50 °C, filtered $CDCl_3$).

	c_0	rate [L/mol^{-1}s^{-1}]	R^2
[**107**] = *const.* 0.334 mol/L	0.0167	$2.07 \cdot 10^{-7}$	0.9753
	0.0334	$2.83 \cdot 10^{-7}$	0.9785
	0.0667	$3.47 \cdot 10^{-7}$	0.9939
[**108**] = *const.* 0.334 mol/L	0.0334	$1.38 \cdot 10^{-7}$	0.9994
	0.0667	$2.42 \cdot 10^{-7}$	0.9988
	0.1334	$3.45 \cdot 10^{-7}$	0.9945

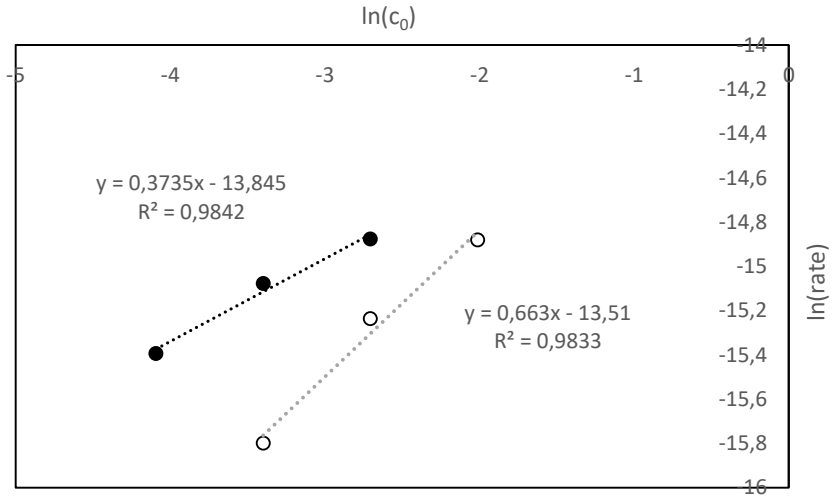

Figure 37. Logarithmic plot of initial concentration of aldehyde **108** *vs.* reaction rate (●, determined *via* imine **109**) and of initial concentration of isocyanide **107** vs. reaction rate (○).

Both plots show a positive slope, indicating a reaction order of >0. However, the slopes are not clean values, possibly influenced by side reactions influencing the accuracy of the measurements (hydrolysis of imine, side reaction of aldehyde). These values therefore only serve as an indication for the final reaction order.

Furthermore, measurements at different loadings of catalyst **XII** were taken and plotted against the initial concentration of **XII** (see fig. 38).

Table 7. Initial rates for the reaction of aldehyde **108** and isocyanide **107** under standard reaction conditions at different loadings of catalyst **XII** (50 °C, filtered $CDCl_3$).

	c_0[a]	rate [L/mol^{-1}s^{-1}]	R^2
[**107**] = *const.*	0.0033	$2.61 \cdot 10^{-7}$	0.9735
0.267 mol/L	0.0067	$3.21 \cdot 10^{-7}$	0.9714
[**108**] = const.	0.0100	$3.39 \cdot 10^{-7}$	0.9695
0.133 mol/L	0.0133	$3.54 \cdot 10^{-7}$	0.9726

[a]initial concentration of catalyst **XII**

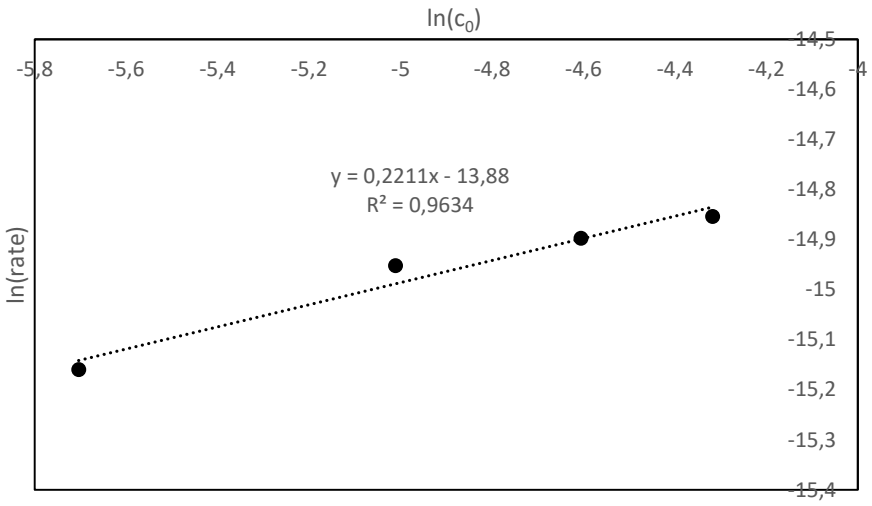

Figure 38. Logarithmic plot of initial concentration of catalyst **XII** *vs.* reaction rate (●).

3.2.2.10 Calculations

Table 8. Computed energies (B3LYP/6-31G*-GD3BJ) for starting materials, transition states, and intermediates for the formation of imine **109** from isocyanide **107** and electron-poor benzaldehyde **108**. [a]free energy (B3LYP/6-31G*-GD3BJ) [b]relative electronic energy with respect to the starting materials **107** and **108**, kcal/mol.

Species	Gibbs B3LYP energies[a]	Profile $E_{rel.}$[b]
107 + **108**	– 800.607570	0.0
TS1a	– 800.559066	+ 30.4
129	– 800.591244	+ 10.2
TS2a	– 800.559703	+ 30.0
130	– 800.607804	– 0.1
TS3a	– 800.543167	+ 40.4
109 + CO	– 800.631331	– 14.9
TS1b	– 800.507869	+ 62.6
131	– 800.558355	+ 30.9
TS2b	– 800.514170	+ 58.6

3.2.2.11 Spectra

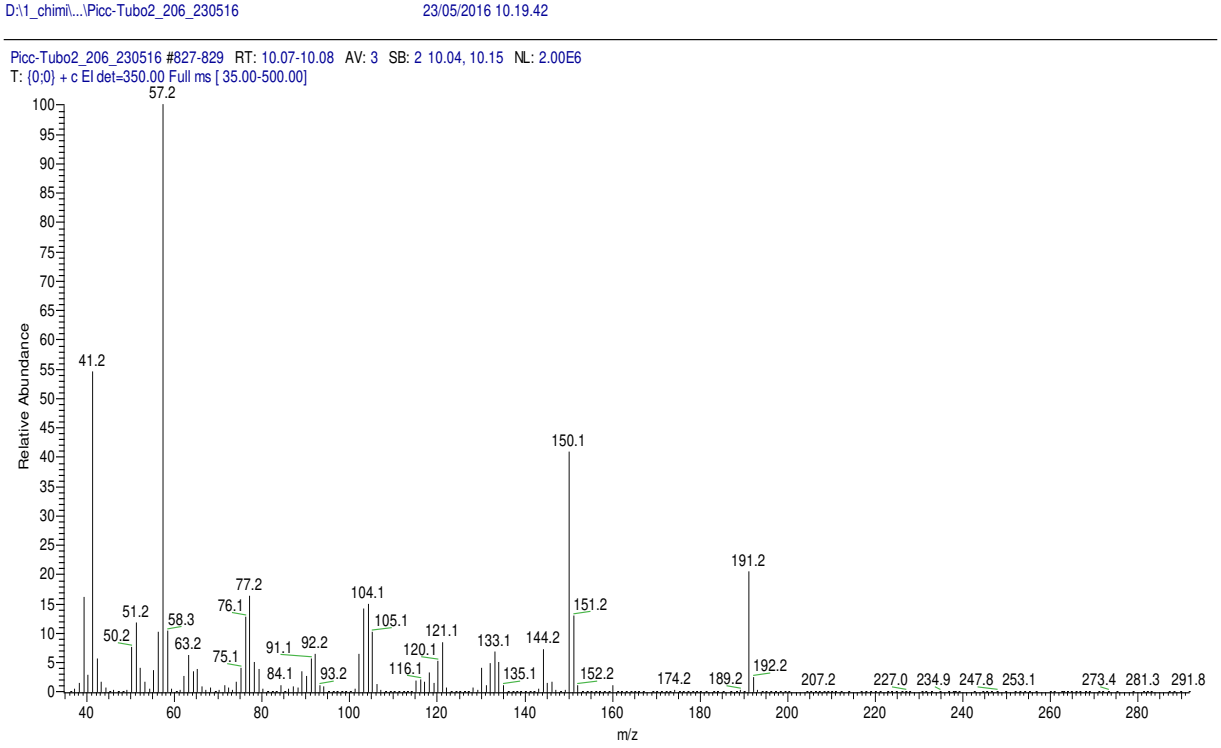

Figure 39. Mass spectrum of imine **109**.

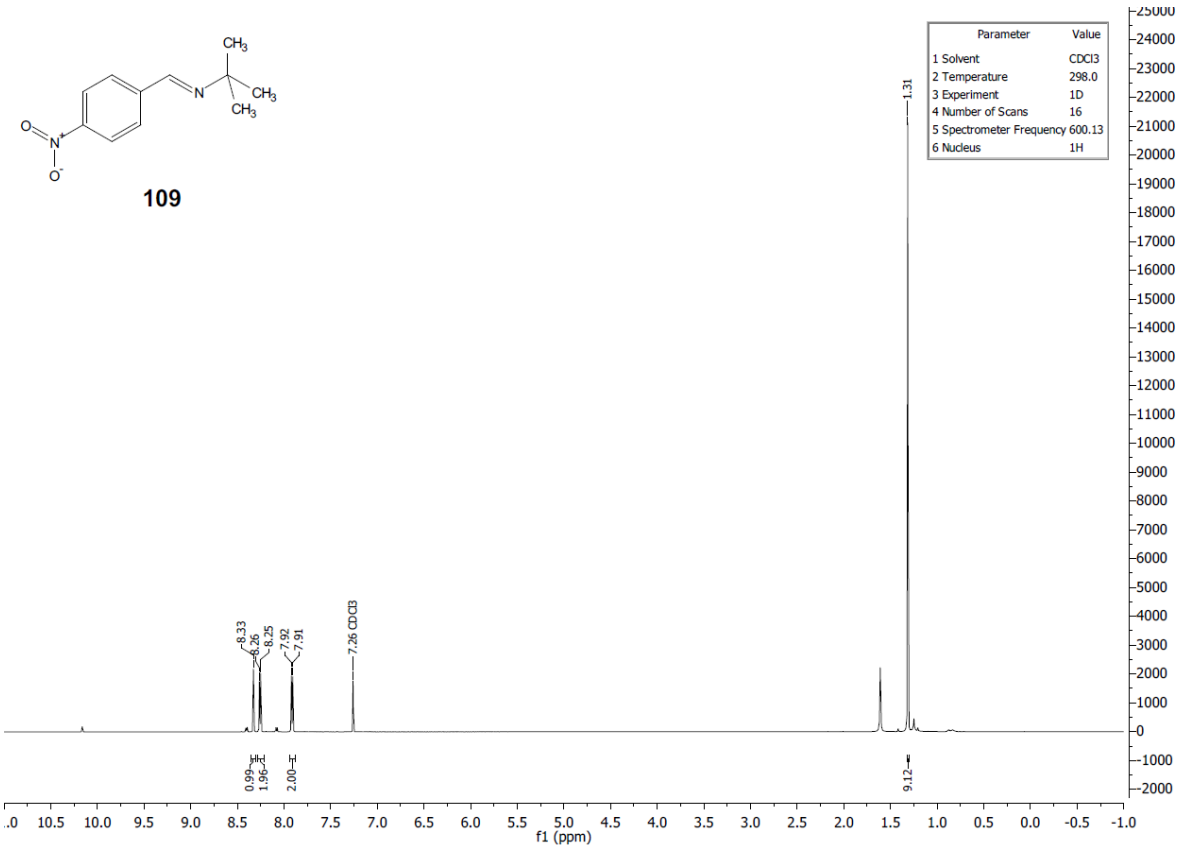

Figure 40. ^{1}H-NMR spectrum of imine **109** in deuterated chloroform.

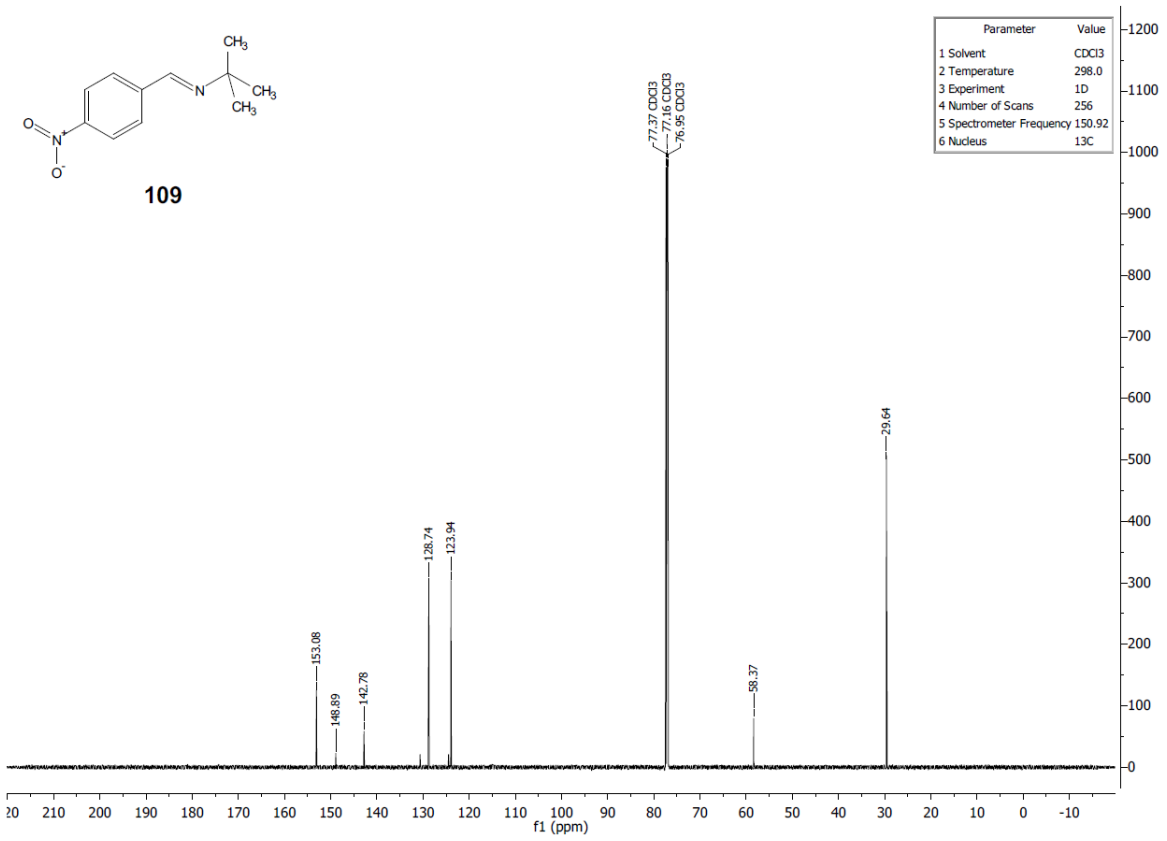

Figure 41. 13C-NMR spectrum of imine **109** in deuterated chloroform.

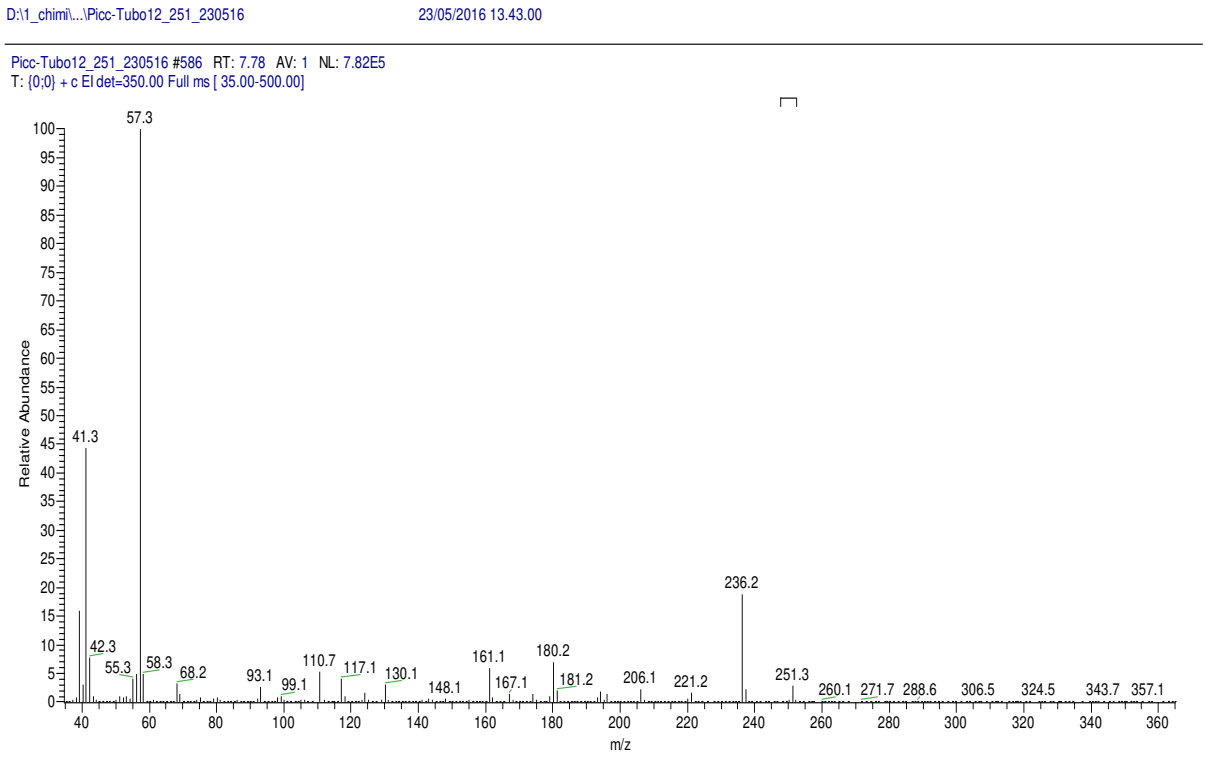

Figure 42. Mass spectrum of pentafluoroimine **132**.

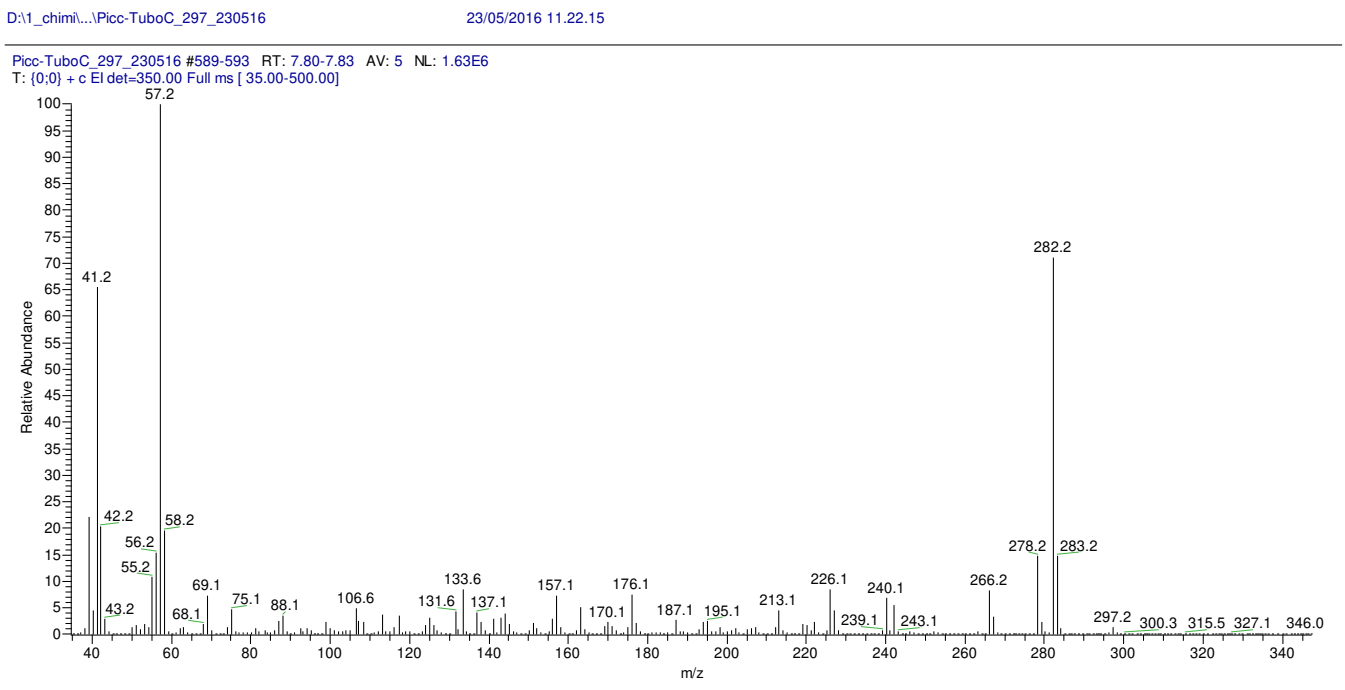

Figure 43. Mass spectrum of 3,5-bis(CF_3) imine **133**.

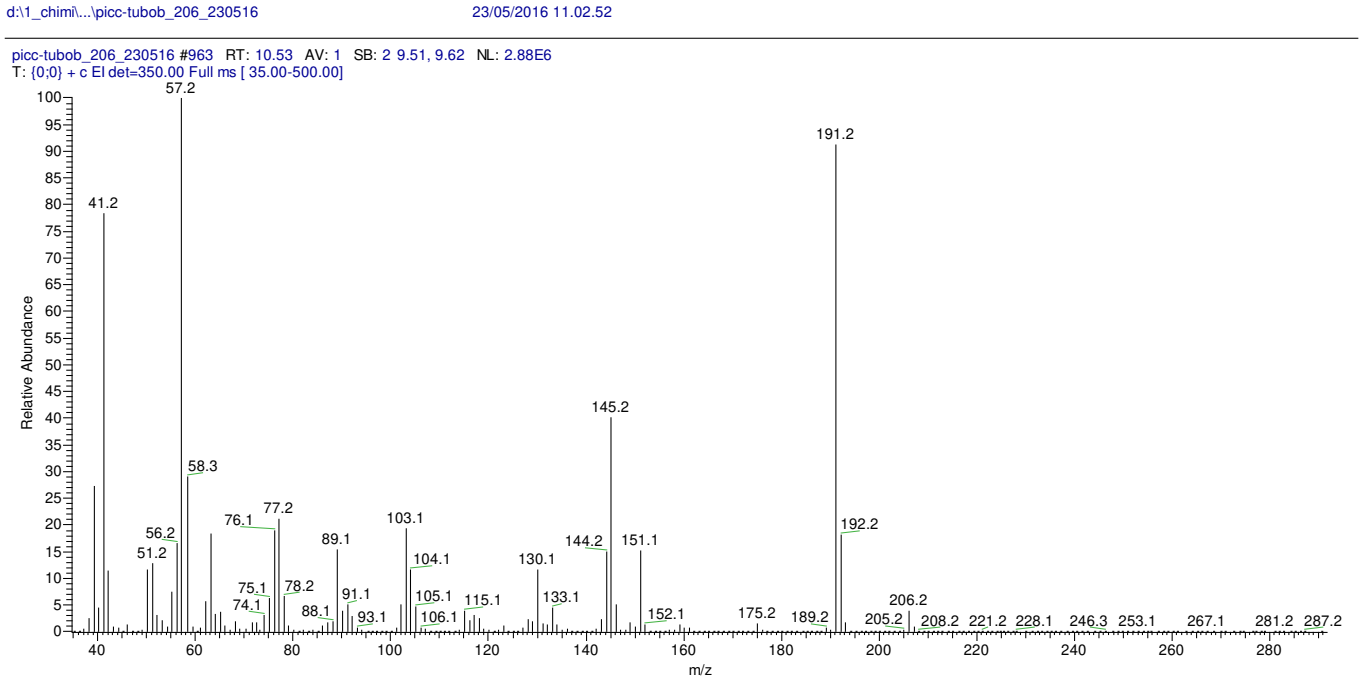

Figure 44. Mass spectrum of *m*-NO_2 imine **134**.

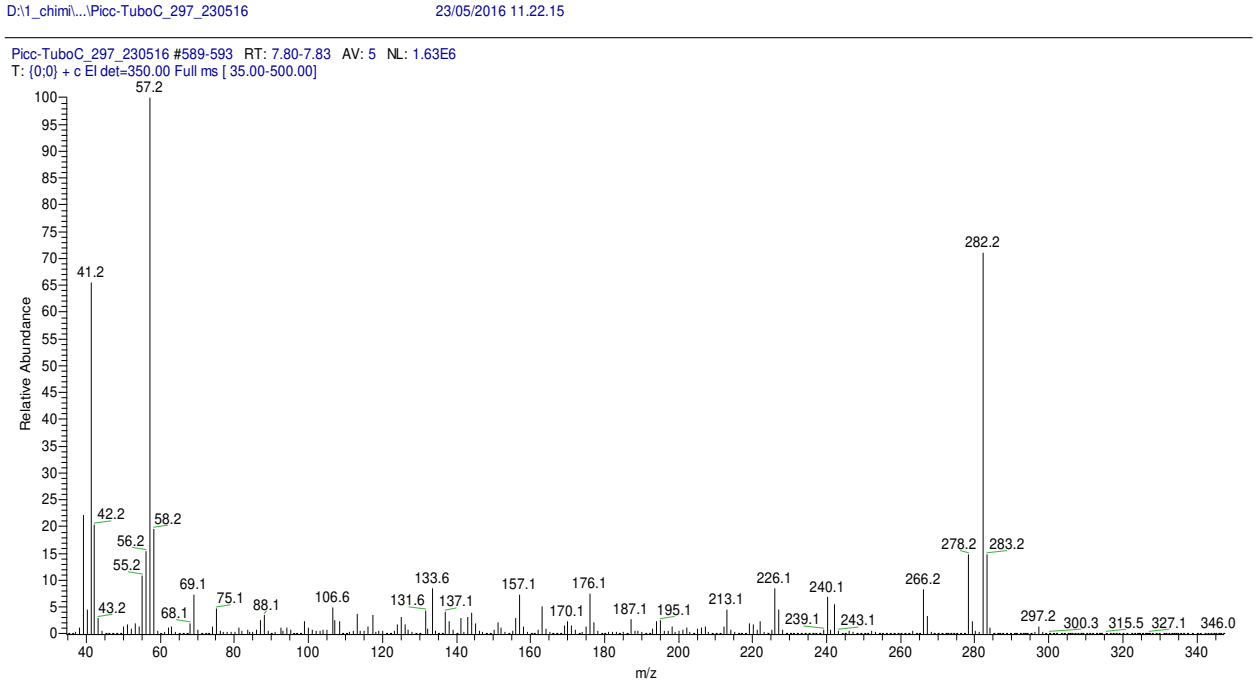

Figure 45. Mass spectrum of *o*-NO_2-*p*-CF_3 imine **135**.

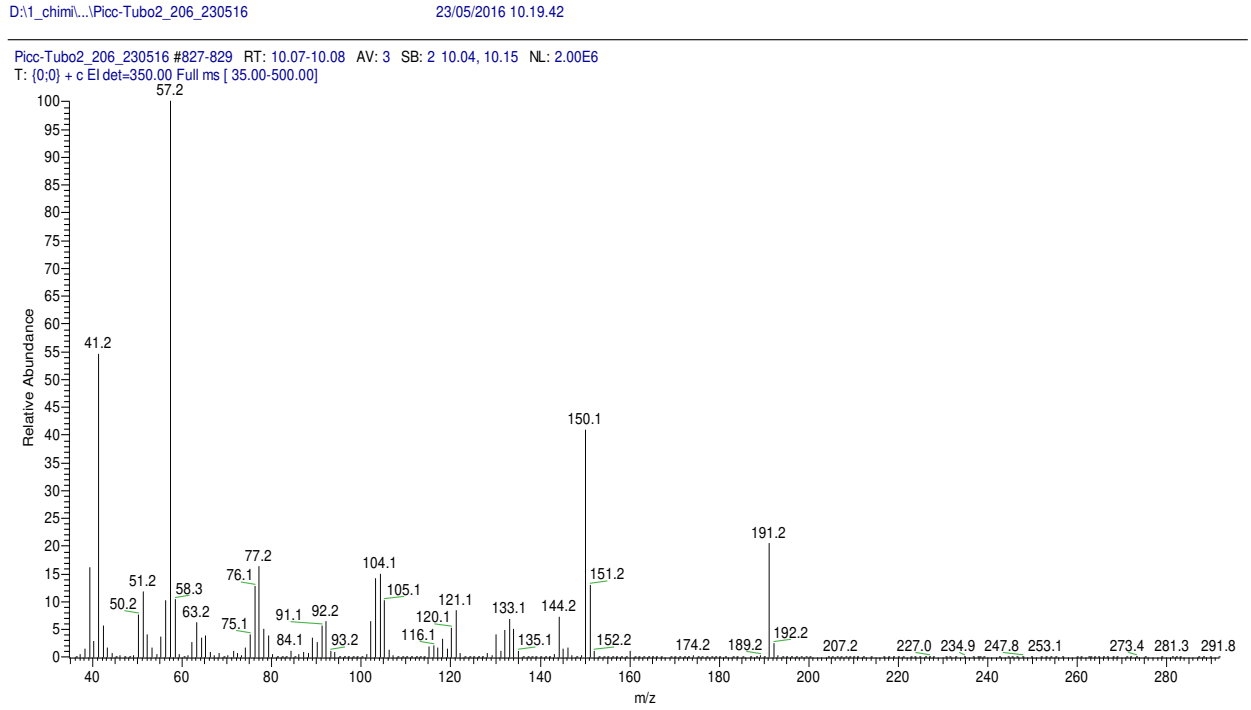

Figure 46. Mass spectrum of *o*-NO_2 imine **136.**

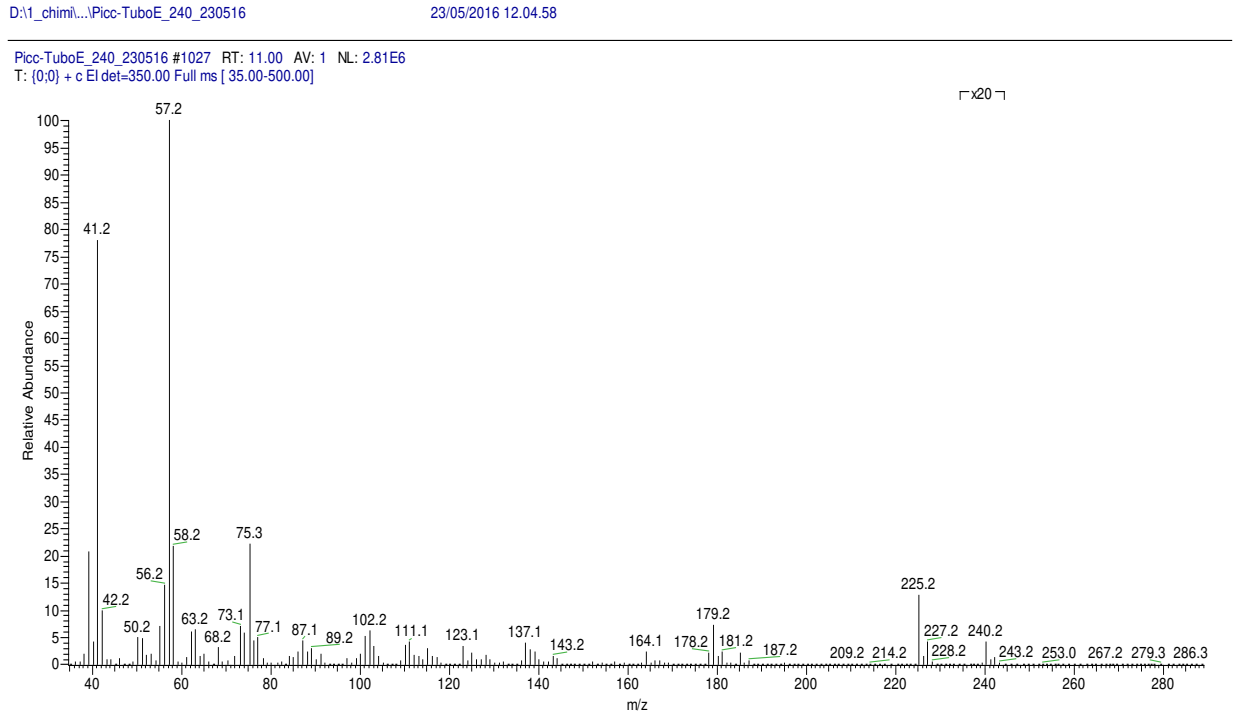

Figure 47. Mass spectrum of *o*-chloro-*m*-NO_2 imine **137**.

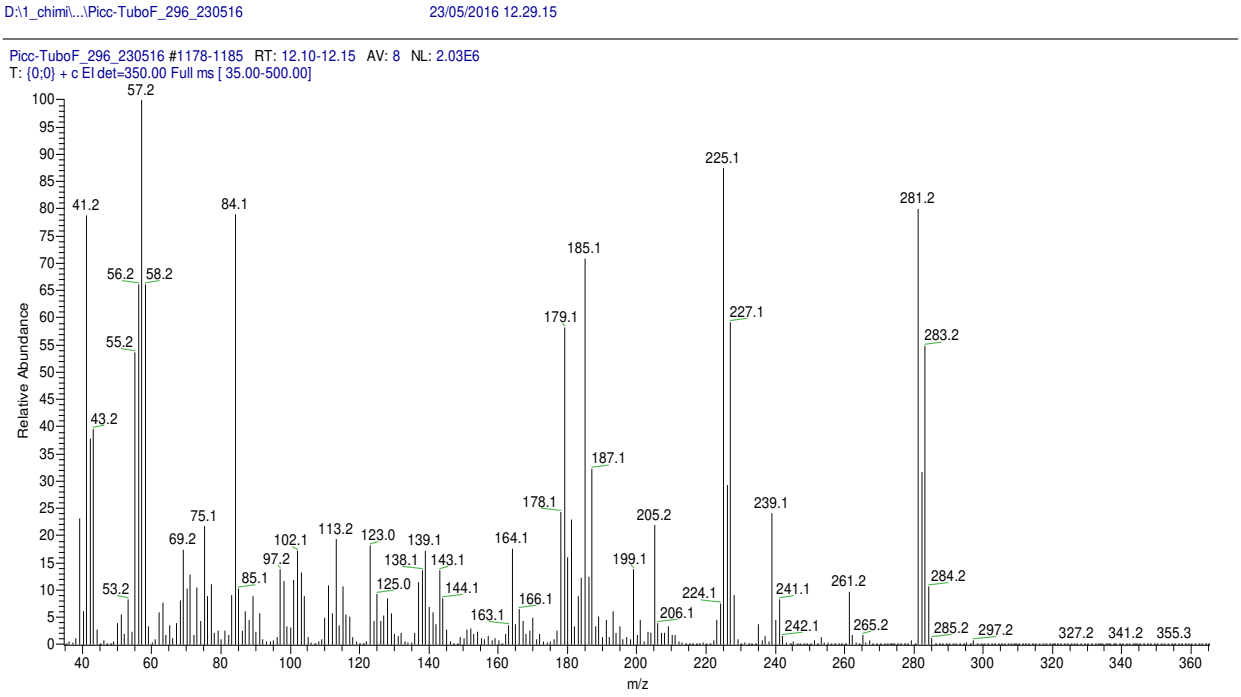

Figure 48. Mass spectrum of nonyl-imine **138**.

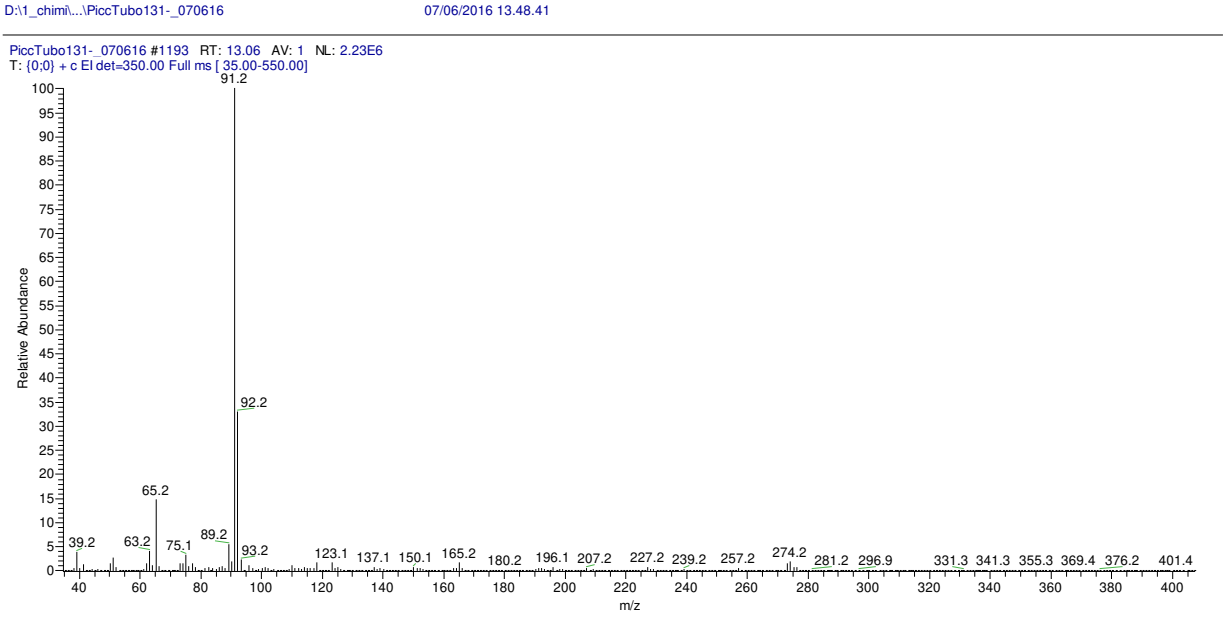

Figure 49. Mass spectrum of benzyl imine **139**.

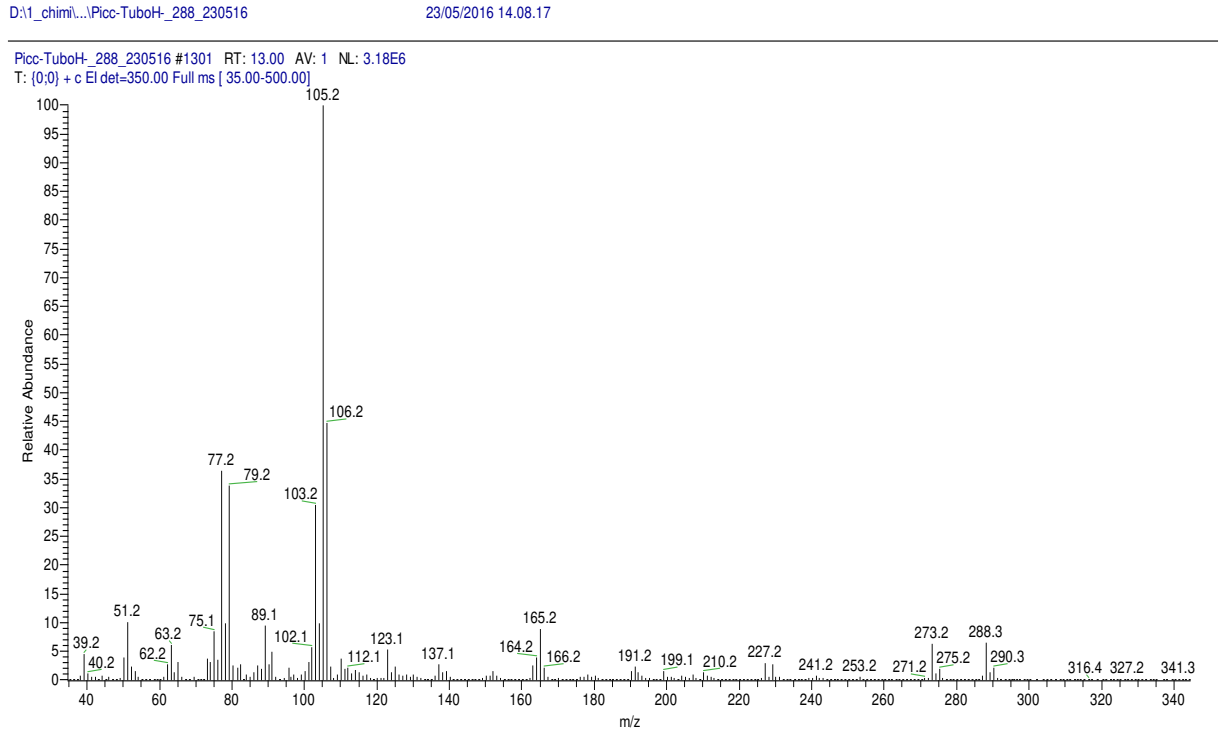

Figure 50. Mass spectrum of methylbenzyl imine **140**.

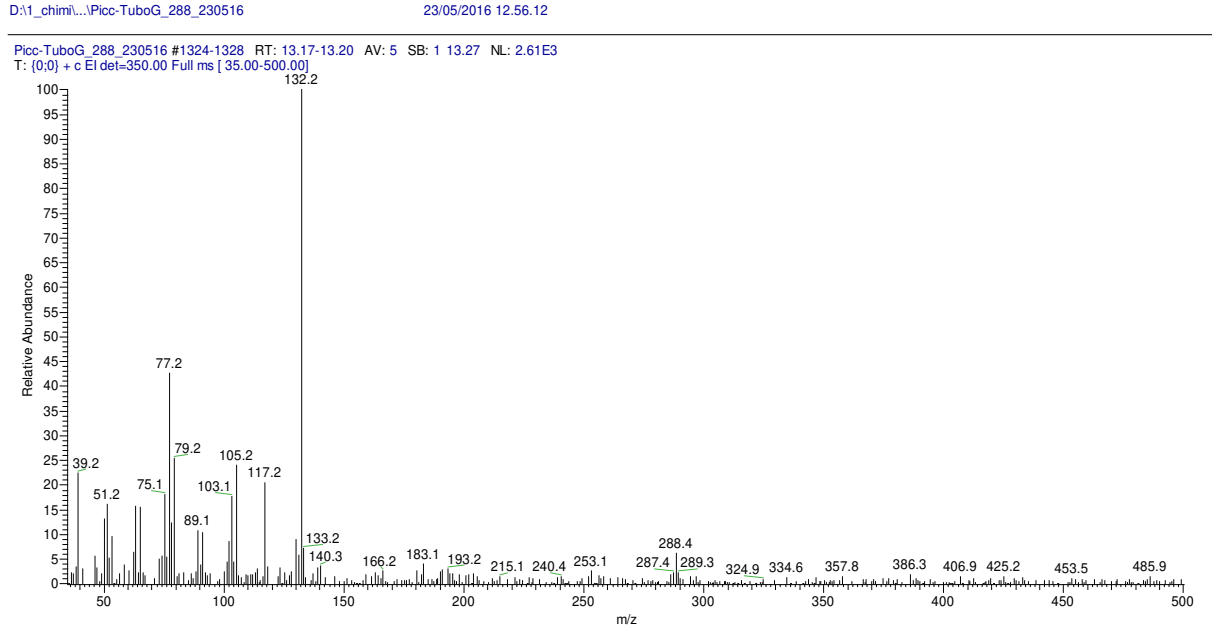

Figure 51. Mass spectrum of xylene imine **141**.

4 Summary and Outlook

Discovering the tail-to-head terpene cyclization being catalyzed inside the hexameric resorcin[4]arene capsule **XII** was a huge milestone in supramolecular catalysis and led to a surge in interest for hydrogen bonded supramolecular assemblies. Exploiting the capsule's ability to stabilize intermediates and transition states *via* cation-π interactions and through hydrogen bonding, multiple new reactions have been published since the first examples of size-selective WITTIG olefinations and acetal hydrolysis.[67] The picture of the exact mode of catalysis remains incomplete, however, sparking interest for further investigations.

We set out to review the role of hydrochloric acid, present in traces in chloroform, the solvent of choice for supramolecularly-assisted transformations, in all relevant reactions published for capsule **XII**. In conclusion, reactions proceeding through cationic intermediates and transition states required the presence of HCl to enable the reaction or accelerate it. A notable exception is the hydration of isocyanides to *N*-formamides, which was thought to progress *via* protonation of the terminal carbon atom and subsequent nucleophilic attack of water on the cationic intermediate. The reaction, however, did not require a cocatalyst, indicating that the transformation may proceed by a different pathway, presumably *via* H-bond activation.

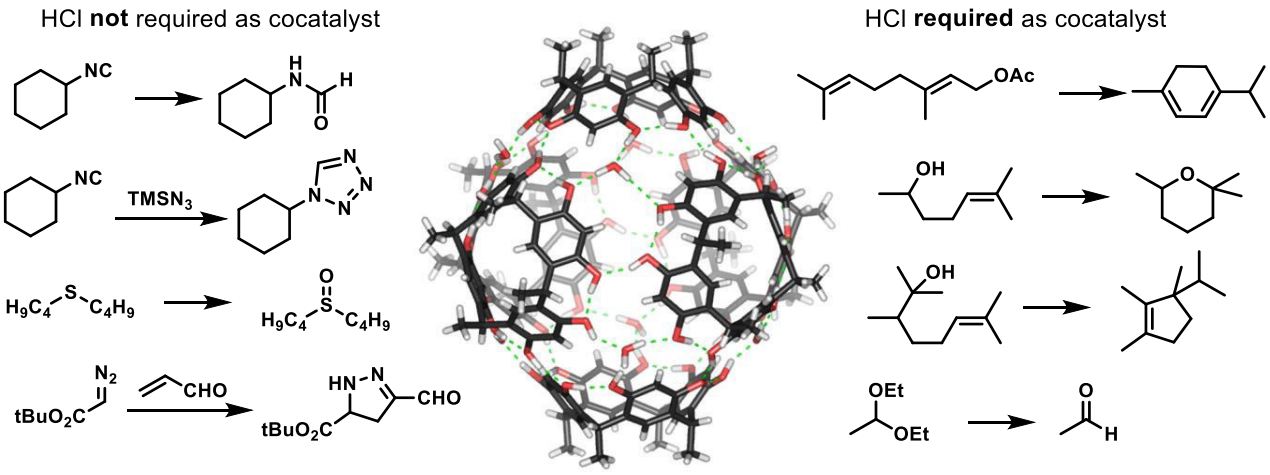

Figure 52. Overview of reactions catalyzed by capsule **XII** and classification into reactions requiring HCl as cocatalyst and reactions not dependent upon its presence.

In a further study we examined the activation of tertiary fluorides, previously facilitated by strong BRØNSTED and LEWIS acids under harsh conditions, inside the cavity of hexameric capsule **XII**. The hydrogen bond network of the supramolecular assembly is able to sufficiently activate tertiary alkyl fluorides as well as primary and secondary benzyl fluorides, giving rise to predominantly elimination products in absence of suitable nucleophiles, ethers from intramolecular interception by alcohols, lactones from esters, and diarylmethanes from FRIEDEL-CRAFTS alkylations. Mechanistic studies indicate a cooperation between the catalyst and hydrogen fluoride, released as a byproduct from the substrate. HF is either sequestered inside the cavity and thus protected from being quenched by reaction with silica glass walls of the reaction vessel and/or increases the inherent BRØNSTED acidity of **XII**, therefore accelerating the reaction.

The supramolecular assembly **XII** exists in an equilibrium in solution between two enantiomers, which arise from subtle differences in the hydrogen bond network between the resorcin[4]arene subunits and water molecules (see fig. 53).

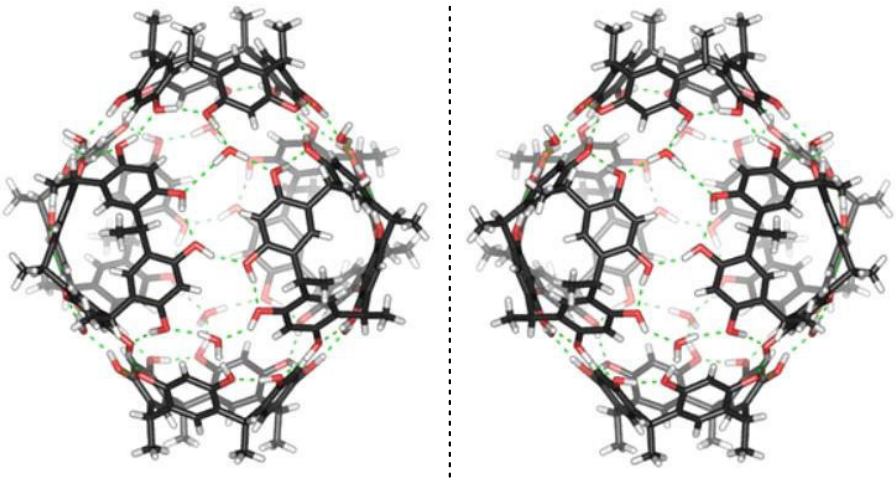

Figure 53. Depiction of the two enantiomers of hexamer **XII** in solution; C_{11}-feet have been omitted for clarity.

COHEN *et al.* demonstrated that substitution of water molecules in the hydrogen bond network of the supramolecular assembly **XII** by alcohols was possible.[99] Replacing water molecules with chiral alcohols may induce a chiral field of sufficient strength to favor the formation of one enantiomer of **XII**, which we hope will in turn induce enantioselectivity in transformations taking place in the interior. Additional strategies to induce a chiral field focus on the introduction of chiral residues on the feet of the capsule.

5 Index of Abbreviations

A ⊃ B	B encapsulated within A
Å	Angstrom, 10^{-10} m
Ac	Acetyl
Ar	Aryl
B3LYP	BECKE, 3-parameter, LEE-YANG-PARR hybrid functional
C	*Celsius*
cat.	catalyst
DMSO	dimethyl sulfoxide
E	energy
ee	enantiomeric excess
eq.	equivalent
et al.	lat. *et alia*, and others
e.g.	lat. *exempli gratia*, for example
eq.	equivalents
Et	Ethyl
FID	flame ionization detector
g	gram
G*	Gaussian
GC	Gas chromatography
GD3BJ	GRIMME D3 dispersion with BECKE-JOHNSON dampening
h	hours
h	Planck's constant, $6.626 \cdot 10^{-34}$ J·s
H-bond	hydrogen bond
Hex	hexyl
Hz	Hertz

i.e.	lat. *id est*, that is to say
k	reaction rate
K	Kelvin
K_a	association constant
k_{cat}	reaction rate for the catalyzed reaction
k_{uncat}	reaction rate for the uncatalyzed reaction
kcal	kilocalorie
L	ligand
L	liter
m	meter
M	metal
M	Molarity, mol
Me	Methyl
MS	mass spectrometry
min	minutes
ν	frequency
NBS	*N*-Bromosuccinimide
NMR	Nuclear Magnetic Resonance
Pa	Pascal
pH	lat. *pondus hydrogenii*, negative base 10 logarithm of the activity of the hydrogen ion in a solution
Ph	phenyl
pK_a	negative base 10 logarithm of the acid dissociation constant (K_a) of a solution
ppm	parts per million, 10^{-6}
Pr	Propyl
R^2	coefficient of determination
r.t.	room temperature

TBAB	tetrabutylammonium bromide
$TEABF_4$	tetraethylamonium tetrafluoroborate
TLC	thin-layer chromatography
TMS	trimethylsilyl
TS	transition state
u	unit
UV	Ultra violet
w	water-saturated

6 References

[1] Lehn, J.-M., *Angew. Chem. Int. Ed.* **1990**, *29*, 1304-1319.

[2] Lehn, J.-M., *Proc. Natl. Acad. Sci. U.S.A.* **2002**, *99*, 4763-4768.

[3] Lehn, J.-M., *Science* **2002**, *295*, 2400-2403.

[4] Fischer, E., *Ber. Dt. Chem. Ges.* **1894**, *27*, 2985-2993.

[5] Koshland, D. E., *Proc. Natl. Acad. Sci. U.S.A.* **1958**, *44*, 98-104.

[6] Dickschat, J. S., *Nat. Prod. Rep.* **2016**, *33*, 87-110.

[7] Kingston, D. G. I., *J. Nat. Prod.* **2000**, *63*, 726-734.

[8] Gürtler, H., Pedersen, R., Anthoni, U., Christophersen, C., Nielsen, P., Wellington, E., Pedersen, C., Bock, K., *J. Antibiot.* **1994**, *47*, 434-439.

[9] a) Wallach, O., *Liebigs Ann. Chem.* **1887**, *239*, 1-54; b) Ruzicka, L., Stoll, M., *Helv. Chim. Acta* **1922**, *5*, 923-936.

[10] Pronin, S. V., Shenvi, R. A., *Nat. Chem.* **2012**, *4*, 915.

[11] Croteau, R., *Chem. Rev.* **1987**, *87*, 929-954.

[12] a) Cram, D. J., *Angew. Chem. Int. Ed.* **1988**, *27*, 1009-1020; b) Lehn, J.-M., *Angew. Chem. Int. Ed.* **1988**, *27*, 89-112; c) Pedersen, C. J., *Angew. Chem. Int. Ed.* **1988**, *27*, 1021-1027.

[13] Pedersen, C. J., *J. Am. Chem. Soc.* **1967**, *89*, 7017-7036.

[14] a) Chao, Y., Cram, D. J., *J. Am. Chem. Soc.* **1976**, *98*, 1015-1017; b) Clement, D., Damm, F., Lehn, J.-M., *Heterocycles* **1976**, *5*, 477-484.

[15] Lehn, J.-M., Sirlin, C., *Chem. Commun.* **1978**, *21*, 949-951.

[16] Brown, C. J., Toste, F. D., Bergman, R. G., Raymond, K. N., *Chem. Rev.* **2015**, *115*, 3012-3035.

[17] Hof, F., Craig, S. L., Nuckolls, C., Rebek, J., *Angew. Chem. Int. Ed.* **2002**, *41*, 1488-1508.

[18] Jordan, J. H., Gibb, B. C., *Chem. Soc. Rev.* **2015**, *44*, 547-585.

[19] a) Oshovsky, G. V., Reinhoudt, D. N., Verboom, W., *J. Am. Chem. Soc.* **2006**, *128*, 5270-5278; b) Beyeh, N. K., Pan, F., Rissanen, K., *Angew. Chem. Int. Ed.* **2015**, *54*, 7303-7307.

[20] a) Dumele, O., Trapp, N., Diederich, F., *Angew. Chem. Int. Ed.* **2015**, *54*, 12339-12344; b) Dumele, O., Schreib, B., Warzok, U., Trapp, N., Schalley, C. A., Diederich, F., *Angew. Chem. Int. Ed.* **2017**, *56*, 1152-1157.

[21] Fujita, M., Oguro, D., Miyazawa, M., Oka, H., Yamaguchi, K., Ogura, K., *Nature* **1995**, *378*, 469-471.

[22] a) Kusukawa, T., Fujita, M., *Angew. Chem. Int. Ed.* 1998, *37*, 3142-3144; b) Kusukawa, T., Fujita, M., *J. Am. Chem. Soc.* **1999**, *121*, 1397-1398.

[23] Yoshizawa, M., Takeyama, Y., Okano, T., Fujita, M., *J. Am. Chem. Soc.* **2003**, *125*, 3243-3247.

[24] Yoshizawa, M., Kusukawa, T., Fujita, M., Sakamoto, S., Yamaguchi, K., *J. Am. Chem. Soc.* **2001**, *123*, 10454-10459.

[25] Murase, T., Nishijima, Y., Fujita, M., *J. Am. Chem. Soc.* **2012**, *134*, 162-164.

[26] Takezawa, H., Kanda, T., Nanjo, H., Fujita, M., *J. Am. Chem. Soc.* **2019**, *141*, 5112-5115.

[27] Caulder, D. L., Powers, R. E., Parac, T. N., Raymond, K. N., *Angew. Chem. Int. Ed.* **1998**, *37*, 1840-1843.

[28] Davis, A. V., Fiedler, D., Ziegler, M., Terpin, A., Raymond, K. N., *J. Am. Chem. Soc.* **2007**, *129*, 15354-15363.

[29] Zhao, C., Sun, Q.-F., Hart-Cooper, W. M., DiPasquale, A. G., Toste, F. D., Bergman, R. G., Raymond, K. N., *J. Am. Chem. Soc.* **2013**, *135*, 18802-18805.

[30] Davis, A. V., Raymond, K. N., *J. Am. Chem. Soc.* **2005**, *127*, 7912-7919.

[31] Leung, D. H., Bergman, R. G., Raymond, K. N., *J. Am. Chem. Soc.* **2006**, *128*, 9781-9797.

[32] Leung, D. H., Bergman, R. G., Raymond, K. N., *J. Am. Chem. Soc.* **2007**, *129*, 2746-2747.

[33] Pluth, M. D., Bergman, R. G., Raymond, K. N., *Science* **2007**, *316*, 85-88.

[34] Hastings, C. J., Fiedler, D., Bergman, R. G., Raymond, K. N., *J. Am. Chem. Soc.* **2008**, *130*, 10977-10983.

[35] Brown, C. J., Bergman, R. G., Raymond, K. N., *J. Am. Chem. Soc.* **2009**, *131*, 17530-17531.

[36] Hart-Cooper, W. M., Clary, K. N., Toste, F. D., Bergman, R. G., Raymond, K. N., *J. Am. Chem. Soc.* **2012**, *134*, 17873-17876.

[37] Kaphan, D. M., Toste, F. D., Bergman, R. G., Raymond, K. N., *J. Am. Chem. Soc.* **2015**, *137*, 9202-9205.

[38] Bolliger, J. L., Belenguer, A. M., Nitschke, J. R., *Angew. Chem. Int. Ed.* **2013**, *52*, 7958-7962.

[39] Salles, A. G., Zarra, S., Turner, R. M., Nitschke, J. R., *J. Am. Chem. Soc.* **2013**, *135*, 19143-19146.

[40] Slagt, V. F., Reek, J. N. H., Kamer, P. C. J., van Leeuwen, P. W. N. M., *Angew. Chem. Int. Ed.* **2001**, *40*, 4271-4274.

[41] Slagt, V. F., Kamer, P. C. J., van Leeuwen, P. W. N. M., Reek, J. N. H., *J. Am. Chem. Soc.* **2004**, *126*, 1526-1536.

[42] a) Kleij, A. W., Lutz, M., Spek, A. L., van Leeuwen, P. W. N. M., Reek, J. N. H., *Chem. Commun.* **2005**, *29*, 3661-3663; b) Bellini, R., Chikkali, S. H., Berthon-Gelloz, G., Reek, J. N. H., *Angew. Chem. Int. Ed.* **2011**, *50*, 7342-7345; c) Bellini, R., Reek, J. N. H., *Chem. Eur. J.* **2012**, *18*, 7091-7099; d) Wang, X., Nurttila, S. S., Dzik, W. I., Becker, R., Rodgers, J., Reek, J. N. H., *Chem. Eur. J.* **2017**, *23*, 14769-14777; e) Nurttila, S. S., Brenner, W., Mosquera, J., van Vliet, K. M., Nitschke, J. R., Reek, J. N. H., *Chem. Eur. J.* **2019**, *25*, 609-620.

[43] a) Slagt, V. F., van Leeuwen, P. W. N. M., Reek, J. N. H., *Angew. Chem. Int. Ed.* **2003**, *42*, 5619-5623; b) Kuil, M., Soltner, T., van Leeuwen, P. W. N. M., Reek, J. N. H., *J. Am. Chem. Soc.* **2006**, *128*, 11344-11345.

[44] Gadzikwa, T., Bellini, R., Dekker, H. L., Reek, J. N. H., *J. Am. Chem. Soc.* **2012**, *134*, 2860-2863.

[45] Palmer, L. C., Rebek, J., *Org. Biomol. Chem.* **2004**, *2*, 3051-3059.

[46] Wyler, R., de Mendoza, J., Rebek., J., *Angew. Chem. Int. Ed.* **1993**, *32*, 1699-1701.

[47] Branda, N., Wyler, R., Rebek, J., *Science* **1994**, *263*, 1267-1268.

[48] Branda, N., Grotzfeld, R. M., Valdes, C., Rebek, J., *J. Am. Chem. Soc.* **1995**, *117*, 85-88.

[49] Valdes, C., Spitz, U. P., Toledo, L. M., Kubik, S. W., Rebek, J., *J. Am. Chem. Soc.* **1995**, *117*, 12733-12745.

[50] Mecozzi, S., Rebek, J., *Chem. Eur. J.* **1998**, *4*, 1016-1022.

[51] Kang, J., Rebek, J., *Nature* **1996**, *382*, 239-241.

[52] Kang, J., Rebek, J., *Nature* **1997**, *385*, 50-52.

[53] Kang, J., Hilmersson, G., Santamaría, J., Rebek, J., *J. Am. Chem. Soc.* **1998**, *120*, 3650-3656.

[54] MacGillivray, L. R., Atwood, J. L., *Nature* **1997**, *389*, 469.

[55] Avram, L., Cohen, Y., *J. Am. Chem. Soc.* **2002**, *124*, 15148-15149.

[56] a) Aoyama, Y., Tanaka, Y., Toi, H., Ogoshi, H., *J. Am. Chem. Soc.* **1988**, *110*, 634-635; b) Aoyama, Y., Tanaka, Y., Sugahara, S., *J. Am. Chem. Soc.* **1989**, *111*, 5397-5404; c) Shivanyuk, A., Rissanen, K., Kolehmainen, E., *Chem. Commun.* **2000**, *13*, 1107-1108.

[57] Shivanyuk, A., Rebek, J., *Proc. Natl. Acad. Sci. U.S.A.* **2001**, *98*, 7662-7665.

[58] Barrett, E. S., Dale, T. J., Rebek, J., *J. Am. Chem. Soc.* **2008**, *130*, 2344-2350.

[59] a) Cavarzan, A., Scarso, A., Sgarbossa, P., Strukul, G., Reek, J. N. H., *J. Am. Chem. Soc.* **2011**, *133*, 2848-2851; b) Bianchini, G., Scarso, A., Sorella, G. L., Strukul, G., *Chem. Commun.* **2012**, *48*, 12082-12084.

[60] Bianchini, G., Sorella, G. L., Canever, N., Scarso, A., Strukul, G., *Chem. Commun.* **2013**, *49*, 5322-5324.

[61] La Sorella, G., Sperni, L., Strukul, G., Scarso, A., *ChemCatChem* **2015**, *7*, 291-296.

[62] Giust, S., La Sorella, G., Sperni, L., Fabris, F., Strukul, G., Scarso, A., *Asian J. Org. Chem.* **2015**, *4*, 217-220.

[63] Giust, S., La Sorella, G., Sperni, L., Strukul, G., Scarso, A., *Chem. Commun.* **2015**, *51*, 1658-1661.

[64] La Sorella, G., Sperni, L., Strukul, G., Scarso, A., *Adv. Synth. Catal.* **2016**, *358*, 3443-3449.

[65] La Sorella, G., Sperni, L., Ballester, P., Strukul, G., Scarso, A., *Catal. Sci. Techol.* **2016**, *6*, 6031-6036.

[66] Caneva, T., Sperni, L., Strukul, G., Scarso, A., *RSC Adv.* **2016**, *6*, 83505-83509.

[67] Zhang, Q., Tiefenbacher, K., *J. Am. Chem. Soc.* **2013**, *135*, 16213-16219.

[68] a) Zhang, Q., Tiefenbacher, K., *Nat. Chem.* **2015**, *7*, 197-202; b) Zhang, Q., Catti, L., Pleiss, J., Tiefenbacher, K., *J. Am. Chem. Soc.* **2017**, *139*, 11482-11492.

[69] Zhang, Q., Rinkel, J., Goldfuss, B., Dickschat, J. S., Tiefenbacher, K., *Nat. Catal.* **2018**, *1*, 609-615.

[70] Zhang, Q., Tiefenbacher, K., *Angew. Chem. Int. Ed.* **2019**, *58*, 12688-12695.

[71] Casey, C. P., *J. Chem. Edu.* **2006**, *83*, 192.

[72] a) Ludwig, J. R., Zimmerman, P. M., Gianino, J. B., Schindler, C. S., *Nature* **2016**, *533*, 374; b) Albright, H., Vonesh, H. L., Becker, M. R., Alexander, B. W., Ludwig, J. R., Wiscons, R. A., Schindler, C. S., *Org. Lett.* **2018**, *20*, 4954-4958.

[73] Catti, L., Tiefenbacher, K., *Angew. Chem. Int. Ed.* **2018**, *57*, 14589-14592.

[74] Catti, L., Tiefenbacher, K., *Chem. Commun.* **2015**, *51*, 892-894.

[75] Catti, L., Pöthig, A., Tiefenbacher, K., *Adv. Synth. Catal.* **2017**, *359*, 1331-1338.

[76] a) Bräuer, T. M., Zhang, Q., Tiefenbacher, K., *Angew. Chem. Int. Ed.* **2016**, *55*, 7698-7701; b) Bräuer, T. M., Zhang, Q., Tiefenbacher, K., *J. Am. Chem. Soc.* **2017**, *139*, 17500-17507.

[77] La Manna, P., De Rosa, M., Talotta, C., Gaeta, C., Soriente, A., Floresta, G., Rescifina, A., Neri, P., *Org. Chem. Front.* **2018**, *5*, 827-837.

[78] Gambaro, S., De Rosa, M., Soriente, A., Talotta, C., Floresta, G., Rescifina, A., Gaeta, C., Neri, P., *Org. Chem. Front.* **2019**, *6*, 2339-2347.

[79] Pellegrino, L. M., Carmen, T., Giuseppe, F., Margherita, D. R., Annunziata, S., Antonio, R., Carmine, G., Placido, N., *Angew. Chem. Int. Ed.* **2018**, *57*, 5423-5428.

[80] La Manna, P., Soriente, A., De Rosa, M., Buonerba, A., Talotta, C., Gaeta, C., Neri, P., *ChemSusChem* **2019**, *12*, 1673-1683.

[81] Kirby, A. J., *Angew. Chem. Int. Ed.* **1996**, *35*, 706-724.

[82] Zhang, Q., Catti, L., Tiefenbacher, K., *Acc. Chem. Res.* **2018**, *51*, 2107-2114.

[83] Köster, J. M., Tiefenbacher, K., *ChemCatChem* **2018**, *10*, 2941-2944.

[84] Köster, J. M., Häussinger, D., Tiefenbacher, K., *Front. Chem.* **2019**, *6*, 639.

[85] a) Yoshizawa, M., Klosterman, J. K., Fujita, M., *Angew. Chem. Int. Ed.* **2009**, *48*, 3418-3438; b) Wiester, M. J., Ulmann, P. A., Mirkin, C. A., *Angew. Chem. Int. Ed.* **2011**, *50*, 114-137; c) Marchetti, L., Levine, M., *ACS Catal.* **2011**, *1*, 1090-1118; d) Raynal, M., Ballester, P., Vidal-Ferran, A., van Leeuwen, P. W. N. M., *Chem. Soc. Rev.* **2014**, *43*, 1734-1787; e) Leenders, S., Gramage-Doria, R., de Bruin, B., Reek, J. N. H., *Chem. Soc. Rev.* **2015**, *44*, 433-448; f) Zarra, S., Wood, D. M., Roberts, D. A., Nitschke, J. R., *Chem. Soc. Rev.* **2015**, *44*, 419-432; g) Otte, M., *ACS Catal.* **2016**, *6*, 6491-6510; h) Catti, L., Zhang, Q., Tiefenbacher, K., *Synthesis* **2016**, *48*, 313-328; i) Catti, L., Zhang, Q., Tiefenbacher, K., *Chem. Eur. J.* **2016**, *22*, 9060-9066.

[86] a) Levin, M. D., Kaphan, D. M., Hong, C. M., Bergman, R. G., Raymond, K. N., Toste, F. D., *J. Am. Chem. Soc.* **2016**, *138*, 9682-9693; b) Cullen, W., Misuraca, M. C., Hunter, C. A., Williams, N. H., Ward, M. D., *Nat. Chem.* **2016**, *8*, 231; c) Gonell, S., Reek, J. N. H., *ChemCatChem* **2019**, *11*, 1458-1464; d) Lu, Z., Lavendomme, R., Burghaus, O., Nitschke, J. R., *Angew. Chem. Int. Ed.* **2019**, *58*, 9073-9077.

[87] Shivanyuk, A., Rebek, J., *J. Am. Chem. Soc.* **2003**, *125*, 3432-3433.

[88] La Manna, P., De Rosa, M., Talotta, C., Gaeta, C., Soriente, A., Floresta, G., Rescifina, A., Neri, P., *Org. Chem. Front.* **2018**, *5*, 827-837.

[89] Avram, L., Cohen, Y., *Org. Lett.* **2002**, *4*, 4365-4368.

[90] a) Nenajdenko, V., *Isocyanide Chemistry: Applications in Synthesis and Material Science*, John Wiley & Sons, **2012**; b) Ramozzi, R., Chéron, N., Braïda, B., Hiberty, P. C., Fleurat-Lessard, P., *New J. Chem.* **2012**, *36*, 1137-1140.

[91] a) Dömling, A., Ugi, I., *Angew. Chem. Int. Ed.* 2000, *39*, 3168-3210; b) Ali Reza, K., Ali, R., *Curr. Org. Chem.* **2012**, *16*, 418-450; c) Sadjadi, S., Heravi, M. M., Nazari, N., *RSC Adv.* **2016**, *6*, 53203-53272.

[92] Okada, I., Kitano, Y., *Synthesis* **2011**, *2011*, 3997-4002.

[93] a) Guchhait, S. K., Madaan, C., *Org. Biomol. Chem.* **2010**, *8*, 3631-3634; b) Zeeh, B., Müller, E., *Liebigs Ann. Chem.* **1968**, *715*, 47-51.

[94] Cohen, A. D., Showalter, B. M., Toscano, J. P., *Org. Lett.* **2004**, *6*, 401-403.

[95] Lengyel, I., Sheehan, J. C., *Angew. Chem. Int. Ed.* **1968**, *7*, 25-36.

[96] Elidrisi, I., Negin, S., Bhatt, P. V., Govender, T., Kruger, H. G., Gokel, G. W., Maguire, G. E. M., *Org. Biomol. Chem.* **2011**, *9*, 4498-4506.

[97] Zultanski, S. L., Zhao, J., Stahl, S. S., *J. Am. Chem. Soc.* **2016**, *138*, 6416-6419.

[98] Moragues, M. E., Esteban, J., Ros-Lis, J. V., Martínez-Máñez, R., Marcos, M. D., Martínez, M., Soto, J., Sancenón, F., *J. Am. Chem. Soc.* **2011**, *133*, 15762-15772.

[99] Slovak, S., Cohen, Y., *Chem. Eur. J.* **2012**, *18*, 8515-8520.

7 Bibliographic Data of Complete Publications

This chapter provides the bibliographic details of the publications summarized in chapters 3.1.1 and 3.1.2. of this thesis to facilitate the retrieval of the complete manuscripts and supporting information.

Elucidating the Importance of Hydrochloric Acid as a Cocatalyst for Resorcinarene-Capsule-catalyzed reactions

Jesper M. Köster[a] and Konrad Tiefenbacher[a,b]*

[a]Department of Chemistry, BPR1096, University of Basel, Mattenstrasse 24a, 4058 Basel, Switzerland

E-mail: konrad.tiefenbacher@unibas.ch

[b]Department of Biosystems Science and Engineering, ETH Zürich, Mattenstrasse 24, 4058 Basel, Switzerland

E-mail: tkonrad@ethz.ch

Originally published in: *ChemCatChem* **2018**, *10*, 2941 – 2944.

DOI: 10.1002/cctc.201800326

Hyperlink: https://onlinelibrary.wiley.com/doi/abs/10.1002/cctc.201800326

Activation of primary and secondary benzylic and tertiary alkyl (sp^3)C-F bonds inside a self-assembled molecular container

Jesper M. Köster[a], Daniel Häussinger[a], Konrad Tiefenbacher[a,b]*

[a]Department of Chemistry, BPR1096, University of Basel, Mattenstrasse 24a, 4058 Basel, Switzerland

E-mail: konrad.tiefenbacher@unibas.ch

[b]Department of Biosystems Science and Engineering, ETH Zürich, Mattenstrasse 24, 4058 Basel, Switzerland

E-mail: tkonrad@ethz.ch

Originally published in: *Front. Chem.* **2019**, **6**, 639.

DOI: 10.3389/fchem.2018.00639

Hyperlink: https://www.frontiersin.org/articles/10.3389/fchem.2018.00639/full

8 Reprint Permissions and Reprints

8.1 John Wiley and Sons

JOHN WILEY AND SONS LICENSE TERMS AND CONDITIONS

Sep 04, 2019

This Agreement between University of Basel -- Jesper Koester ("You") and John Wiley and Sons ("John Wiley and Sons") consists of your license details and the terms and conditions provided by John Wiley and Sons and Copyright Clearance Center.

License Number	4661970904955
License date	Sep 04, 2019
Licensed Content Publisher	John Wiley and Sons
Licensed Content Publication	ChemCatChem
Licensed Content Title	Elucidating the Importance of Hydrochloric Acid as a Cocatalyst for Resorcinarene-Capsule-Catalyzed Reactions
Licensed Content Author	Konrad Tiefenbacher, Jesper M. Köster
Licensed Content Date	May 8, 2018
Licensed Content Volume	10
Licensed Content Issue	14
Licensed Content Pages	4
Type of use	Dissertation/Thesis
Requestor type	Author of this Wiley article
Format	Print and electronic
Portion	Full article
Will you be translating?	No
Title of your thesis / dissertation	Catalysis in Supramolecular Containers
Expected completion date	Oct 2019
Expected size (number of pages)	100
Requestor Location	University of Basel Petersplatz 1 Basel, 4056 Switzerland Attn: University of Basel
Publisher Tax ID	EU826007151
Total	0.00 EUR

8.2 Frontiers Media SA

The manuscript published in *Frontiers in Chemistry* was reproduced with permission (**open access**) of Frontiers Media SA.

Activation of Primary and Secondary Benzylic and Tertiary Alkyl (sp^3)C-F Bonds Inside a Self-Assembled Molecular Container

J. Köster, D. Häussinger, K. Tiefenbacher, *Front. Chem.* **2019**, *6*, 639.

8.3 American Chemical Society

PERMISSION/LICENSE IS GRANTED FOR YOUR ORDER AT NO CHARGE

This type of permission/license, instead of the standard Terms & Conditions, is sent to you because no fee is being charged for your order. Please note the following:

- Permission is granted for your request in both print and electronic formats, and translations.
- If figures and/or tables were requested, they may be adapted or used in part.
- Please print this page for your records and send a copy of it to your publisher/graduate school.
- Appropriate credit for the requested material should be given as follows: "Reprinted (adapted) with permission from (COMPLETE REFERENCE CITATION). Copyright (YEAR) American Chemical Society." Insert appropriate information in place of the capitalized words.
- One-time permission is granted only for the use specified in your request. No additional uses are granted (such as derivative works or other editions). For any other uses, please submit a new request.

ChemPubSoc Europe

DOI: 10.1002/cctc.201800326

CHEMCATCHEM Communications

Elucidating the Importance of Hydrochloric Acid as a Cocatalyst for Resorcinarene-Capsule-Catalyzed Reactions

Jesper M. Köster[a] and Konrad Tiefenbacher*[a, b]

This survey of resorcinarene-capsule-catalyzed reactions demonstrates that HCl functions as a crucial cocatalyst by increasing the capsule's inherent Brønsted acidity to enable or accelerate cationic reactions. The presence of HCl appears to be without consequences for other reactions.

Supramolecular catalysts have emerged as promising enzyme mimics[1,2] that are able to influence reactions accelerated inside their cavity. The main differences between reactions catalyzed inside a supramolecular container and those catalyzed in bulk solution include the following:[1j] 1) product selectivity; in several cases different products are obtained inside the supramolecular container. 2) substrate selectivity; this hallmark feature is generally used as a control experiment. Large substrates that do not bind the cavity, or at least to a much lower extent, are converted at significantly reduced rates. 3) multicatalyst tandem reactions; the encapsulation of the active site enables the simultaneous use of several otherwise incompatible catalysts in solution. One of the more versatile representatives is resorcinarene (**1**, Figure 1 a), which self-assembles in apolar solvents such as chloroform and benzene under the incorporation of eight water molecules to hexameric capsule **I** (Figure 1 b).[3] The assembly displays high affinity for cations, which are stabilized through cation–π interactions with the aromatic cavity walls.[4] Furthermore, capsule **I** was shown to be reasonably Brønsted acidic ($pK_A = 5.6–5.9$).[5] It has been employed as a catalyst for the hydrolysis of acetals,[5] the tail-to-head cyclization of terpenes,[6] the intramolecular hydroalkoxylation of alkenes,[7] the cyclodehydration of alkenols,[8] the hydration of isonitriles,[9] [2+3]-cycloaddition reactions,[10] the Meinwald rearrangement of epoxides,[11] the hydration of alkynes to ketones,[12] and the oxidation of thioethers.[13] In a recent report concerning tail-to-head terpene cyclization,[14] it was found that trace amounts of hydrochloric acid, formed through the photodegradation of the solvent chloroform, acted as an essential cocatalyst. It was established that HCl

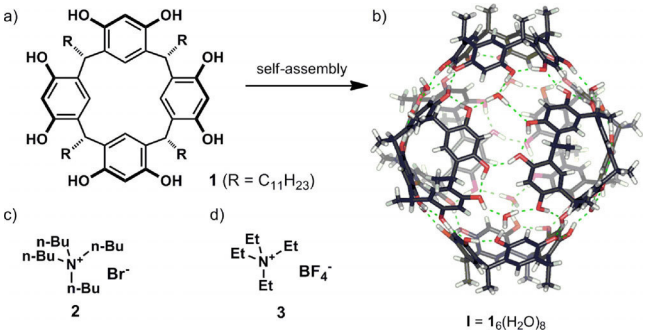

Figure 1. a) Resorcinarene monomer **1**. b) Hexameric capsule **I**; C_{11}-alkyl feet are omitted for clarity. c) High-affinity guests tetrabutylammonium bromide (TBAB, **2**) and d) tetraethylammonium tetrafluoroborate ($TEABF_4$, **3**).

protonated the capsule,[14] which was then believed to transfer the proton onto the encapsulated substrate (Figure 2 a, right). Control experiments without the capsule under otherwise identical conditions did not lead to any observable conversion. Additionally, size-competition experiments as well as blocking experiments provided convincing evidence that the reaction took place inside the capsule. It was also found that the presence of trace amounts of HCl could be easily detected by in-

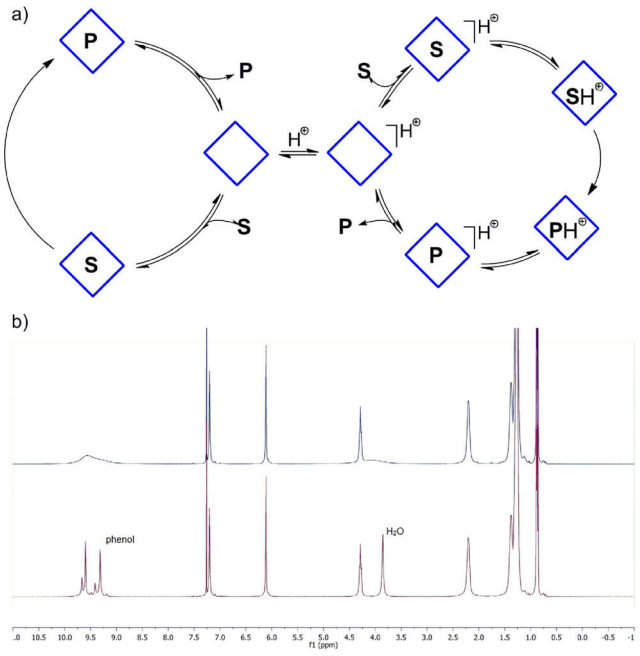

Figure 2. a) Possible reaction pathways for reactions catalyzed inside capsule **I** with and without HCl as a cocatalyst. b) ^1H NMR spectra of capsule **I** in $CDCl_3$ (3.3 mM) before and after the addition of HCl (0.3 equiv. with respect to capsule **I**). S = substrate, P = product.

[a] J. M. Köster, Prof. Dr. K. Tiefenbacher
Department of Chemistry, BPR1096
University of Basel
Mattenstrasse 24a, 4058 Basel (Switzerland)
E-mail: konrad.tiefenbacher@unibas.ch

[b] Prof. Dr. K. Tiefenbacher
Department of Biosystems Science and Engineering
ETH Zürich
Mattenstrasse 24, 4058 Basel (Switzerland)
E-mail: tkonrad@ethz.ch

Supporting Information and the ORCID identification number(s) for the author(s) of this article can be found under: https://doi.org/10.1002/cctc.201800326.

specting the ^{1}H NMR spectrum of the capsule solution (Figure 2 b). In the absence of HCl, sharp signals for the phenols and water signals were observed. Trace amounts of HCl led to significant broadening of these signals. In all previously published reactions employing capsule **I** as a catalyst, untreated chloroform (not filtered through basic Al_2O_3) was used as a solvent. Therefore, we wondered if the presence of an acid cocatalyst (HCl) was generally required for catalytic activity or if the inherent Brønsted acidity of capsule **I** itself was sufficient for other reactions.

To elucidate the importance of HCl, all reaction classes reported were repeated under precisely controlled conditions. One suitable substrate (high yielding, high selectivity) was chosen for each reaction class and was investigated under the conditions published in the absence and presence of defined amounts of HCl. To exclude background reactions outside of capsule **I**, control experiments were performed as described in the literature by blocking the cavity of the supramolecular capsule through the addition of the high-affinity guest tetrabutylammonium bromide (**2**, Figure 1 c) or tetraethylammonium tetrafluoroborate (**3**, Figure 1 d). The results from this screening are summarized in Table 1.

For the hydrolysis of acetaldehyde diethyl acetal (**4**) inside container **I**,[5] a clear correlation between the amount of HCl

Table 1. Overview of reactions investigated including yields obtained.[a]

Entry	Reaction	Yield [%] A	B	C	D
1	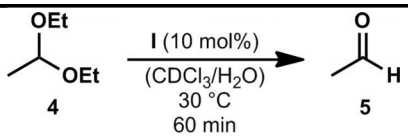	0 ± 1	86 ± 5[b]	0[c]	0[b,c]
2	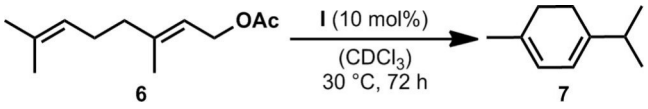	0	27 ± 3	0[c]	0[c]
3	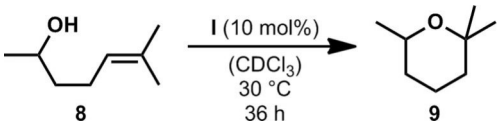	0	95 ± 2	0[c]	7 ± 2[c]
4	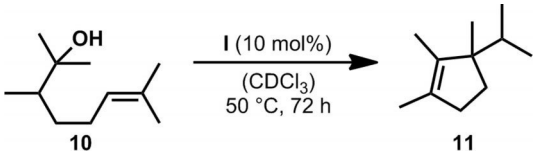	32 ± 1	65 ± 1	0[c]	3 ± 2[c]
5	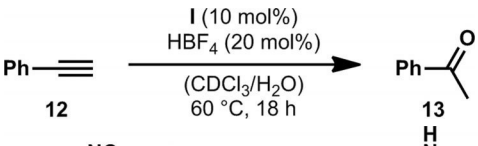	81 ± 3	79 ± 3	2 ± 0[d]	12 ± 5[d]
		acid HBF_4 was present in entries 5A-D			
6	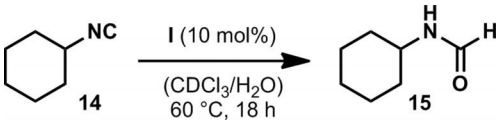	95 ± 4	95 ± 1	13 ± 0[d]	14 ± 1[d]
7	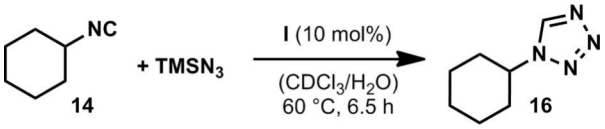	90 ± 4	92 ± 5	43 ± 1[d]	41 ± 1[d]
8	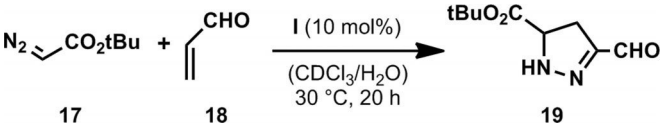	93 ± 2	90 ± 1	0[d]	0[d]
9	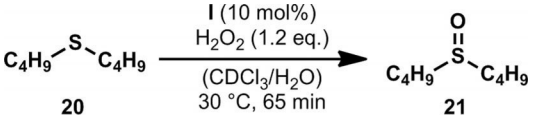	92 ± 1	94 ± 1	70 ± 1[d]	70 ± 0[d]

[a] Reactions were performed in triplicate and standard deviations were determined; all reactions were performed in $CDCl_3$ that was filtered through basic Al_2O_3 to remove trace amounts of acid with capsule **I** (10 mol%). Conditions A: no additive; conditions B: HCl (3 mol%) was added; conditions C: literature inhibition conditions (ammonium salt **2** or **3**); conditions D: literature inhibition conditions (ammonium salt **2** or **3**) and HCl (3 mol%) was added. [b] HCl (0.1 mol%) was added. [c] TBAB (**2**, 1.5 equiv.) was added. [d] $TEABF_4$ (**3**, 10 equiv.) was added.

added and the formation of the product was revealed. In initial experiments (10 mol% capsule **I**, 3 mol% HCl), almost instantaneous hydrolysis of the acetal was observed. To reproduce the published findings, the HCl content was gradually lowered to 0.1 mol%, which led to a yield of (86±5)% after a reaction time of 60 min (Table 1, entry 1B); this is in good agreement with the yield reported in the literature. Without the addition of the cocatalyst, no conversion was observed. In this case, the acidity of the hexameric assembly was not sufficient for catalysis inside **I**.[5] Control experiments, for which the catalytically active cavity of **I** was blocked by a strong binding guest, tetrabutylammonium bromide (TBAB, **2**; Table 1, entry 1C), indicated that the reaction was limited to the interior of capsule **I**, even in the presence of 0.1 mol% HCl (Table 1, entry 1D). Furthermore, very convincing evidence was provided in the original report by size-competition experiments.[5]

For the cyclization of geranyl acetate (**6**), the published findings were reproduced,[6] and conversion was only observed in the presence of HCl as a cocatalyst (Table 1, entry 2B). Control experiments again confirmed that access to the cavity of **I** was required for activity, even in the presence of 3 mol% HCl (Table 1, entry 2D).

The intramolecular hydroalkoxylation[7] of alkene **8** was also revealed to be highly dependent on the presence of HCl, and a (95±2)% yield was obtained after 36 h in the presence of 3 mol% HCl (Table 1, entry 3B). The requirement of HCl as a cocatalyst for this reaction was overlooked in the original report. Nevertheless, all control experiments performed in the initial report (size-competition and blocking experiments) strongly support the fact that the reaction takes place predominantly inside the cavity. The formation of small amounts of product (7±2%) with blocked capsule in the presence of 3 mol% HCl indicates only a slow background reaction outside of capsule **I** (Table 1, entry 3D).

The cyclodehydration of alkenol **10** took place under HCl-free conditions inside capsule **I** (Table 1, entry 4A),[8] but the presence of HCl greatly accelerated the reaction (Table 1, entry 4B). The acceleration effect on this reaction was not known at the time of the initial report. Negligible amounts of product [(3±2)%] were formed in the presence of 3 mol% HCl upon adding competitive guest **2** (Table 1, entry 4D). Although HCl is not required as a cocatalyst for the reaction, the addition of a catalytic amount led to significant acceleration of the reaction.

The hydration of alkyne **12** to acetophenone (**13**) was already shown to require the presence of an acid cocatalyst (i.e., HBF_4).[12] Supplementing the reaction with additional acid (i.e., HCl) led to no significant change in reactivity (Table 1, entries 5A and 5B). The addition of 10 equivalents of **3** efficiently blocked the reactive cavity, as evidenced by the drastically lower yield of acetophenone.

In contrast to the examples discussed so far, the hydration of cyclohexyl isocyanide (**14**) did not depend on an acid cocatalyst (Table 1, entries 6A and 6B).[9] Control experiments with 10 equivalents of competitive guest **3** led to significant retardation of the reaction progress, even in the presence of HCl (Table 1, entries 6C and 6D). This might indicate that protonation of the carbenic-like carbon atom is not rate determining in this process.

The [2+3] cycloaddition of **14** with trimethylsilyl azide was also unaffected by the addition of HCl (Table 1, entries 7A and 7B).[10a] Employing inhibitor **3** in a large excess did not lead to efficient suppression of the cycloaddition (Table 1, entries 7C and 7D), which might indicate that a significant background reaction takes place outside of capsule **I**.

Also, in the case of the [2+3] cycloaddition between *tert*-butyl diazoacetate (**17**) and acrolein (**18**), no significant impact of HCl was observed (Table 1, entries 8A and 8B).[10b] Blocking of the cavity by the addition of 10 equivalents of tetraethylammonium tetrafluoroborate (**3**) completely suppressed product formation.

HCl was also not required for the oxidation of thioether **20** by H_2O_2 (Table 1, entries 9A and 9B).[13] A very significant background reaction was observed in all control experiments (Table 1, entries 9C and 9D). This may be explained by the activation of H_2O_2 by replacing water in the hydrogen-bonding network of the hexameric assembly, which was already proposed in the original report.[13] The activated peroxide was also accessible from outside of capsule **I**, which led to oxidation of the thioether upon contact from the bulk solution.

Inspection of Table 1 reveals that the experiments performed can be readily divided into two groups: 1) reactions that are enabled or at least significantly accelerated by an acid cocatalyst (Table 1, entries 1–5); 2) reactions that are not accelerated by an acid cocatalyst (Table 1, entries 6–9).

For reactions in group 1, the acidity of capsule **I** is not sufficient to promote the acid-catalyzed reaction even in the inside of the cavity, in which cationic/protonated intermediates and transition states are stabilized. The addition of HCl as a cocatalyst in substoichiometric amounts increases the acidity of the capsule and facilitates catalytic turnovers inside the cavity of **I**. Control experiments reported in the literature clearly indicate that the reactions take place inside the container and that they are not catalyzed by HCl alone. In addition, control experiments with HCl were performed (Chapter S5.5 in the Supporting Information), and they also confirmed that HCl alone was not able to catalyze the reactions investigated. Interestingly, one would expect to find the hydration of isonitriles (Table 1, entry 6) in group 1, as protonation of the carbenic-like carbon atom is thought to be crucial for activation of the isonitrile for nucleophilic attack of water. The results from Table 1, however, indicate that the inherent Brønsted acidity of capsule **I** is sufficient to facilitate the reaction.

Reactions in group 2 are accelerated by capsule **I** itself and do not require an external acid for activation. Even the initial rates of the reactions seem not to be influenced by the presence of HCl, as experiments with cyclohexyl isocyanide (Table 1, entry 6) demonstrated (see the Supporting Information). In two cases (Table 1, entries 7 and 9), significant background reactions were observed, and this might indicate that the reactions can also take place outside of capsule **I**.

In conclusion, literature results with capsule **I** as a catalyst were reproduced under strictly controlled conditions. Reactions involving cationic intermediates showed a strong de-

pendency upon the presence of HCl or HBF_4 as a cocatalyst. The transformations of isocyanides into formamides and tetrazoles, which are believed to progress through initial protonation of the carbenic-like carbon atom, displayed no dependence upon the presence of HCl; this may indicate that the inherent acidity of hexamer **I** is already sufficient for catalysis in these reactions. Oxidation and cycloaddition reactions displayed no dependency on an additional acid cocatalyst. These results clarify the role of HCl as a cocatalyst in resorcinarene-capsule-catalyzed reactions. As HCl can play a significant role in such reactions, we highly encourage scientists to run future studies under strictly controlled conditions only. It is recommended that the solvent be filtered through basic Al_2O_3 directly before the start of the experiment to remove trace amounts of acid and that resorcinarene **1**, which is synthesized under acidic (HCl) conditions, be washed with large amounts of water to remove trace amounts of acid (see the Supporting Information).

Acknowledgements

This work was supported by funding from the European Research Council Horizon 2020 Programme [ERC Starting Grant 714620-TERPENECAT], the Swiss National Science Foundation as part of the NCCR Molecular Systems Engineering, and the Bayerische Akademie der Wissenschaften (Junges Kolleg).

Conflict of interest

The authors declare no conflict of interest.

Keywords: acidity · host–guest systems · self-assembly · supramolecular chemistry · π interactions

[1] a) M. Yoshizawa, J. K. Klosterman, M. Fujita, *Angew. Chem.* **2009**, *121*, 3470 – 3490; b) M. J. Wiester, P. A. Ulmann, C. A. Mirkin, *Angew. Chem. Int. Ed.* **2011**, *50*, 114 – 137; *Angew. Chem.* **2011**, *123*, 118 – 142; c) L. Marchetti, M. Levine, *ACS Catal.* **2011**, *1*, 1090 – 1118; d) M. Raynal, P. Ballester, A. Vidal-Ferran, P. W. N. M. van Leeuwen, *Chem. Soc. Rev.* **2014**, *43*, 1734 – 1787; e) C. J. Brown, F. D. Toste, R. G. Bergman, K. N. Raymond, *Chem. Rev.* **2015**, *115*, 3012 – 3035; f) S. H. A. M. Leenders, R. Gramage-Doria, B. de Bruin, J. N. H. Reek, *Chem. Soc. Rev.* **2015**, *44*, 433 – 448; g) S. Zarra, D. M. Wood, D. A. Roberts, J. R. Nitschke, *Chem. Soc. Rev.* **2015**, *44*, 419 – 432; h) M. Otte, *ACS Catal.* **2016**, *6*, 6491 – 6510; i) L. Catti, Q. Zhang, K. Tiefenbacher, *Synthesis* **2016**, *48*, 313 – 328; j) L. Catti, Q. Zhang, K. Tiefenbacher, *Chem. Eur. J.* **2016**, *22*, 9060 – 9066.

[2] For recent examples, see: a) W. Cullen, M. C. Misuraca, C. A. Hunter, N. H. Williams, M. D. Ward, *Nat. Chem.* **2016**, *8*, 231; b) M. D. Levin, D. M. Kaphan, C. M. Hong, R. G. Bergman, K. N. Raymond, F. D. Toste, *J. Am. Chem. Soc.* **2016**, *138*, 9682 – 9693; c) A. C. H. Jans, A. Gómez-Suárez, S. P. Nolan, J. N. H. Reek, *Chem. Eur. J.* **2016**, *22*, 14836 – 14839; d) Q.-Q. Wang, S. Gonell, S. H. A. M. Leenders, M. Dürr, I. Ivanović-Burmazović, J. N. H. Reek, *Nat. Chem.* **2016**, *8*, 225; e) P. F. Kuijpers, M. Otte, M. Dürr, I. Ivanović-Burmazović, J. N. H. Reek, B. de Bruin, *ACS Catal.* **2016**, *6*, 3106 – 3112; f) X. Wang, S. S. Nurttila, W. I. Dzik, R. Becker, J. Rodgers, J. N. H. Reek, *Chem. Eur. J.* **2017**, *23*, 14769 – 14777; g) Y. Ueda, H. Ito, D. Fujita, M. Fujita, *J. Am. Chem. Soc.* **2017**, *139*, 6090 – 6093; h) T. M. Bräuer, Q. Zhang, K. Tiefenbacher, *J. Am. Chem. Soc.* **2017**, *139*, 17500 – 17507; i) P. La Manna, M. De Rosa, C. Talotta, C. Gaeta, A. Soriente, G. Floresta, A. Rescifina, P. Neri, *Org. Chem. Front.* **2018**, *5*, 827 – 837; j) L. Catti, K. Tiefenbacher, *Angew. Chem. Int. Ed.* **2018**, https://doi.org/10.1002/anie.201712141; *Angew. Chem.* **2018**, https://doi.org/10.1002/ange.201712141.

[3] L. Avram, Y. Cohen, *Org. Lett.* **2002**, *4*, 4365 – 4368.

[4] a) L. Avram, Y. Cohen, *J. Am. Chem. Soc.* **2003**, *125*, 16180 – 16181; b) L. Avram, Y. Cohen, *J. Am. Chem. Soc.* **2004**, *126*, 11556 – 11563.

[5] Q. Zhang, K. Tiefenbacher, *J. Am. Chem. Soc.* **2013**, *135*, 16213 – 16219.

[6] Q. Zhang, K. Tiefenbacher, *Nat. Chem.* **2015**, *7*, 197 – 202.

[7] L. Catti, K. Tiefenbacher, *Chem. Commun.* **2015**, *51*, 892 – 894.

[8] L. Catti, A. Pöthig, K. Tiefenbacher, *Adv. Synth. Catal.* **2017**, *359*, 1331 – 1338.

[9] G. Bianchini, G. L. Sorella, N. Canever, A. Scarso, G. Strukul, *Chem. Commun.* **2013**, *49*, 5322 – 5324.

[10] a) S. Giust, G. La Sorella, L. Sperni, F. Fabris, G. Strukul, A. Scarso, *Asian J. Org. Chem.* **2015**, *4*, 217 – 220; b) G. La Sorella, L. Sperni, G. Strukul, A. Scarso, *ChemCatChem* **2015**, *7*, 291 – 296.

[11] T. Caneva, L. Sperni, G. Strukul, A. Scarso, *RSC Adv.* **2016**, *6*, 83505 – 83509.

[12] G. La Sorella, L. Sperni, P. Ballester, G. Strukul, A. Scarso, *Catal. Sci. Technol.* **2016**, *6*, 6031 – 6036.

[13] G. La Sorella, L. Sperni, G. Strukul, A. Scarso, *Adv. Synth. Catal.* **2016**, *358*, 3443 – 3449.

[14] Q. Zhang, L. Catti, J. Pleiss, K. Tiefenbacher, *J. Am. Chem. Soc.* **2017**, *139*, 11482 – 11492.

Manuscript received: February 27, 2018
Revised manuscript received: April 4, 2018

Version of record online: ■■ ■■, 0000

COMMUNICATIONS

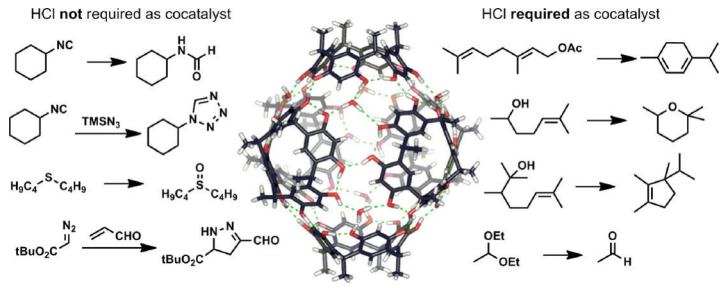

*J. M. Köster, K. Tiefenbacher**

■■ – ■■

Elucidating the Importance of Hydrochloric Acid as a Cocatalyst for Resorcinarene-Capsule-Catalyzed Reactions

Reactivity inspection: Detailed investigations of published resorcinarene-capsule-catalyzed reactions reveal a dependency on the presence of HCl, a common photodegradation product of the solvent $CDCl_3$, for some reactions. Other reactions do not depend on an acid cocatalyst.

frontiers in Chemistry

ORIGINAL RESEARCH
published: 04 January 2019
doi: 10.3389/fchem.2018.00639

Activation of Primary and Secondary Benzylic and Tertiary Alkyl (sp^3)C-F Bonds Inside a Self-Assembled Molecular Container

Jesper M. Köster[1], *Daniel Häussinger*[1] *and Konrad Tiefenbacher*[1,2]*

[1] Department of Chemistry, University of Basel, Basel, Switzerland, [2] Department of Biosystems Science and Engineering, ETH Zürich, Basel, Switzerland

Alkyl fluorides are generally regarded as chemically inert. However, several literature examples describe the activation of alkyl (sp3)C-F bonds via strong Brønsted or Lewis acids under harsh conditions. We here report that catalytic amounts of the self-assembled resorcinarene capsule are able to activate alkyl (sp3)C-F bonds under mild conditions (40°C, no strong Brønsted or Lewis acid present). Kinetic measurements display a sigmoidal reaction progress after an initial induction period. Control experiments indicate that the presence of the supramolecular capsule is required for an efficient reaction acceleration.

Keywords: supramolecular catalysis, molecular capsules, supramolecular chemistry, acid catalysis, elimination

OPEN ACCESS

Edited by:
Pablo Ballester, Catalan Institution for Research and Advanced Studies, Spain

Reviewed by:
Yevgen Karpichev, Tallinn University of Technology, Estonia
Guzman Gil-Ramirez, University of Lincoln, United Kingdom
Joost Reek, UvA Minds, Netherlands

***Correspondence:**
Konrad Tiefenbacher
konrad.tiefenbacher@unibas.ch; tkonrad@ethz.ch

Specialty section:
This article was submitted to Supramolecular Chemistry, a section of the journal Frontiers in Chemistry

Received: *26 June 2018*
Accepted: *07 December 2018*
Published: *04 January 2019*

Citation:
Köster JM, Häussinger D and Tiefenbacher K (2019) Activation of Primary and Secondary Benzylic and Tertiary Alkyl (sp^3)C-F Bonds Inside a Self-Assembled Molecular Container. Front. Chem. 6:639. doi: 10.3389/fchem.2018.00639

INTRODUCTION

Catalysis inside closed binding pockets, much like inside enzymes, has been a challenging research area but in recent decades active supramolecular systems have been reported (Marchetti and Levine, 2011; Wiester et al., 2011; Raynal et al., 2014; Brown et al., 2015; Leenders et al., 2015; Zarra et al., 2015; Catti et al., 2016a,b; Cullen et al., 2016; Jans et al., 2016; Kuijpers et al., 2016; Levin et al., 2016; Otte, 2016; Wang et al., 2016, 2017; Bräuer et al., 2017; Ueda et al., 2017; Catti and Tiefenbacher, 2018; La Manna et al., 2018a). Drawing upon a multitude of structural classes such as coordination cages, metal-organic frameworks, and non-covalent assemblies, a whole series of reactions were successfully catalyzed. One of the catalytically active supramolecular containers is the hexameric resorcinarene capsule **I** (see **Figure 1B**), which self-assembles in non-polar solvents (e.g., chloroform or benzene) from six molecules of resorcinarene (**1**, **Figure 1A**) and eight water molecules (MacGillivray and Atwood, 1997; Avram and Cohen, 2002). It possesses an internal volume of ~1,400 A^3 and is readily accessible in a one-step condensation from resorcinol and dodecanal. It was demonstrated to serve as a mild Brønsted acid ($pK_A \sim 5.5$–6) and functions as a non-nucleophilic counterion due to the extensive delocalization of the negative charge (Zhang and Tiefenbacher, 2013).

The supramolecular capsule **I** was used as a catalyst in the hydrolysis of acetals (Zhang and Tiefenbacher, 2013), the tail-to-head cyclization of terpenes (Zhang and Tiefenbacher, 2015), the hydroalkoxylation of alkenes (Catti and Tiefenbacher, 2015), the cyclodehydration of alcohols (Catti et al., 2017), the carbonyl-olefin metathesis (Catti and Tiefenbacher, 2018), the hydration of isonitriles (Bianchini et al., 2013), [2+3]-cycloaddition reactions (Giust et al., 2015; La Manna et al., 2018a), the Meinwald rearrangement of epoxides (Caneva et al., 2016), the hydration of alkynes (La Sorella et al., 2016a), the oxidation of thioethers (La Sorella et al., 2016b), and Friedel-Crafts reactions (La Manna et al., 2018b).

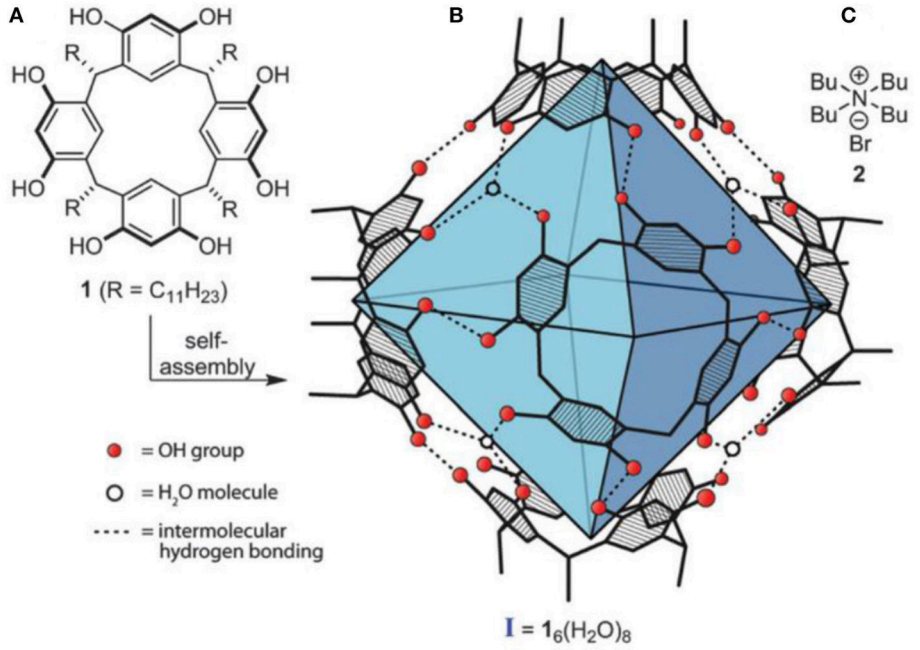

FIGURE 1 | (A) C_{11}-resorcinarene (**1**); **(B)** hexameric capsule **I**, C_{11}-feet omitted; **(C)** competitive guest TBAB (**2**).

Recently, we investigated "inert" fluorinated acyclic terpenes as probes to quantify substrate encapsulation via ^{19}F-NMR. Surprisingly, the C-F bond of tertiary fluoride **10** (**Table 1**) was activated in the presence of catalytic amounts of capsule (10 mol%). This observation prompted us to investigate this reaction more closely and here we present the results.

Alkyl halides, known for their broad spectrum of reactivity (substitution, elimination, metalation), are a cornerstone of organic chemistry. In contrast to iodides, bromides, and chlorides alkyl fluorides display a general lack of reactivity under typical conditions for halide chemistry. Contrary to intuition, the exceptionally high electronegativity of fluorine does not facilitate nucleophilic attacks on the adjacent carbon but instead strengthens the (sp^3)C-F bond (105.4 kcal/mol, C-H: 98.8 kcal/mol, C-Cl: 78.5 kcal/mol), due to substantial electrostatic attraction between the highly polarized bonding partners (O'Hagan, 2008). Strategies that work for alkyl chlorides, bromides, or iodides seem to fail to sufficiently activate fluorides for further reactions. Nevertheless, some successful approaches for C-F bond activation have been developed (Burdeniuc et al., 1997; Amii and Uneyama, 2009; Kuehnel et al., 2013; Shen et al., 2015). Exploiting fluorine's high affinity toward boron, and aluminum, most examples cover activation by Lewis acids. Activation by Brønsted acids, known since 1949, when Le Fave found that heating trifluorotoluene in concentrated sulfuric acid facilitated the hydrolysis to benzoic acid (Fave, 1949), has received relatively little attention by contrast. Wang et al. recently published an improved take on this approach to activate trifluorotoluyl substrates by employing an excess of triflic acid at ambient temperature (Wang and Hu, 2009). The benzyl acylium ions generated by this method were then converted to benzophenone derivatives by adding arene nucleophiles to promote a Friedel-Crafts acylation. The inert nature of the CF_3 group requires the use of superstoichiometric amounts of strong acids, which limits the functional group tolerance considerably.

Although the topic of organic fluorides as hydrogen bond acceptors is controversial, increasing evidence indicates a weak interaction (Champagne et al., 2015a). A mild method of activation for benzylic fluorides via hydrogen bonding was recently developed by Paquin et al. (Champagne et al., 2014, 2015b). Hexafluoroisopropanol (HFIP) serves as hydrogen bond donor to the fluorine atom, which destabilizes the C-F bond to then generate a benzylic cation, which can be intercepted by an arene nucleophile in a Friedel-Crafts reaction. HF is liberated after the conversion and replaces HFIP as the catalytically active species because of its higher hydrogen bond donating ability (Rosenberg, 2012; Champagne et al., 2014).

Activation of non-benzylic fluorides remains challenging under Brønsted acidic conditions. Under harsh Brønsted acidic conditions (HCl, 80–110°C) elimination of tertiary alkyl fluorides was reported (**Figures 2A,B**). Primary and secondary fluorides show no reactivity due to the poor stabilization of the respective intermediate carbocations (Wenckens et al., 1998; Bellezza et al., 2005). Interestingly, the enzyme pocket of isopenicillin N synthase facilitated the elimination of a tertiary fluoride under mild conditions (**Figure 2C**).

TABLE 1 | Substrate overview with yields; product denominations: **a**, alcohol; **e**, cyclic ether; **i**, internal alkene; **t**, terminal alkene; all reactions run in filtered $CDCl_3$.

Entry	Substrate	Products		Background
1	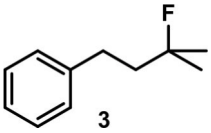 **3**	**3i** 69%[a] (16 h) **3t** 13%[a]		0[b] 0[c]
2	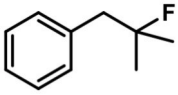 **4**	**4i** 45%[a] (16 h) **4a** 35%[a] **4t** 16%[a]		0[b] 0[c]
3	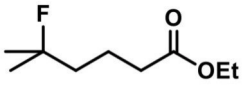 **5**	**5l** 60%[a] (20 h) **5i** 29%[a] **5t** 3%[a]	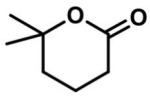 **5l**	0[b] 0[c]
4	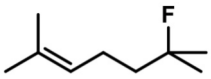 **6**	**6e** 81%[a] (21 h) **6i** 11%[a]	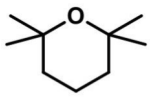 **6e**	0[b] 0[c]
5	 **7**	**7t** 98%[a] (2 h)		**7t** 98%[b] (20 h) 0[c]
6	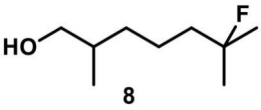 **8**	**8e** 72%[a] (4 h)	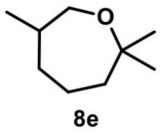 **8e**	**8e** 71%[b] (7d) 0[c]
7	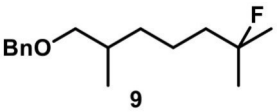 **9**	**9i** 65%[a](4 h) **9t** 6%[a]		**9i** 5%[b](7d) 0[c]
8	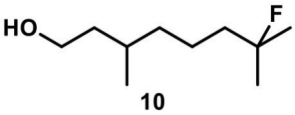 **10**	**10i** 60%[a] (4 h) **10a** 6%[a] **10t** 16%[a]		**10i** 52%[b] (7d) **10a** 6%[b] **10t** 13%[a] 0[c]

*All reactions run in $CDCl_3$ (filtered over basic Al_2O_3 prior to use) at 40°C; [a]determined via ^1H NMR [b]addition of TBAB (1.5 eq. relative to capsule **I**), reaction run for 7 d at 40°C [c] addition of HOAc (10 mol%), no hexamer present, 7d, 40°C.*

RESULTS AND DISCUSSION

Similarly to the enzyme pocket (see above), catalytic amounts of capsule **I** (10 mol%) also facilitated the activation of tertiary alkyl fluorides. In light of our recent investigations (Köster and Tiefenbacher, 2018) concerning the role of HCl as a cocatalyst for some reactions catalyzed by capsule **I**, it is important to note that the activation of tertiary fluorides reported here does not require an acid cocatalyst.

The aryl-substituted substrates **3** and **4** (**Table 1**, entries 1 and 2) were mainly transformed to the corresponding homostyrene **3i** and styrene **4i**, respectively. In both cases the formation of the trisubstituted alkene was favored and the terminal alkenes **3t** and **4t** were observed to a smaller degree. Brønsted-acid catalyzed isomerization of homostyrene **3i** to the corresponding styrene was not observed. Furthermore, an intramolecular Friedel-Crafts alkylation could not be observed. Considerable amounts of homobenzylic alcohol **4a** were formed as a side product. It is important to note that no background reaction was observed when the capsule was blocked with inhibitor **2** (see **Figure 1C**, 1.5 eq. tetrabutylammonium bromide per capsule) or when the capsule was omitted and replaced with an acid of similar acidity (acetic acid). These control experiments indicate that the reaction takes place inside the binding pocket of capsule **I**.

The main product of the reaction of ester **5** was found to be lactone **5l**, presumably resulting from a nucleophilic attack of the ester carbonyl oxygen on the tertiary carbocation. The elimination pathway also led to the formation of the trisubstituted alkene **5i** and of terminal alkene **5t** in trace amounts. Again, no background reactions were observed.

When the unsaturated fluoride **6** was investigated, the main product was found to be cyclic ether **6e** (see **Table 1**). Nucleophilic interception of the initially formed tertiary carbocation by water (from the hexameric assembly or the bulk solution) presumably leads to the formation of an alkenol. The ensuing cyclization is known to be catalyzed by capsule **I** (Catti and Tiefenbacher, 2015). As a side reaction, elimination to the trisubstituted alkene was observed.

Camphene-derived fluoride **7** was converted to the alkene **7t** within 2 h quantitatively. The addition of inihibitor **2** did not result in suppression of the reaction but only slowed down the reaction (completion after 20 h). The complete selectivity toward elimination may be explained by the steric constrains of the carbocation, with a quaternary center and a bridgehead atom in close proximity, which effectively shield the cation from the attack of any nucleophiles.

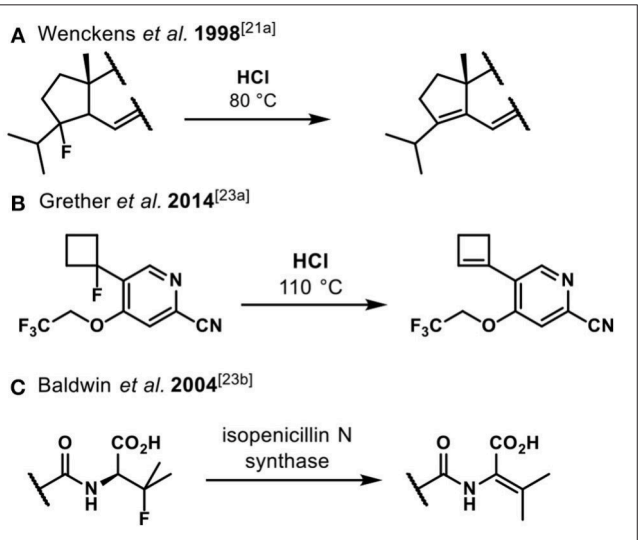

FIGURE 2 | Examples of Brønsted acid- and enzyme-promoted elimination of tertiary fluorides **(A)** Wenckens et al. (1998), **(B)** Grether et al. (2013) and **(C)** Grummitt et al. (2004).

The fluoroalcohol **8** was converted to the seven-membered cyclic ether with good selectivity. The addition of inhibitor **2** did not prevent the reaction but slowed it down significantly (7 d instead of 4 h). The benzyl-protected analog **9** was transformed mainly to the corresponding trisubstituted alkene **9i** because the cyclization pathway was blocked. Experiments with a blocked cavity revealed only marginal conversion after 7 d. The β-Citronellol-derived fluoride **10** showed complete conversion within 4 h with the major product being the trisubstituted alkene. The formation of the corresponding eight-membered cyclic ether could not be observed. As observed with **8**, substantial conversion could be observed in presence of **2**, although at reduced rates (7 d instead of 4 h).

A possible explanation for the conversion of substrates in the presence of inhibitor may lie in the ability of capsule **I** to bind substrates via H-bonds from the outside. However, the significantly reduced reaction rates point toward an acceleration of the reaction on the inside of **I**. All substrates remained intact upon prolonged exposure to 10 mol% acetic acid ($pK_A = 4.75$), indicating that the hexamer's ($pK_A \sim 5.5$–6) mode of activation is likely based on hydrogen bonding to the substrate and stabilization of the resulting cation via cation-π interactions instead of Brønsted acidity alone.

After having demonstrated the ability of capsule **I** to activate tertiary alkyl fluorides, we wondered whether the Friedel-Crafts alkylation with benzylic fluoride electrophiles was also possible inside the hexameric capsule **I**. Starting with 4-tert-butyl benzyl fluoride (**11**) and *p*-xylene (**Scheme 1**), a reaction to the expected product could be observed, albeit in low yield (17%). Since it is known that unfunctionalized guests

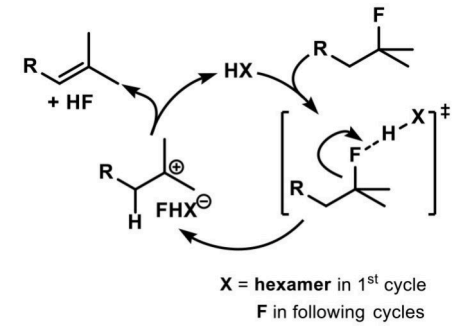

SCHEME 2 | Proposed mechanism of the HF elimination inside container **I**.

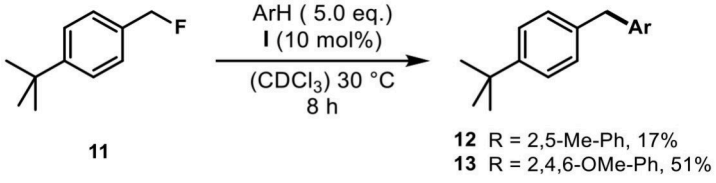

SCHEME 1 | Friedel-Crafts benzylation with benzyl fluoride **11** inside the cavity.

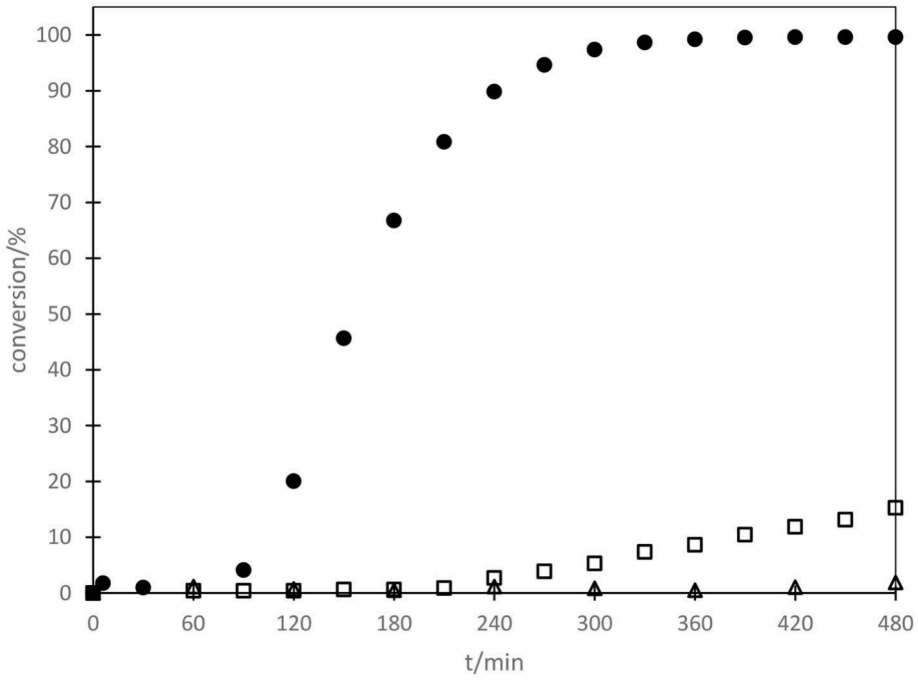

FIGURE 3 | Reaction progress for the elimination of HF from **3** in presence of capsule **I**; 30 °C (□); 40 °C (•), 10 mol% HF, no capsule present, 40°C (Δ).

are taken up poorly by container **I**, we employed 1,3,5-trimethoxybenzene as arene nucleophile to take advantage of the efficient uptake of oxygenated species by capsule **I**. This indeed resulted in an increase in yield to 51%. These results clearly indicate that the activation of benzylic fluorides is also possible and further corroborate capsule **I**'s ability to accelerate Friedel-Crafts reactions as was recently demonstrated by La Manna et al. (2018b). In the absence of suitable nucleophiles, oligomerization was observed with primary and secondary benzyl fluorides. When benzylic di- and trifluorides were investigated, no reaction could be observed. Attempts to use tertiary alkyl fluorides as electrophiles for Friedel-Crafts reactions were unsuccessful, leading only to the respective elimination products.

Following the findings of Paquin et al. (Champagne et al., 2014, 2015a,b) we propose an autocatalytic cycle starting with the encapsulation of a substrate molecule (see **Scheme 2**). The fluorine substituent likely is interacting *via* a hydrogen bond to a water molecule of the assembly. Subsequent cleavage of the activated C-F bond then leads to formation of a carbocation and hydrogen bonded fluoride[1]. After elimination of a proton and subsequent recombination with fluoride to form HF, the alkene is released from the inner cavity. With its superior hydrogen bond donating ability (Checinska and Grabowski, 2006; Champagne et al., 2014) hydrogen fluoride acts as catalytically active species in ensuing cycles.

[1]If X = F, the ion is known as bifluoride, however, more equivalents of HF could be involved.

This mechanistic proposal was underlined by kinetic measurements of the reaction of **3** inside container **I**. After an induction period a sigmoidal reaction progress can be observed at 40°C, a typical indication of an autocatalytic reaction (see **Figure 3**) (Anslyn and Dougherty, 2006).

Interestingly, the addition of HF did not initiate a rapid autocatalytic conversion in the absence of capsule **I**. Conversion of the starting fluoride after addition of catalytic amounts of hydrogen fluoride was sluggish, reaching only 2% after 8 h. A probable cause of this observation might be the fast equilibration of hydrogen fluoride with silicon of the glass reaction vessel walls, which greatly diminishes the local concentration of the catalytically active species. Although HF has been shown to exist in equilibrium with glass walls (Chapman and Levy, 1952), only minuscule amounts of HF may exist at any given time in solution. Interestingly, experiments in plastic vials (see **SI chapter 5.2**) indicated that this is not true. Addition of HF in the absence of hexamer **I** did not lead to a significant conversion even when the reaction was run in plastic vials. However, in the presence of hexamer **I** the addition of HF initiated the reaction immediately (no induction period observed). This strongly suggests a synergistic catalysis mediated by HF and capsule **I**. Control reactions with a large substrate (see **SI chapter 5.5**) that is unable to enter the cavity of **I**, showed no conversion within 4 days under standard reaction conditions (40°C, acid-free $CDCl_3$, 10 mol% **I**). However, a competition experiment together with benzyl ether **9** resulted in the full conversion of both substrates within 4 h (see **SI-Figure 6**). It is clearly visible that the smaller substrate **9** initiated the reaction and subsequently the larger substrate reacted, obviously outside of capsule **I**. In summary, this

suggests that: (1) capsule **I** is necessary to activate the substrate, (2) HF is only catalytically active in conjunction with capsule **I** (3) if HF has been liberated large substrates can also react outside of capsule **I**, in accordance with the proposed mechanism (see **Scheme 2**).

Kinetic experiments with monodeuterated substrate **3d** (see **SI chapter 5.3**) to elucidate the reaction mechanism resulted in a KIE of 1.16 ± 0.03. This is indicative of a secondary deuterium KIE arising from hyperconjugative stabilization of the formed cation, thereby indicating fluoride abstraction as rate-limiting (Anslyn and Dougherty, 2006). This result is in agreement with earlier observations made in the acid-catalyzed solvolysis of tertiary alkyl fluorides (Chapman and Levy, 1952).

In conclusion, we have demonstrated the ability of **I** to activate tertiary alkyl fluorides and primary and secondary benzylic fluorides. The hexameric assembly **I** presumably not only functions as a hydrogen bond donor to activate the C-F bond but is also able to stabilize the intermediate carbocations *via* cation-π interactions. The stabilized intermediates underwent several transformations inside the cavity, ranging from elimination, cyclization to intermolecular nucleophilic attack in the case of benzyl fluorides. The displayed ability of hexamer **I** to activate aliphatic C-F bonds is noteworthy since the reaction conditions are unusually mild: 40°; no strong Brønsted or Lewis acids present.

AUTHOR CONTRIBUTIONS

KT conceived and supervised the project. KT and JK planned the project. JK carried out all the experiments. DH performed kinetic NMR measurements. JK and KT compiled the first draft of the manuscript. All authors contributed to the final version of the manuscript.

ACKNOWLEDGMENTS

This work was supported by funding from the European Research Council Horizon 2020 Programme [ERC Starting Grant 714620-TERPENECAT], the Swiss National Science Foundation as part of the NCCR Molecular Systems Engineering and the Bayerische Akademie der Wissenschaften (Junges Kolleg).

SUPPLEMENTARY MATERIAL

The Supplementary Material for this article can be found online at: https://www.frontiersin.org/articles/10.3389/fchem.2018.00639/full#supplementary-material

REFERENCES

Amii, H., and Uneyama, K. (2009). C–F bond activation in organic synthesis. *Chem. Rev.* 109, 2119–2183. doi: 10.1021/cr800388c

Anslyn, E. V., and Dougherty, D. A. (2006). *Modern Physical Organic Chemistry*. Sausalito, CA: University Science Books.

Avram, L., and Cohen, Y. (2002). The role of water molecules in a resorcinarene capsule as probed by NMR diffusion measurements. *Org. Lett.* 4, 4365–4368. doi: 10.1021/ol0271077

Bellezza, F., Cipiciani, A., Ricci, G., and Ruzziconi, R. (2005). On the enzymatic hydrolysis of methyl 2-fluoro-2-arylpropionates by lipases, *Tetrahedron* 61, 8005–8012. doi: 10.1016/j.tet.2005.06.007

Bianchini, G., La Sorella, G. L., Canever, N., Scarso, A., and Strukul, G. (2013). Efficient isonitrile hydration through encapsulation within a hexameric self-assembled capsule and selective inhibition by a photo-controllable competitive guest. *Chem. Commun.* 49, 5322–5324. doi: 10.1039/c3cc42233j

Bräuer, T. M., Zhang, Q., and Tiefenbacher, K. (2017). Iminium catalysis inside a self-assembled supramolecular capsule: scope and mechanistic studies. *J. Am. Chem. Soc.* 139, 17500–17507. doi: 10.1021/jacs.7b08976

Brown, C. J., Toste, F. D., Bergman, R. G., and Raymond, K. N. (2015). Supramolecular catalysis in metal–ligand cluster hosts. *Chem. Rev.* 115, 3012–3035. doi: 10.1021/cr4001226

Burdeniuc, J., Jedicka, B., and Crabtree, R. H. (1997). Recent advances in C–F bond activation. *Chem. Ber.* 130, 145–154. doi: 10.1002/cber.19971300203

Caneva, T., Sperni, L., Strukul, G., and Scarso, A. (2016). Efficient epoxide isomerization within a self-assembled hexameric organic capsule. *RSC Adv.* 6, 83505–83509. doi: 10.1039/C6RA20271C

Catti, L., Pöthig, A., and Tiefenbacher, K. (2017). Host-catalyzed cyclodehydration–rearrangement cascade reaction of unsaturated tertiary alcohols. *Adv. Synth. Catal.* 359, 1331–1338. doi: 10.1002/adsc.201601363

Catti, L., and Tiefenbacher, K. (2015). Intramolecular hydroalkoxylation catalyzed inside a self-assembled cavity of an enzyme-like host structure. *Chem. Commun.* 51, 892–894. doi: 10.1039/C4CC08211G

Catti, L., and Tiefenbacher, K. (2018). Brønsted acid-catalyzed carbonyl-olefin metathesis inside a self-assembled supramolecular host. *Angew. Chem. Int. Ed.* 57, 14589–14592. doi: 10.1002/anie.201712141

Catti, L., Zhang, Q., and Tiefenbacher, K. (2016a). Self-assembled supramolecular structures as catalysts for reactions involving cationic transition states. *Synthesis* 48, 313–328. doi: 10.1055/s-0035-1560362

Catti, L., Zhang, Q., and Tiefenbacher, K. (2016b). Advantages of catalysis in self-assembled molecular capsules. *Chem. Eur. J.* 22, 9060–9066. doi: 10.1002/chem.201600726

Champagne, P. A., Benhassine, Y., Desroches, J., and Paquin, J. F. (2014). Friedel–crafts reaction of benzyl fluorides: selective activation of C-F bonds as enabled by hydrogen bonding. *Angew. Chem.* 126, 14055–14059. doi: 10.1002/ange.201406088

Champagne, P. A., Desroches, J., and Paquin, J.-F. (2015a). Organic fluorine as a hydrogen-bond acceptor: recent examples and applications. *Synthesis* 47, 306–322. doi: 10.1055/s-0034-1379537

Champagne, P. A., Drouin, M., Legault, C. Y., Audubert, C., and Paquin, J.-F. (2015b). Revised mechanistic explanation for the alcohol-promoted amination of benzylic fluorides under highly concentrated conditions: computational and experimental evidence on a model substrate. *J. Fluor. Chem.* 171, 113–119. doi: 10.1016/j.jfluchem.2014.08.018

Chapman, N. B., and Levy, J. L. (1952). Nucleophilic displacement of fluorine from organic compounds. Part III. Acid-catalysed solvolysis of alkyl fluorides in aqueous ethanol. *J. Chem. Soc.* 1677–1682. doi: 10.1039/jr9520001677

Checinska, L., and Grabowski, S. J. (2006). F–H···F–C hydrogen bonds–The influence of hybridization of carbon atom connected with F-acceptor on their properties. *Chem. Phys.* 327, 202–208. doi: 10.1016/j.chemphys.2006.04.011

Cullen, W., Misuraca, M. C., Hunter, C. A., Williams, N. H., and Ward, M. D. (2016). Highly efficient catalysis of the Kemp elimination in the cavity of a cubic coordination cage. *Nat. Chem.* 8:231. doi: 10.1038/nchem.2452

Fave, G. M. L. (1949). Some reactions of the trifluoromethyl group in the benzotrifluoride series. I. Hydrolysis. *J. Am. Chem. Soc.* 71, 4148–4149. doi: 10.1021/ja01180a507

Giust, S., La Sorella, G., Sperni, L., Fabris, F., Strukul, G., and Scarso, A. (2015). Supramolecular catalysis in the synthesis of substituted 1 H-tetrazoles from isonitriles by a self-assembled hexameric capsule. *Asian J. Org. Chem.* 4, 217–220. doi: 10.1002/ajoc.201402229

Grether, U., Kimbara, A., Nettekoven, M., Ricklin, F., Roever, S., Rogers-Evans, M., et al. (2013). WO/2014/086805.

Grummitt, A. R., Rutledge, P. J., Clifton, I. J., and Baldwin, J. E. (2004). Active-site-mediated elimination of hydrogen fluoride from a fluorinated substrate analogue by isopenicillin N synthase. *Biochem. J.* 382, 659–666. doi: 10.1042/BJ20040529

Jans, A. C., Gómez-Suárez, A., Nolan, S. P., and Reek, J. N. (2016). A Switchable gold catalyst by encapsulation in a self-assembled cage. *Chem. Eur. J.* 22, 14836–14839. doi: 10.1002/chem.201603162

Köster, J., and Tiefenbacher, K. (2018). Elucidating the importance of hydrochloric acid as a cocatalyst for resorcinarene-capsule-catalyzed reactions. *ChemCatChem* 10, 2941–2944. doi: 10.1002/cctc.201800326

Kuehnel, M. F., Lentz, D., and Braun, T. (2013). Synthesis of fluorinated building blocks by transition-metal-mediated hydrodefluorination reactions. *Angew. Chem. Int. Ed.* 52, 3328–3348. doi: 10.1002/anie.201205260

Kuijpers, P. F., Otte, M., Dürr, M., Ivanović-Burmazović, I., Reek, J. N. H., and de Bruin, B. (2016). A self-assembled molecular cage for substrate-selective epoxidation reactions in aqueous media. *ACS Catal.* 6, 3106–3112. doi: 10.1021/acscatal.6b00283

La Manna, P., De Rosa, M., Talotta, C., Gaeta, C., Soriente, A., Floresta, G., et al. (2018a). The hexameric resorcinarene capsule as an artificial enzyme: ruling the regio and stereochemistry of a 1,3-dipolar cycloaddition between nitrones and unsaturated aldehydes. *Org. Chem. Front.* 5, 827–837. doi: 10.1039/C7QO00942A

La Manna, P., Talotta, C., Floresta, G., De Rosa, M., Soriente, A., Rescifina, A. et al. (2018b). Mild friedel–crafts reactions inside a hexameric resorcinarene capsule: C–Cl bond activation through hydrogen bonding to bridging water molecules. *Angew. Chem. Int. Ed.* 57, 5423–5428. doi: 10.1002/anie.201801642

La Sorella, G., Sperni, L., Ballester, P., Strukul, G., and Scarso, A. (2016a). Hydration of aromatic alkynes catalyzed by a self-assembled hexameric organic capsule. *Catal. Sci. Techol.* 6, 6031–6036. doi: 10.1039/C6CY00307A

La Sorella, G., Sperni, L., Strukul, G., and Scarso, A. (2016b). Supramolecular activation of hydrogen peroxide in the selective sulfoxidation of thioethers by a self-assembled hexameric capsule. *Adv. Synth. Catal.* 358, 3443–3449. doi: 10.1002/adsc.201600430

Leenders, S., Gramage-Doria, R., de Bruin, B., and Reek, J. N. H. (2015). Transition metal catalysis in confined spaces. *Chem. Soc. Rev.* 44, 433–448. doi: 10.1039/C4CS00192C

Levin, M. D., Kaphan, D. M., Hong, C. M., Bergman, R. G., Raymond, K. N., and Toste, F. D. (2016). Scope and mechanism of cooperativity at the intersection of organometallic and supramolecular catalysis. *J. Am. Chem. Soc.* 138, 9682–9693. doi: 10.1021/jacs.6b05442

MacGillivray, L. R., and Atwood, J. L. (1997). A chiral spherical molecular assembly held together by 60 hydrogen bonds. *Nature* 389, 469. doi: 10.1038/38985

Marchetti, L., and Levine, M. (2011). Biomimetic catalysis. *ACS Catal.* 1, 1090–1118. doi: 10.1021/cs200171u

O'Hagan, D. (2008). Understanding organofluorine chemistry. An introduction to the C-F bond. *Chem. Soc. Rev.* 37, 308–319. doi: 10.1039/B711844A

Otte, M. (2016). Size-selective molecular flasks. *ACS Catal.* 6, 6491–6510. doi: 10.1021/acscatal.6b01776

Raynal, M., Ballester, P., Vidal-Ferran, A., and van Leeuwen, P. W. (2014). Supramolecular catalysis. Part 2: artificial enzyme mimics. *Chem. Soc. Rev.* 43, 1734–1787. doi: 10.1039/C3CS60037H

Rosenberg, R. E. (2012). Does fluoromethane form a hydrogen bond with water? *J. Phys. Chem. A* 116, 10842–10849. doi: 10.1021/jp308533b

Shen, Q., Huang, Y.-G., Liu, C., Xiao, J.-C., Chen, Q.-Y., and Guo, Y. (2015). Review of recent advances in CF bond activation of aliphatic fluorides. *J. Fluor. Chem.* 179, 14–22. doi: 10.1016/j.jfluchem.2015.07.007

Ueda, Y., Ito, H., Fujita, D., and Fujita, M. (2017). Permeable self-assembled molecular containers for catalyst isolation enabling two-step cascade reactions. *J. Am. Chem. Soc.* 139, 6090–6093. doi: 10.1021/jacs.7b02745

Wang, F., and Hu, J. (2009). Brønsted Acid Mediated (sp3)carbon-fluorine bond activation: inter- and intramolecular arylation of trifluoromethylated arenes. *Chin. J. Chem.* 27, 93–98. doi: 10.1002/cjoc.200990032

Wang, Q.-Q., Gonell, S., Leenders, S. H., Dürr, M., Ivanović-Burmazović, I., and Reek, J. N. (2016). Self-assembled nanospheres with multiple endohedral binding sites pre-organize catalysts and substrates for highly efficient reactions. *Nat. Chem.* 8:225. doi: 10.1038/nchem.2425

Wang, X., Nurttila, S. S., Dzik, W. I., Becker, R., Rodgers, J., and Reek, J. N. H. (2017). Tuning the porphyrin building block in self-assembled cages for branched-selective hydroformylation of propene. *Chem. Eur. J.* 23, 14769–14777. doi: 10.1002/chem.201703135

Wenckens, M., Grønvald, F., and Hansen, J. B. (1998). Synthesis of meiosis-activating sterols containing fluorine. *Acta Chem. Scand.* 52, 503–507 doi: 10.3891/acta.chem.scand.52-0503

Wiester, M. J., Ulmann, P. A., and Mirkin, C. A. (2011). Enzyme mimics based upon supramolecular coordination chemistry. *Angew. Chem. Int. Ed.* 50, 114–137. doi: 10.1002/anie.201000380

Zarra, S., Wood, D. M., Roberts, D. A., and Nitschke, J. R. (2015). Molecular containers in complex chemical systems. *Chem. Soc. Rev.* 44, 419–432. doi: 10.1039/C4CS00165F

Zhang, Q., and Tiefenbacher, K. (2013). Hexameric resorcinarene capsule is a brønsted acid: investigation and application to synthesis and catalysis. *J. Am. Chem. Soc.* 135, 16213–16219. doi: 10.1021/ja4080375

Zhang, Q., and Tiefenbacher, K. (2015). Terpene cyclization catalysed inside a self-assembled cavity. *Nat. Chem.* 7, 197–202. doi: 10.1038/nchem.2181

Conflict of Interest Statement: The authors declare that the research was conducted in the absence of any commercial or financial relationships that could be construed as a potential conflict of interest.